CONTRACTOR REPORT

SAND82—7157/2 of 4
Unlimited Release
UC—63

Analysis of Concentrating PV-T Systems for the Commercial/Industrial Sector

Volume II. PV-T State-of-the-Art Survey and Site/Application Pair Selection and Analysis

W. E. Schwinkendorf
The BDM Corporation
1801 Randolph Rd, SE
Albuquerque, NM 87106

Prepared by Sandia National Laboratories Albuquerque, New Mexico 87185 and Livermore, California 94550 for the United States Department of Energy under Contract DE-AC04-76DP00789

Printed September 1984

When printing a copy of any digitized SAND Report, you are required to update the markings to current standards.

Issued by Sandia National Laboratories, operated for the United States Department of Energy by Sandia Corporation.
NOTICE: This report was prepared as an account of work sponsored by an agency of the United States Government. Neither the United States Government nor any agency thereof, nor any of their employees, nor any of their contractors, subcontractors, or their employees, makes any warranty, express or implied, or assumes any legal liability or responsibility for the accuracy, completeness, or usefulness of any information, apparatus, product, or process disclosed, or represents that its use would not infringe privately owned rights. Reference herein to any specific commercial product, process, or service by trade name, trademark, manufacturer, or otherwise, does not necessarily constitute or imply its endorsement, recommendation, or favoring by the United States Government, any agency thereof or any of their contractors or subcontractors. The views and opinions expressed herein do not necessarily state or reflect those of the United States Government, any agency thereof or any of their contractors or subcontractors.

Printed in the United States of America
Available from
National Technical Information Service
U.S. Department of Commerce
5285 Port Royal Road
Springfield, VA 22161

NTIS price codes
Printed copy: A08
Microfiche copy: A01

SAND82–7157/2 of 4
Unlimited Release
Printed September 1984

Distribution
Category UC–63

Analysis of Concentrating PV-T Systems for the Commercial/Industrial Sector

Volume II. PV-T State-of-the-Art Survey and Site/Application Pair Selection and Analysis

W. E. Schwinkendorf
The BDM Corporation
1801 Randolph Rd, SE
Albuquerque, NM 87106

Abstract

As part of a project to develop feasibility assessments, design procedures, and reference designs for total energy systems that could use actively cooled concentrating photovoltaic collectors, a survey was conducted to provide an overview of available photovoltaic-thermal (PV-T) technology. General issues associated with the design and installation of a PV-T system are identified. Electrical and thermal efficiencies for the line-focus Fresnel, the linear parabolic trough, and the point-focus Fresnel collectors are specified as a funtion of operating temperature, ambient temperature, and insolation. For current PV-T technologies, the line-focus Fresnel collector proved to have the highest thermal and electrical efficiencies, lowest array cost, and lowest land area requirement. But a separate feasibility analysis involving 11 site/application pairs showed that for most applications, the cost of the photovoltaic portion of a PV-T system is not recovered through the displacement of an electrical load, and use of a thermal-only system to displace the therml load would be a more economical alternative. PV-T systems are not feasible for applications that have a small thermal load, a large steam requirement, or a high load return temperature. SAND82–7157/3 identifies the technical issues involved in designing a photovoltaic-thermal system and provides guidance for resolving such issues. Detailed PV-T system designs for three selected applications and the results of a trade-off study for these applications are presented in SAND82–7157/4. A summary of the major results of this entire study and conclusions concerning PV-T systems and applications is presented in SAND82–7157/1.

FOREWORD

This volume of technical report BDM/A-82-458-TR-R1 is submitted by The BDM Corporation, 1801 Randolph Road, S.E., Albuquerque, New Mexico to Sandia National Laboratories. This report documents an analysis of PV-T systems and selected applications performed under contract 68-0361. This volume documents the state-of-the-art survey of PV-T systems and the analysis of these systems. Current operating systems are reviewed and issues associated with overall design of a PV-T array are discussed. Various site/application pairs are selected for further detailed analysis using SOLCEL-III and the Perino Economic Analysis Methodology. Economic and performance analyses are presented for PV-T, thermal only, and PV-only systems for several site/application pairs.

The support and helpful comments of Miguel Rios, the Sandia Contract Monitor, are acknowledged and greatly appreciated.

TABLE OF CONTENTS

Chapter		Page
I	INTRODUCTION	I-1
II	STATE OF THE ART OF CONCENTRATING PV-T SYSTEMS	II-1
	A. GENERAL SUMMARY	II-1
	1. Photovoltaic-Thermal Concentrators	II-1
	2. System Development Status	II-1
	B. SUBSYSTEM SPECIFICATIONS	II-4
	1. Collector Modules	II-4
	2. Other System Components	II-28
	C. SYSTEM DESIGN ISSUES	II-36
	1. Array Field Layout	II-36
	2. Constant Versus Variable Fluid Flow Rate	II-48
	3. Freeze Protection and Fluid Selection	II-48
	D. SUMMARY OF PV-T APPLICATIONS	II-51
	1. The DOE Program	II-51
	2. The BDM CAPVC Project	II-52
	3. The E-Systems Dallas-Fort Worth Airport Project	II-54
	4. The Acurex Hawaiian Hospital Project	II-56
	5. The BDM/SKI MCC College Project	II-57
	E. REFERENCES	II-59
III	SITE/APPLICATION PAIR SELECTION, LOAD PROFILE DEVELOPMENT, AND ECONOMIC ANALYSIS	III-1
	A. INTRODUCTION	III-1
	B. COMMERCIAL SECTOR ANALYSIS	III-4
	1. Ranking of Commercial Site/Application Pairs	III-4
	2. Development of Commercial Load Profiles	III-9
	C. INDUSTRIAL SECTOR ANALYSIS	III-30

TABLE OF CONTENTS (Concluded)

Chapter		Page
	D. SITE/APPLICATION PAIR ANALYSIS	III-68
	1. Economic Parameters	III-71
	2. Industrial Site/Application Pairs	III-75
	3. Commercial Site/Application Pairs	III-80
	E. SIDE-BY-SIDE STUDY	III-80
	1. Collector Array Costs	III-82
	2. Results of Side-By-Side Analysis	III-83
	F. REFERENCES	III-93
IV	CONCLUSIONS	IV-1

LIST OF ILLUSTRATIONS

Figure		Page
II-1	PV-T Technologies	II-2
II-2	SKI Concentrator with BDM Receiver	II-5
II-3	Cross Section of E-Systems Line Focus Fresnel Lens Collector	II-8
II-4	Second Generation Array	II-9
II-5	MMC PV-T Array	II-11
II-6	MMC Insulated PV-T Receiver Extrusion	II-12
II-7	Results of SOLCEL Thermal Performance Calculations for Concentrating PV-T Systems	II-21
II-8	Results of SOLCEL Electrical Performance Calculation for Concentrating PV-T Systems	II-24
II-9	Collector Field Layout Patterns	II-38
II-10	Energy Incident on Collector Aperture (LPT)	II-41
II-11	Annual Nonfirst Row Shading	II-42
II-12	Monthly Shadowing of E/W and N/S Parabolic Troughs	II-42
II-13	Maximum Effect of Tracking Thresholds, Cosine Factor, and Row Shading for a N/S LPT	II-44
III-1	Conceptual PV-T System for Preliminary Analysis and Sizing	III-3
III-2	Uniform Building Code U Values for Walls	III-17
III-3	Thermal System Configuration for PV-T Application to Commercial Buildings	III-26
III-4	Fresno, California Hospital Load Profile on a Cold, Clear Winter Day (350)	III-29
III-5	Fresno, California Hospital Load Profile on a Warm, Clear Summer Day (160)	III-31

LIST OF ILLUSTRATIONS (Continued)

Figure		Page
III-6	Seattle, Washington Hospital Load Profile on a Cold, Clear Winter Day (350)	III-32
III-7	Seattle, Washington Hospital Load Profile on a Warm, Clear Summer Day (173)	III-33
III-8	Albuquerque, New Mexico School Load Profile on a Cool, Clear Winter Day (340)	III-34
III-9	Albuquerque, New Mexico School Load Profile on a Warm, Clear Fall Day (250)	III-35
III-10	Boston, Massachusetts School Load Profile on a Cold, Clear Winter Day (350)	III-36
III-11	Boston, Massachusetts School Load Profile on a Warm, Clear Fall Day (251)	III-37
III-12	Phoenix, Arizona Public Administration Building Load Profile on a Cool, Clear Winter Day (361)	III-38
III-13	Phoenix, Arizona Public Administration Building Load Profile on a Hot, Clear Summer Day (176)	III-39
III-14	Denver, Colorado Bread Bakery Thermal Load Profile	III-53
III-15	Denver, Colorado Bread Bakery Electrical Load Profile	III-54
III-16	Dixon, California Meat Packing Plant Thermal Load Profile	III-56
III-17	Dixon, California Meat Packer Electrical Load Profile (Armor Meat Packing Co.)	III-57
III-18	Thomaston, Georgia Fiber Finishing Plant Thermal Load Profile (Thomaston Mills)	III-59
III-19	Thomaston, Georgia Fiber Finishing Plant Electrical Load Profile	III-60
III-20	El Paso, Texas Fluid Milk Plant Thermal Load Profile	III-63

LIST OF ILLUSTRATIONS (Concluded)

Figure		Page
III-21	El Paso, Texas Fluid Milk Plant Electrical Load Profile	III-64
III-22	Tucson, Arizona Concrete Block Plant Thermal Load Profile	III-65
III-23	Tucson, Arizona Concrete Block Plant Electrical Load Profile	III-66
III-24	Electrical and Thermal Load Profiles for a Typical Laundromat	III-69
III-25	Life Cycle Cost Ratio Versus Array Area for LFF Collectors and for the Industrial Sector--Income Tax Credit is 10 Percent	III-76
III-26	Life Cycle Cost Ratio Versus Array Area of LFF Collectors for the Industrial Sector--Income Tax Credit is 25 Percent	III-77
III-27	Life Cycle Cost Ratio Versus Array Area for Commercial Applications Using LFF Collectors and a 25 Percent Tax Credit	III-81
III-28	Solar Collector Thermal Performance SKI T-800	III-87
III-29	Life Cycle Cost Ratio Versus Array Area for Concentrating Solar Thermal Collectors Only and Industrial Applications	III-88
III-30	Life Cycle Cost Ratio Versus Array Area for Concentrating Solar Thermal Collectors Only and Commercial Applications	III-89
III-31	Life Cycle Cost Ratio Versus Array Size for a LFF PV System Only and Industrial Applications	III-91
III-32	Life Cycle Cost Ratio Versus Array Area for a LFF PV System Only and Commercial Applications	III-92

LIST OF TABLES

Table		Page
II-1	SURVIVAL WIND SPEEDS m/sec (mph)	II-14
II-2	SOLCEL II COLLECTOR INPUT VALUES	II-18
II-3	EFFICIENCY PARAMETERS	II-22
II-4	ANNUAL EFFICIENCIES (%)	II-25
II-5	CAPITAL COST SUMMARY IN $\$/m^2$ ($\$/FT^2$)	II-26
II-6	LEVELIZED ANNUAL COSTS IN $\$/m^2$ ($\$/FT^2$)	II-27
II-7	OPERATION AND MAINTENANCE COST SUMMARY	II-29
II-8	FIELD LAYOUT TRADE-OFFS	II-37
II-9	SEASONAL VARIATIONS IN SHADING FACTORS	II-43
II-10	LFF SHADING IN ALBUQUERQUE	II-46
II-11	PFF SHADING IN ALBUQUERQUE	II-46
II-12	COMPARISON OF LAND USE	II-47
II-13	METHODS OF FREEZE PROTECTION FOR PV-T SYSTEMS	II-50
III-1	ILLUSTRATIVE COMPUTATION OF Pq FOR HOSPITALS BASED ON TOTAL NATIONAL ENERGY CONSUMPTION	III-6
III-2	RTI RANKING FACTORS FOR PV-T APPLICATIONS IN THE COMMERCIAL SECTOR	III-7
III-3	REGIONS FOR INSOLATION DATA FOR FULLY TRACKING COLLECTORS	III-8
III-4	RANKING OF THE COMMERCIAL SECTOR BY REGION	III-10
III-5	TEN TOP RANKED SITE/APPLICATION PAIRS	III-11
III-6	CLASSIFICATION OF COMMERCIAL LOADS	III-12
III-7	SOLCEL COMMERCIAL LOAD INPUT VALUES	III-14

LIST OF TABLES (Concluded)

Table		Page
III-8	TYPICAL BUILDING STRUCTURES	III-18
III-9	OCCUPANCY PROFILES	III-19
III-10	HOSPITAL LOAD PROFILES	III-21
III-11	HIGH SCHOOL LOAD PROFILES	III-22
III-12	TABULATION OF SYSTEMS ENERGY CONSUMPTION FOR THE PHOENIX, ARIZONA PUBLIC ADMINISTRATION BUILDING	III-23
III-13	PUBLIC ADMINISTRATION BUILDING LOAD PROFILES	III-25
III-14	ANNUAL COMMERCIAL LOADS	III-28
III-15	INDUSTRIAL REGIONS	III-40
III-16	ENERGY COST - SIC 203 (FRUIT AND VEGETABLE PROCESSING)	III-42
III-17	RANKING OF THE INDUSTRIAL SECTOR FOR POTENTIAL PV-T APPLICATION	III-48
III-18	SELECTED SITE/APPLICATION PAIRS	III-70
III-19	ECONOMIC PARAMETERS FOR PV-T LIFE CYCLE COST ANALYSIS	III-74
III-20	CONVENTIONAL ENERGY COSTS, 1982 DOLLARS	III-74
III-21	ENERGY COST ESCALATION RATES (23 YEAR AVERAGE OF JANUARY, 1980 FEDERAL REGISTER VALUES INCLUDING GENERAL INFLATION)	III-75
III-22	GE INSTALLATION COSTS USING 1980 TECHNOLOGY AND A PRODUCTION RATE OF 10^5 m^2/YEAR	III-84
III-23	GE COST STUDIES USING 1980 TECHNOLOGY AND 10^5 m^2/YEAR PRODUCTION LEVELS	III-85
III-24	PROJECTED 1990 COSTS WITH NEW TECHNOLOGY AND 7.5 x 10^6 m^2 PRODUCTION LEVEL	III-86

CHAPTER I
INTRODUCTION

This volume of the study of actively cooled photovoltaic systems, or combined photovoltaic-thermal (PV-T) systems, combined a state-of-the-art survey of existing PV-T systems and an analysis of the application of PV-T systems to selected site/application pairs.

In chapter II the results of the PV-T state-of-the-art survey are described, including the characteristics of current PV-T collectors, the characteristics and problems associated with current operating systems, and "lessons learned" about the design, installation, and operation of a PV-T system. This study was designed to provide an overview of currently available PV-T technology, to identify general issues associated with designing and installing a PV-T system, and to identify problems associated with first generation PV-T installations, so that similar problems will not recur.

The types of collectors studied include the line focus Fresnel (LFF), the linear parabolic trough (LPT), and the point focus Fresnel (PFF) collectors. A detailed analysis was performed for each collector using SOLCEL-II to determine electrical and thermal efficiencies for each collector as a function of operating temperature, ambient temperature, and insolation. In addition, an analysis was performed for each collector type to determine the land area and array cost required for a specified electrical power output. These analyses indicated that the LFF collector had the highest thermal and electrical efficiencies, lowest array cost, and lowest land area requirement of the three systems studied.

In chapter III a methodology is described for ranking the industrial and commercial sector applications to allow selection of the best site/application pairs for further detailed analysis. This methodology was based on the assumption that the PV-T system should be designed to displace the entire electrical load and whatever thermal energy was available would be used to displace the thermal load. At the time, this

appeared to be a reasonable basis to select a limited number of site/application pairs for further study. Unfortunately, detailed hour-by-hour simulation has indicated that PV-T systems should be optimized in size for the thermal load, and that the electrical load plays a negligible part in defining the system size. Thus, this ranking should have been based on displacing the thermal load rather than the electric load. However, if a PV-T system can economically provide thermal energy, then the added cost of the PV portion of the system may be recoverable through displacement of an electrical load or selling power to the utility.

Eleven site/application pairs were selected for further analysis, six from the industrial sector and five from the commercial sector. From this analysis it was found that those applications with a small thermal load, or a thermal load which could not be met to a large extent by the PV-T system (i.e., a large steam load), were not economically feasible.

A study was also performed to determine the feasibility of using a thermal-only system to displace the thermal load of the 11 site/application pairs, and a PV-only system to displace the electrical loads. The thermal-only array consisted of LPT collectors, and the PV-only array consisted of passively cooled, two-axis tracking LFF collectors. These analyses indicated that the thermal-only systems had an economic advantage over the PV-T systems for most of the applications. In no case was the PV-only system economically feasible. However, only conventional financing for load connected systems with utility sellback of electrical power was considered. Third-party financing may change the results obtained for the PV-only systems.

The conclusions derived from the studies reported in this volume are discussed in more detail in chapter IV.

CHAPTER II
STATE OF THE ART OF CONCENTRATING PV-T SYSTEMS

A. GENERAL SUMMARY

1. Photovoltaic-Thermal Concentrators

Solar photovoltaic concentrators focus sunlight on small PV cells, which convert sunlight directly to electricity (ref. II-1). Since PV cells operate more efficiently at low temperatures, a cooling fluid is pumped through the cell receiver section, or fins are attached to the back of the receiver, to promote natural radiative and convective heat transfer. When the former option is employed, thermal energy becomes available in the form of hot water or oil, and the system is called a photovoltaic-thermal (PV-T) concentrator.

This study of PV-T concentrators initially considered three collector types--the linear parabolic trough (LPT) reflector, the line focus Fresnel (LFF) lens, and the point focus Fresnel (PFF) lens. Representative collectors in these categories are shown in figure II-1. In the development of LPT and LFF photovoltaic concentrators, active cooling was the first choice of designers. In the case of the PFF, active cooling was later introduced in an attempt to provide useful thermal energy. The major portion of this study deals with LPT and LFF techniques, which currently represent the most economical candidates for PV-T systems.

2. System Development Status

Since PV-T systems are a combination of PV and thermal technologies, progress made in each area has been applied to the combined systems. In the electrical area, the analysis of photovoltaic cell and array performance has a history dating back to the space program of the 1950's. The analysis of PV arrays for terrestrial applications received considerable interest in the 1970's. During that decade, the development of performance analyses was led by Sandia National Laboratories (SNLA) in Albuquerque, New Mexico. This work included the development of SOLCEL II

TECHNOLOGY	LINEAR PARABOLIC TROUGHS		LINEAR FOCUS FRESNEL	POINT FOCUS FRESNEL
ORG.	BDM/SKI	ACUREX	E-SYSTEMS	MARTIN MARIETTA
MODULE	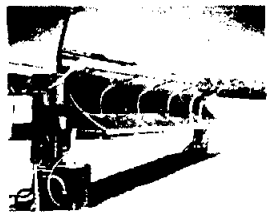	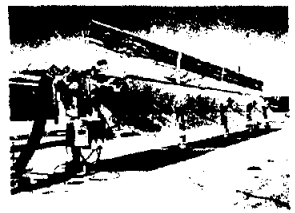	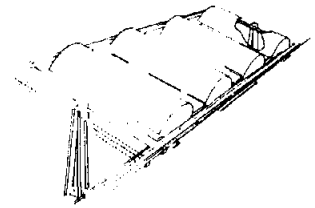	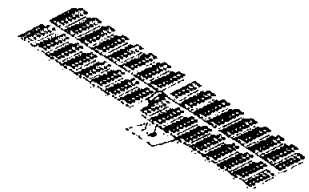
RECEIVER	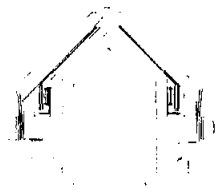	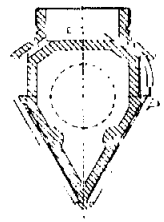	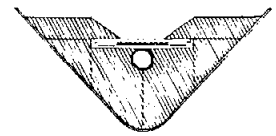	
PHYSICAL SPECIFICATIONS	• CONCENTRATION RATIO 42 • TRACKING N-S AXIS • MODULE LENGTH - m 6.1 • MODULE WIDTH - m 2.1 • MODULES/DRIVE UNIT 6 • m^2/DRIVE UNIT 78	36 N-S AXIS 3.05 1.8 12 67	40 TWO AXIS 3.05 0.9 72 201	50 TWO AXIS 1.2 0.3 68 25.3
ELECTRICAL PERFORMANCE I = 800 w/m^2 T_{CELL} = 28°C	% ARRAY EFFICIENCY 9 kWp/DRIVE UNIT 5.6 CELL MANUFACTURER ASEC	9.1 4.8 ASEC	12.7 1.7 ASEC	12.1 2.1 ASEC
THERMAL PERFORMANCE	% ARRAY EFFICIENCY 50 $\dot{m}$ (m^3/sec) 6.3×10^{-4}	60 5×10^{-4}	47 3.2×10^{-4}	37 5×10^{-4}

Figure II-1. PV-T Technologies

(ref. II-2), a computer simulation code originally written by SNLA with assistance by The BDM Corporation and later modified by BDM under contract with SNLA. Several private companies have also written their own PV simulation programs. Comprehensive guidelines for the design of PV electrical circuits have been provided in an SNLA report by BDM (ref. II-3).

In the area of hardware development, Sandia National Laboratories has tested PV flat plate and concentrating arrays developed by several companies (ref. II-4). The Department of Energy (DOE), through SNLA, has funded the construction of nine large-scale experimental and demonstration PV installations in the commercial and industrial sector. Three of these projects, which are listed below, use actively cooled PV concentrators:

(1) Commercial Application of a PV Concentrator (CAPVC), The BDM Office Building, Albuquerque, New Mexico, by The BDM Corporation and Solar Kinetics, Inc. (SKI); an LPT system operational in July, 1982.

(2) A Fresnel/Photovoltaic Concentrator Application Experiment for the Dallas-Fort Worth Airport, by E-Systems, Inc.; first generation LFF system operational in July 1982.

(3) Photovoltaic Energy System for a Hawaiian hospital, by the Acurex Corporation; an LPT system operational in the fall of 1981.

In addition, DOE has funded through a grant program the Mississippi County Community College Concentrating Photovoltaic Array Project, by TEAM, Inc., Solar Kinetics, Inc., and The BDM Corporation. This LPT system was operational in the fall of 1981. Passively cooled point focus Fresnels have also been installed in large-scale experimental projects (primarily by the Martin-Marietta Corporation), but to date PFFs with active cooling have only been built as prototypes.

The development of solar thermal systems also accelerated in the 1970's. Analysis methods were primarily based on the earlier works of Liu and Jordon (ref. II-5), Hottel and Whillier (ref. II-6), and Lof

and Duffie (ref. II-7). Detailed computer simulations of active collector systems were written by the staff at the University of Wisconsin (TRNSYS) (ref. II-8) and by Sandia National Laboratories (SOLTES) (ref. II-9). Other codes were written by various private companies, and less expensive design tools have also been developed. Many design and installation guides have been generated, but primarily for residential flat plate solar energy systems.

Commercial and industrial solar thermal energy systems have been installed in all regions of the country, with limited success (ref. II-10). Many installations have been fraught with design and installation problems, in addition to component reliability and operational difficulties. In view of these problems, the Solar Energy Research Institute has recently developed design guidelines for solar thermal IPH systems (ref. II-11).

The current literature specific to combined PV-T systems consists mainly of reports on the early phases of the DOE-funded experimental PV projects. The study herein was initiated to provide design information and specific design models for PV-T systems. The following sections describe the components of a PV-T system and the state of the art of PV-T systems design as it existed at the start of this study.

B. SUBSYSTEM SPECIFICATIONS

1. Collector Modules

a. Linear Parabolic Troughs

1) Concentrator Description

PV-T collectors of this type consist of a parabolic reflector with a receiver mounted at the focal line. Two LPT collector modules are considered in this study--the Acurex Model 3001 and the Solar Kinetics, Inc. Model T-700, shown in figure II-2. Both track the sun by rotating on a horizontal axis parallel to the focal line, which can be oriented in either a north-south or an east-west direction.

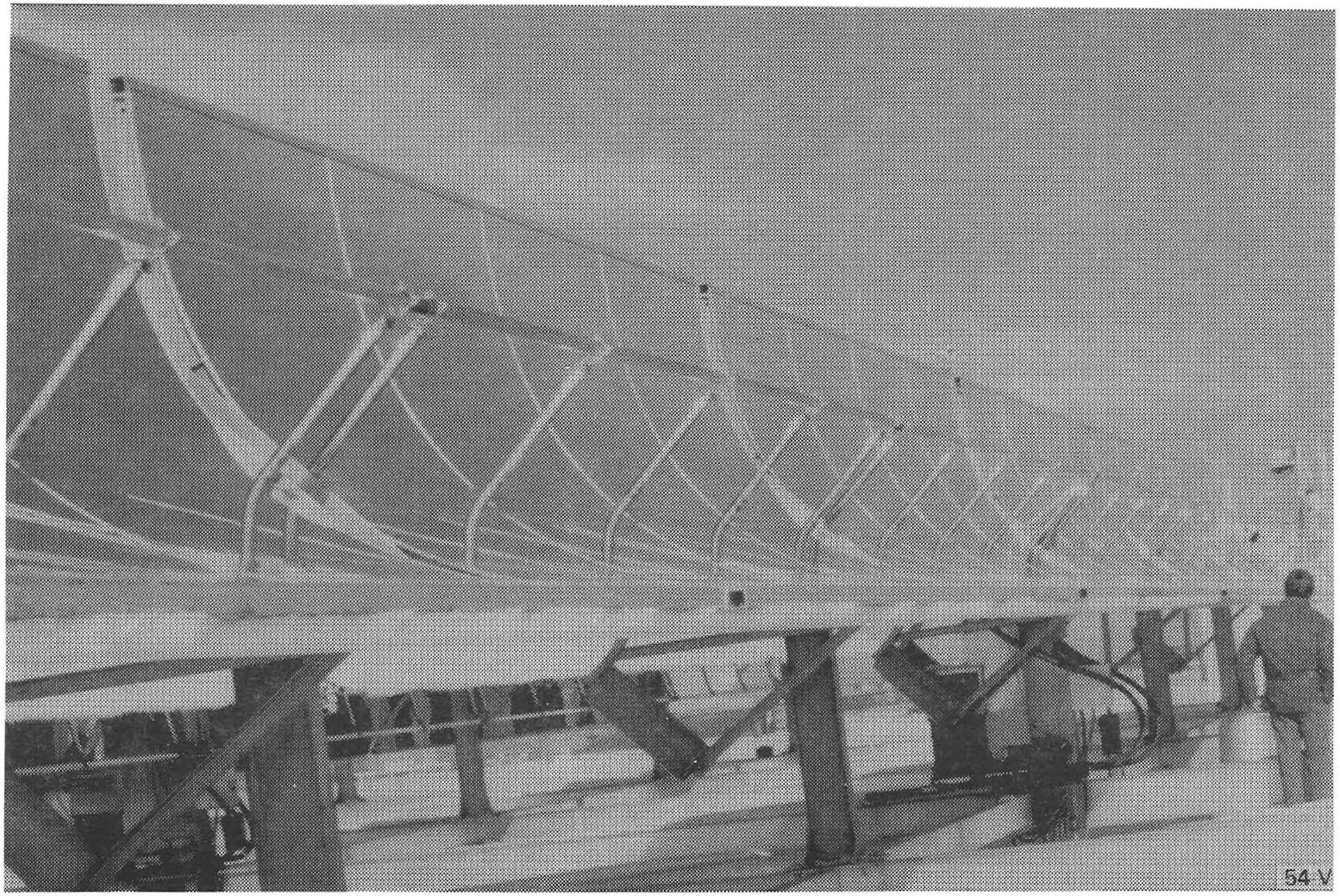

Figure II-2. SKI Concentrator with BDM Receiver

The Acurex trough structure consists of reinforced sheet metal, and the SKI structure is an aluminum monocoque. Both use an aluminized acrylic reflector bonded to the structure. The Acurex 3001 reflector is 3.05 m (10 ft) long by 1.8 m (6 ft) wide, providing an aperture area of 5.6 m^2 (60 ft^2). The SKI T-700 is 2.1 m (7 ft) by 6.1 m (20 ft)--a 13 m^2 (140 ft^2) module. Both companies are actively pursuing further collector development. Acurex is enlarging their module to 1.8 m (6 ft) by 6.1 m (20 ft), and SKI is developing an 2.4 m (8 ft) wide collector. They are also experimenting with prototypes that have glass reflectors. None of these more recent designs, however, have been operated in a large-scale system with a PV-T receiver.

2) Receiver Description

Typical receiver designs for collectors of this type consist of a V-shaped aluminum extrusion with PV cell modules bonded to each face of the V. A dielectric film (such as Kapton tape) is placed between the cells and the extrusion to provide electrical isolation between the cells and aluminum cooling channel. Heat transfer from the cells to the coolant channel is enhanced by the use of a conductive adhesive and thermal grease. The coolant channel in the Acurex receiver, shown in figure II-1, has a cross-sectional area of approximately 4.5 cm^2 (0.7 in^2).

Two different receivers have been used with the Solar Kinetics collector; SKI developed their own extrusion, and one was designed by The BDM Corporation. The SKI receiver is a one-piece unit, while the BDM design, shown in figure II-1, consists of two extrusions clamped together. The latter design reflects a concern for quick and convenient replacement of the PV cells without the need to open the coolant line. As confidence in cell and system reliability grows, this concern may be less important. The cross-sectional area of the coolant channel in the BDM design is approximately 4 cm^2 (0.63 in^2). (A thorough review of the state of the art in PV receiver design and cell bonding techniques is given in SAND 83-7036, reference II-12.)

The piping connections between collectors in an array are made with short sections of flexible hose covered with an ultra-violet-resistant material. When the fluid line leaves a collector string, it does so via a hose designed to flex without interfering with the rotation of the trough. These flexible hoses may be insulated if necessary.

Most PV-T systems use water as the basic cooling fluid with ethylene glycol added to prevent freezing. A 60 percent solution may be required in very cold climates, while in milder locations a 40 percent glycol mixture may be adequate. A 50 percent solution has a viscosity of 2.27×10^{-3} Pa·s (5.5 lb/hr ft), a thermal conductivity of 0.424 W/m^{o}K (0.245 Btu/hr ft^{o}F), and a specific heat of 3391 J/Kg^{o}K (0.81 Btu/lb ^{o}F) at 38°C (100°F). A corrosion inhibitor (such as NALCO 2755) is also added to the coolant.

3) PV Cell Modules

The PV cell modules are glass-covered and typically 1.2 to 1.5 m (4 to 5-ft) long with 2.54 cm (1-in) wide cells. The modules include bypass circuits with diode protection to reduce the effects of partial shading, which results from both the gaps between modules and shadows from receiver supports, as well as external objects. An extensive explanation of these design considerations is given in reference II-3. Solarex Corporation and Applied Solar Energy Corporation (ASEC) are two major suppliers of PV cell modules.

b. Line Focus Fresnel

1) Concentrator Description

E-Systems, Inc. has developed a line focus collector module with a curved plastic fresnel lens, which is illustrated in figure II-3. The second generation array design shown in figure II-4 consists of four modules each 0.915 m (3 ft) wide by 3.28 m (10 ft) long, providing an aperture area of 11.2 m^2 (120 ft^2) per frame. The long axis of each module is oriented north-south, and the tracking system follows the sun about two axes by rotating each module and varying the tilt of the entire array as needed. The PV cells are approximately 2.29 cm (0.9 in) wide, resulting in a geometric concentration of 40.

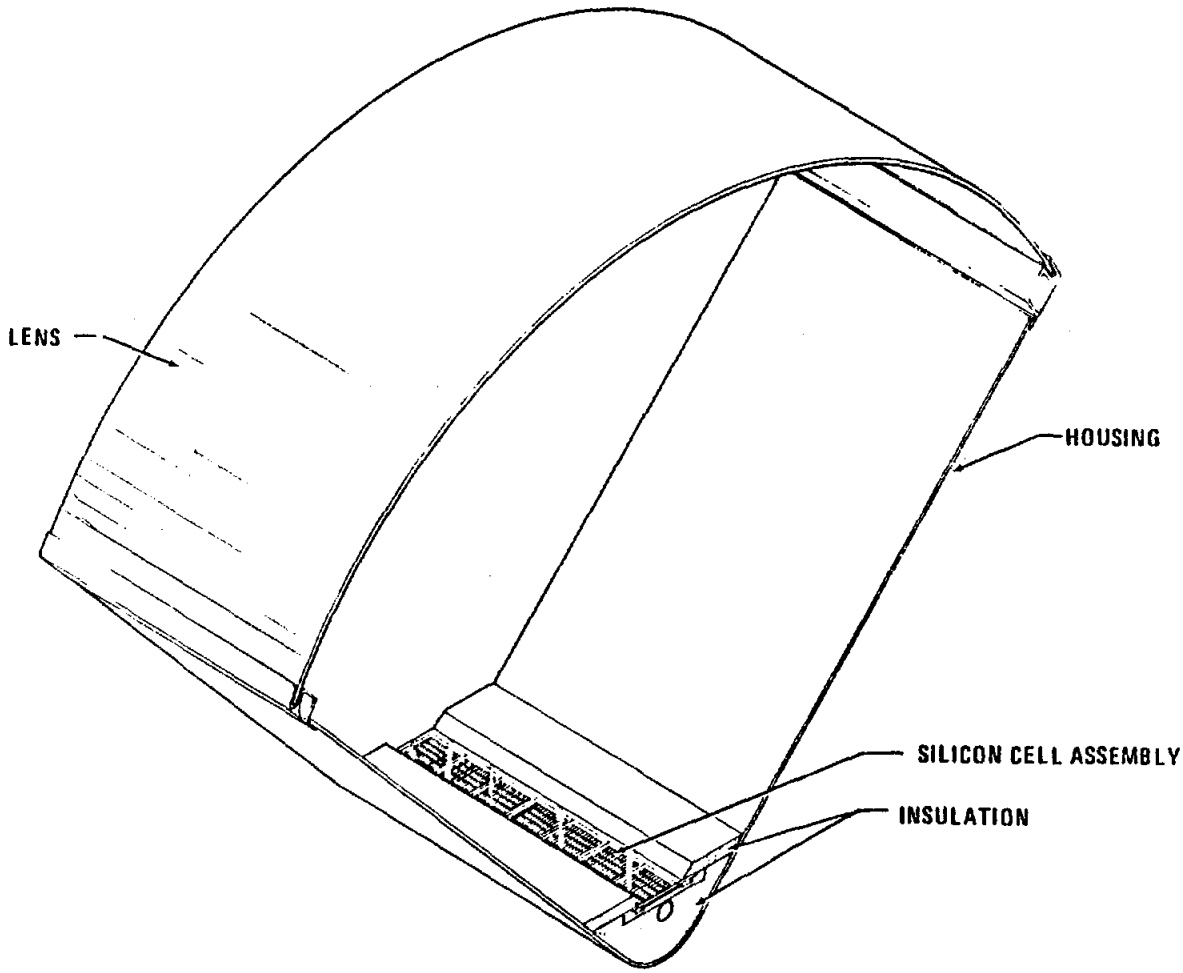

BDM/A-82-458-TR-R1

Figure II-3. Cross Section of E-Systems Line Focus Fresnel Lens Collector

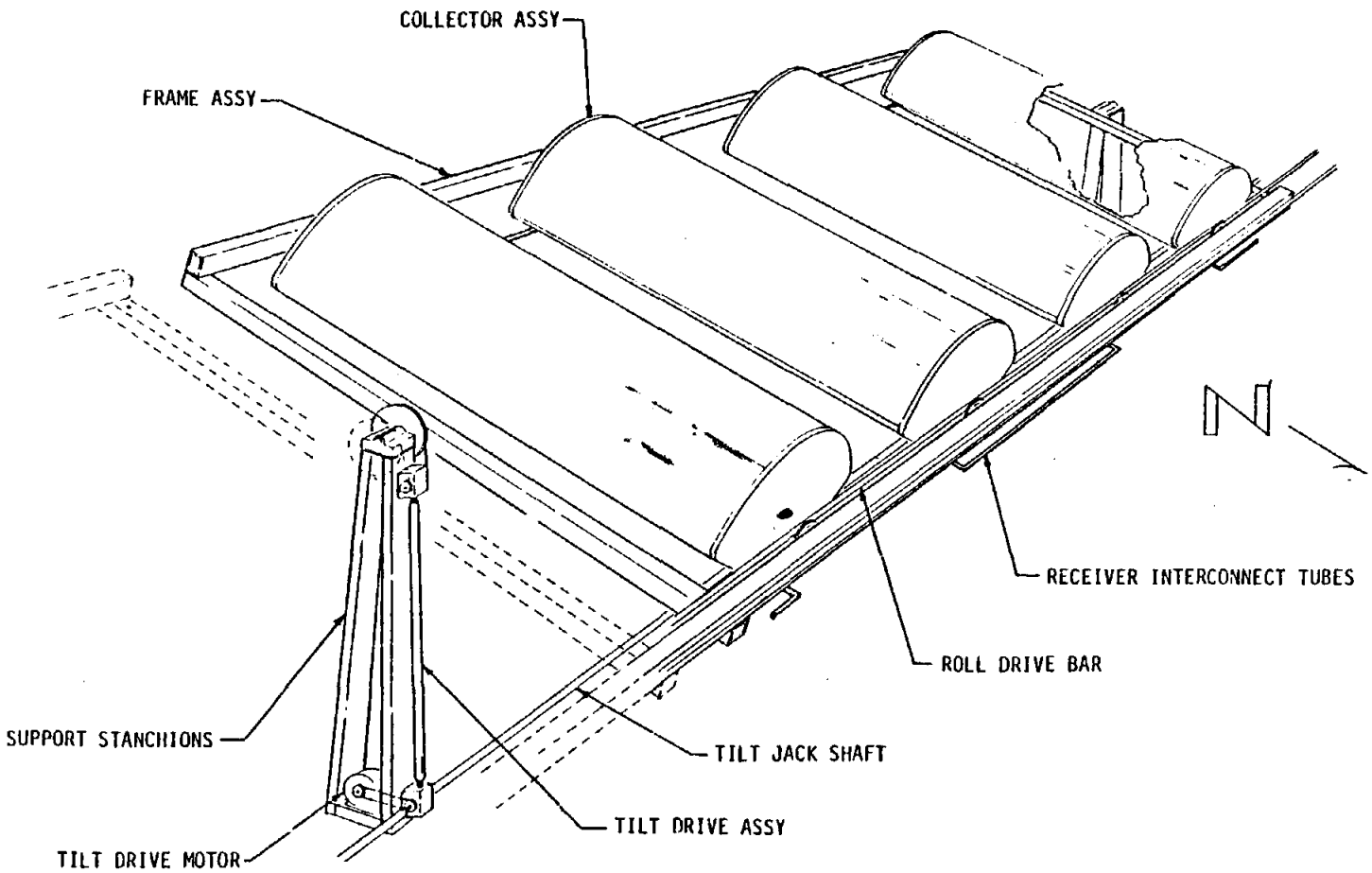

BDM/A-82-458-TR-R1

Figure II-4. Second Generation Array

2) Receiver Description

The E-Systems receiver consists of a one-piece aluminum extrusion, which consists of a plate and coolant tube. A thermally conducting adhesive (GE RTV 615 filled with AL_2O_3 particles) provides the dielectric standoff and heat conduction path to the fluid. The coolant tube has a diameter of 1.9 cm (0.75 in). The back of the receiver is insulated with approximately 2.54 cm (1 in) of polyurethane. The piping connections between modules are made with an insulated flexible hose. Ethylene glycol is used as the coolant fluid at sites where freezing temperatures are expected.

3) PV Cells

The PV cells used by E-Systems are similar to those used in the linear parabolic concentrators. The 2.29 cm by 2.29 cm cells are bonded to a 0.3175 cm (1/8-in) thick Sunadex glass superstrate 0.5 m long. Six of these cell modules are bonded to the receiver with the conducting adhesive.

c. Point Focus Fresnel

1) Concentrator Description

Point focus Fresnel lenses for PV collectors are made by molding concentric prismatic rings in a plastic sheet. The lens made by the Martin-Marietta Corporation (MMC) is 0.093 m^2 (1 ft^2), and circular cells 0.002129 m^2 (3.3 in^2) in area are located at the focal point about 0.457 m (1.5 ft) below the lens. The resulting geometric concentration ratio is 44. In the MMC PV-T prototype, 272 of these modules were mounted in an array as shown in figure II-5. The array tilts about the center torque tube and turns about the center pedestal for two-axis tracking.

2) Receiver Description

The MMC receiver extrusion consists of a 2.74-m (9-ft) aluminum plate with an integral coolant channel. The cross section of the extrusion is shown with back insulation in figure II-6. The coolant channel is 5.4 cm by 1.4 cm (2.125 in by 0.563 in). The circular cells are soldered to an alumina substrate, which serves as the

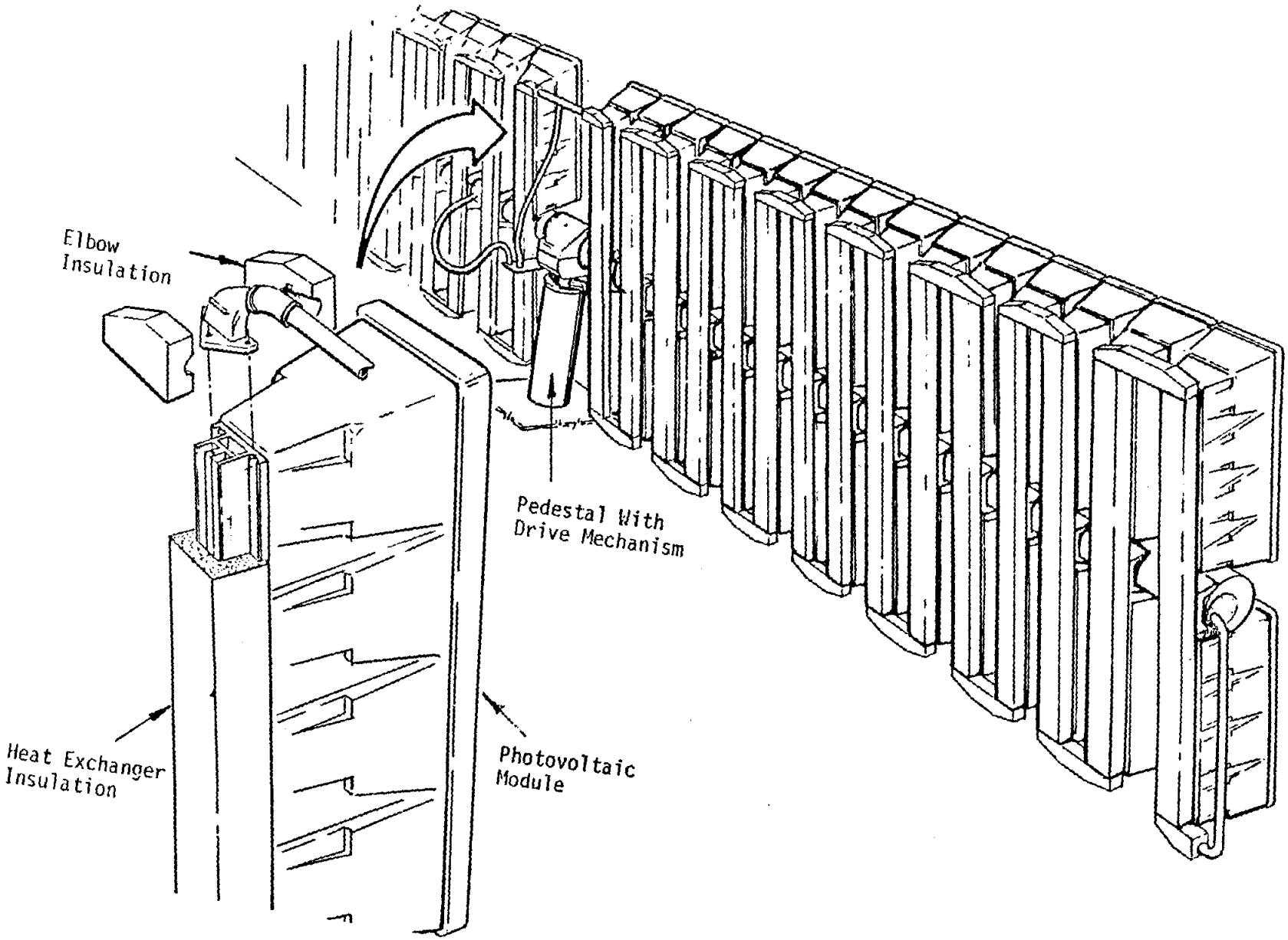

Figure II-5. MMC PV-T Array

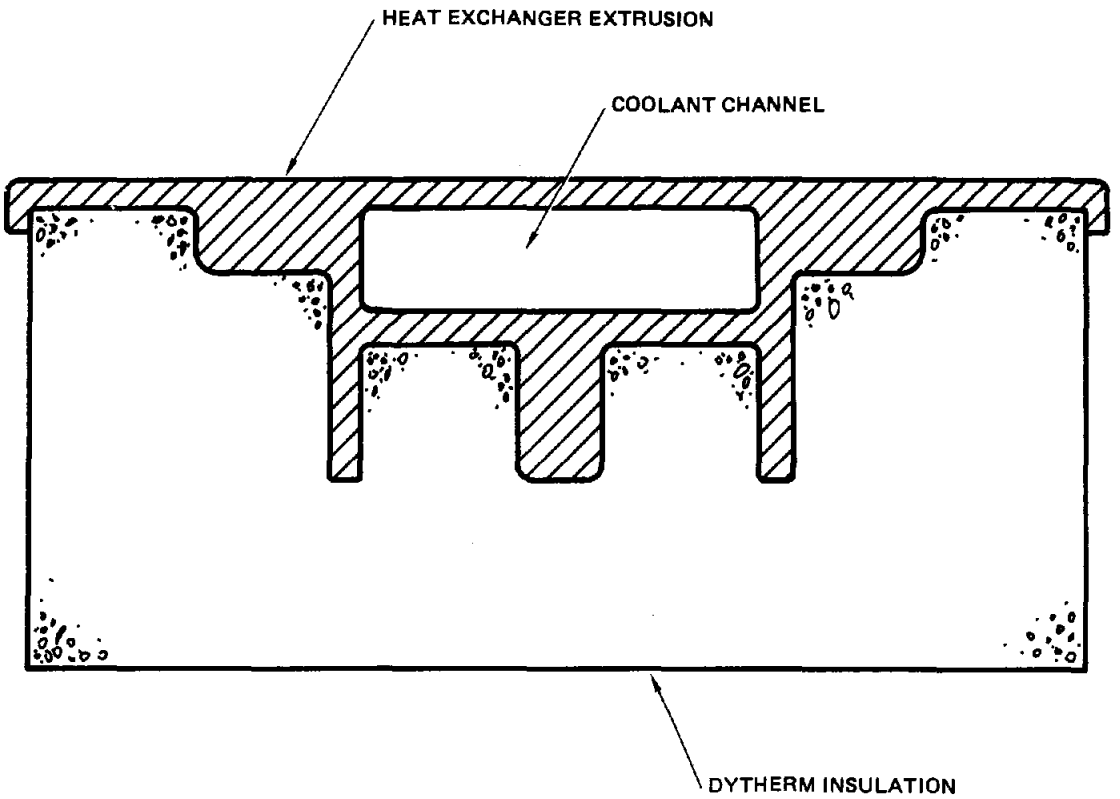

BDM/A-82-458-TR-R1

Figure II-6. MMC Insulated PV-T Receiver Extrusion

dielectric between the cells and the aluminum extrusion. This assembly is mechanically attached on 0.305-m (1-ft) centers with thermal grease between the alumina wafer and aluminum heat sink to improve the heat conduction to the extrusion.

d. Temperature Limitations

Concentrating collectors that provide only heat can be used to produce temperatures of 280°C (536°F) and higher to meet steam loads. PV-T concentrators, however, are presently limited to far lower temperatures for two reasons: (1) the electrical efficiency of the PV cell decreases as the operating temperature increases; and (2) the materials used with the PV modules degrade at high temperatures. The BDM/SKI receiver is designed to operate at a cell temperature below 74°C (165°F); near that temperature the collector is de-focused to prevent overheating. The cell encapsulant, polyvinyl butyral (PVB), will bubble and discolor under concentrated ultraviolet radiation at 90°C (194°F). Thus, assuming typical temperature gradients of 20°C in the receiver, the fluid outlet temperature must be limited to about 55°C (130°F). E-Systems uses an RTV encapsulant that can tolerate approximately 205°C (400°F); however, the rated limit for the E-Systems receiver insulation is 177°C (350°F). The melting point of the solder that is commonly used in PV-T receivers is 185°C (365°F). Various materials are available for wiring insulation, including PVC, which is limited to 105°C (221°F), and Teflon, which can be used up to 200°C (392°F). E-Systems recommends a maximum cell operating temperature of 130°C (265°F) for their collector due to the degradation in electrical performance at higher temperatures. This would produce a fluid outlet temperature of about 110°C (230°F). The ethylene glycol coolant solution must be maintained below its boiling point during operation so hot spots do not develop. At atmospheric pressure, a 50 percent solution will boil at about 108°C (225°F).

If higher fluid temperatures were desired, more expensive materials including advanced PV cells with higher efficiencies at high temperatures would be required.

e. Structural Integrity and Base Support

Structures currently used to support linear parabolic troughs, linear focus Fresnel, and the point focus Fresnel concentrators can be noted in the previous figures II-1, II-4, and II-5. The central purpose of all of these systems is to furnish economical, repetitive structural and foundation elements with sufficient strength, stiffness, and reliability to sustain the dominating lateral wind-induced drag loads which are accompanied by moments, and by upward or downward acting vertical loads. These loads are transferred by pylons into foundation elements in soil or into the roof structure of a building. Although wind loads are the dominant factor in the structural design, gravity (dead loads), earthquake, snow, rain, hail, and ice loads must also be considered.

Concentrating collectors are typically designed to withstand only moderate winds in an operating position. In high winds, the control systems are designed to move the collectors to a stowed (low profile) position. Table II-1 gives survival wind speeds as a function of position.

TABLE II-1. SURVIVAL WIND SPEEDS, m/sec (mph)

MODULE	FOCUSSED	MOVING TO STOW	STOWED
LPT (Average Values)	15.6 (35)	22.4 (50)	40.2 (90)
LFF (E-Systems)	13.4 (30)	22.4 (50)	40.2 (90)
PFF (Martin Marietta)	11.6-13.4 (26-30)	22.4 (50)	44.7 (100)

The bearings, pylons, and roof mounts or foundations in soil are required to safely support the optical assemblies in these winds with appropriate allowance for dynamic effects, wind gusts, and the other loadings previously referred to.

The determination of wind forces on a PV-T collector depends on the lift, drag, and moment coefficients, which are best determined from wind tunnel data. Several wind tunnel tests have been

performed on LPT and PFF systems. A number of these have been conducted by the staff at Colorado State University (CSU) using a boundary layer wind tunnel (refs. II-13, II-14, II-15). For the LPT systems, values of the coefficients depend on the presence of a wind fence or berm, the collector aspect ratio, and other factors. Randall, of SNLA, has summarized the results of available wind tunnel tests on LPTs (refs. II-16, II-16, II-17). The coefficients for the E-Systems LFF array have only been estimated because wind tunnel tests have yet to be accomplished.

If the system is roof-mounted, a special roof member design is required to resist the solar array forces. Each roof design or retrofit is usually a unique project. Ground-mounted systems require an adequate foundation system, several of which have been investigated by Sandia National Laboratories in Albuquerque (refs. II-18 through II-21). Dunder, at SNLA in Livermore, has reported on the use of a computer code for pier design (refs. II-22, II-23). Reinforced concrete piers provide an effective, economical foundation element where appropriate soil conditions are found. (Sample pier designs are presented in a later section of this report.) Piers are inappropriate under some circumstances, such as where boulders or rocks are encountered, or where expansive clays are encountered. Installation of ground-mounted systems requires a soil survey and consultation with a geotechnical engineer to ensure that an economical and structurally adequate foundation element is provided.

f. Tracking Methods

Various collector positioning systems have been developed for maintaining concentrating collectors in focus. Most manufacturers of PV-T collectors currently use a photocell (light sensing) system of some type to control a mechanical drive system. The BDM/SKI light sensor consists of two photocells, one on each side of a shading bar. If one cell receives more light than the other, the drive mechanism is actuated to move the collector until the intensities are equalized. Wake-up and shut-down are controlled by a light sensor that activates the shadow bar unit. After initial installation, the system is completely automatic.

Manual override is provided from a control box located on the collector pylon. The primary control switches are located at a central station.

The same tracking approach is used for the Martin-Marietta array, which uses a sensor consisting of photocells arranged on a rectangular pyramid. The E-Systems design uses two shadow-band sensors, one for each tracking axis.

Although problems were experienced with early shadow-band tracking systems, particularly with tracking of reflections and with sensitivity adjustments, the systems have been improved and are now generally satisfactory. Recent designs track the sun only through a 150° dome to eliminate tracking problems early and late in the day. More reliable systems, such as coded drive shafts with programmed positioning, are significantly more costly.

In regard to the drive systems, mechanical drives have proved to be less costly and more reliable than hydraulic systems. They do, however, require a back-up power supply so the collectors can be stowed in the event of a power failure (hydraulic systems automatically defocus the collectors when power is lost). LPT systems typically incorporate the drive mechanism into the support pylons and turn the collectors through a torque tube. The MMC mechanical drive is housed in the central pedestal shown in figure II-5, while the E-Systems collector utilizes a system with a long drive shaft as illustrated in figure II-4. In the E-Systems design a 373-watt (1/2-hp) motor is used to position up to 72 modules in the declination mode, and a 12.4-watt (1/60-hp) motor turns them in the longitudinal mode. Duty cycles for these motors are typically only 10 percent.

g. SOLCEL Performance Simulation

In most cases, the electrical and thermal performance of the various PV-T systems was not available. An exception to this is the E-Systems LFF, which has been tested extensively by the manufacturer, who has reported electrical and thermal efficiencies in terms of fluid and ambient temperature and insolation. The LPT systems have been tested thoroughly for electrical efficiencies, which are reported in terms of

cell temperature. The actively cooled PFF is currently undergoing testing. Since thermal performance was not available for the LPT and PFF systems, each of the three PV-T collector types was simulated using SOLCEL-II (ref. II-2). Although test data were available for the LFF system, its performance was also simulated as a check on our modeling technique. The SOLCEL-II results and LFF test data are consistent, providing confidence in the modeling methodology.

1) Input Values

The existing SOLCEL-II model for a linear concentrator was modified for the E-Systems case to include the thermal effects of the enclosure in the same manner that they are modeled in the point focus subroutine. The model for the PFF was extended to include: (1) an additional thermal node to model the heat transfer to and from the connecting channel between the cells; and (2) realistic insulation on the back of the flow channel (previously the back was assumed to be perfectly insulated).

The SOLCEL-II input values for collector characteristics are shown in table II-2. These values were selected based on PRDA-35 Phase I reports, related BDM studies (ref. II-12), and interviews with manufacturer's representatives.

Instantaneous efficiencies were determined for the following conditions:

Flow rate: 0.311 and 0.933 kg/s (5 and 15 gpm)
Incident radiation (I_{DN}): 900 and 1000 W/m^2
Incident angle modifier (R_b): 1.0
Inlet temperature (TFI): 30, 55, and 80°C
Ambient temperature (TA): 0, 15, and 30°C
Wind speed (VW): 2 and 8 m/s
Coolant fluid: water (100 percent)

2) Instantaneous Efficiency Results

Since a systems designer is typically interested in performance as a function of fluid temperature and ambient conditions, the SOLCEL-II results for the thermal performance were plotted using the following linear model:

Table II-2. SOLCEL II COLLECTOR INPUT VALUES

VARIABLE DESCRIPTION	VARIABLE NAME	UNITS	VALUES LPT	LFF	PFF
CELL EFFICIENCY DEGRADATION FACTOR: $(\eta @ T)=(\eta @ 28^oC)(1 - COEF(T - 28^oC))$	COEF	$1/^oC$	0.004	0.004	0.0046
AVERAGE CELL EFFICIENCY AT 28^oC AND 1000 W/m^2	EFFC	NONE	0.165	0.180	0.166
CELL VISIBLE ENERGY ABSORPTANCE	ABSCV	NONE	0.80	0.80	0.80
LENS OR APERTURE AREA FOR EACH CELL IN POINT FOCUS ARRAY	ARLENS	m^2	N/A	N/A	0.0929
HEATSINK BASE PLATE AREA FOR EACH CELL IN POINT-FOCUS ARRAY	ARSINK	m2	N/A	N/A	0.0232
LENGTH OF THE FLOW CHANNEL AND COLLECTOR APERTURE	CL	m	6.10	12.2	41.45
GEOMETRIC CONCENTRATION RATIO	CONRA	NONE	45	40	44
FLOW CHANNEL WETTED PERIMETER	CTP	m	0.071	0.060	0.137
WIDTH OF THE COLLECTOR APERTURE	CW	m	2.13	0.914	0.305
WIDTH OF ONE LINE FOCUS MODULE	CWTH	m	2.13	0.914	N/A
INFRARED EMITTANCE OF THE CELL ENCAPSULANT	EMTCI	NONE	0.81	0.81	0.81
INFRARED EMMITTANCE OF THE THERMAL INSULATION SURFACE (OR COVER)	EMTII	NONE	0.80	0.80	0.80

Table II-2. SOLCEL II COLLECTOR INPUT VALUES (Continued)

VARIABLE DESCRIPTION	VARIABLE NAME	UNITS	VALUES		
			LPT	LFF	PFF
FLOW CHANNEL CROSS-SECTIONAL AREA	FA	m^2	4.1×10^{-4}	2.85×10^{-4}	7.71×10^{-4}
THERMAL INSULATION CONDUCTIVITY/ THICKNESS	HINS	W/m^2C	N/A	1.0	1.5
CELL BOND CONDUCTIVITY/THICKNESS	HINCEL	W/m^2C	1030	7972	4834
OVERALL OPTICAL EFFICIENCY (FOR ELECTRICAL PURPOSES)	OPEFF	NONE	0.73	0.83	0.80
CELL PACKING FACTOR	PACFAC	NONE	0.94	0.97	N/A

$$\eta = \eta_{int} - \beta \left[\frac{TF - TA}{I_{DN} R_b} \right] \qquad \text{(Eq. II-1)}$$

In SOLCEL-II the assumption is made that the fluid temperature varies linearly over the length of the module, so the mean fluid temperature is

$$TF = \frac{TFO + TFI}{2} \qquad \text{(Eq. II-2)}$$

where TFO is the outlet temperature. Both the efficiency intercept, η_{int}, and the slope, β, are functions of the collector's characteristics. The following relationships have been defined for thermal systems (refs. II-24, II-25):

The intercept is:

$$\eta_{int} = F_m \eta_o \qquad \text{(Eq. II-3)}$$

and the slope is:

$$\beta = F_m U_L \qquad \text{(Eq. II-4)}$$

where F_m is the heat transfer factor based on the mean temperature, η_o is the optical efficiency, and U_L is the overall energy loss coefficient. In the case of PV-T systems, both F_m and U_L include the energy "lost" to the cell in the direct conversion to electricity. The optical efficiency was an input to the SOLCEL-II model:

$$\eta_o = ABSCV * OPEFF \qquad \text{(Eq. II-5)}$$

The SOLCEL-II thermal performance results are plotted in figure II-7, and the values of the efficiency parameters obtained from these calculations are shown in table II-3.

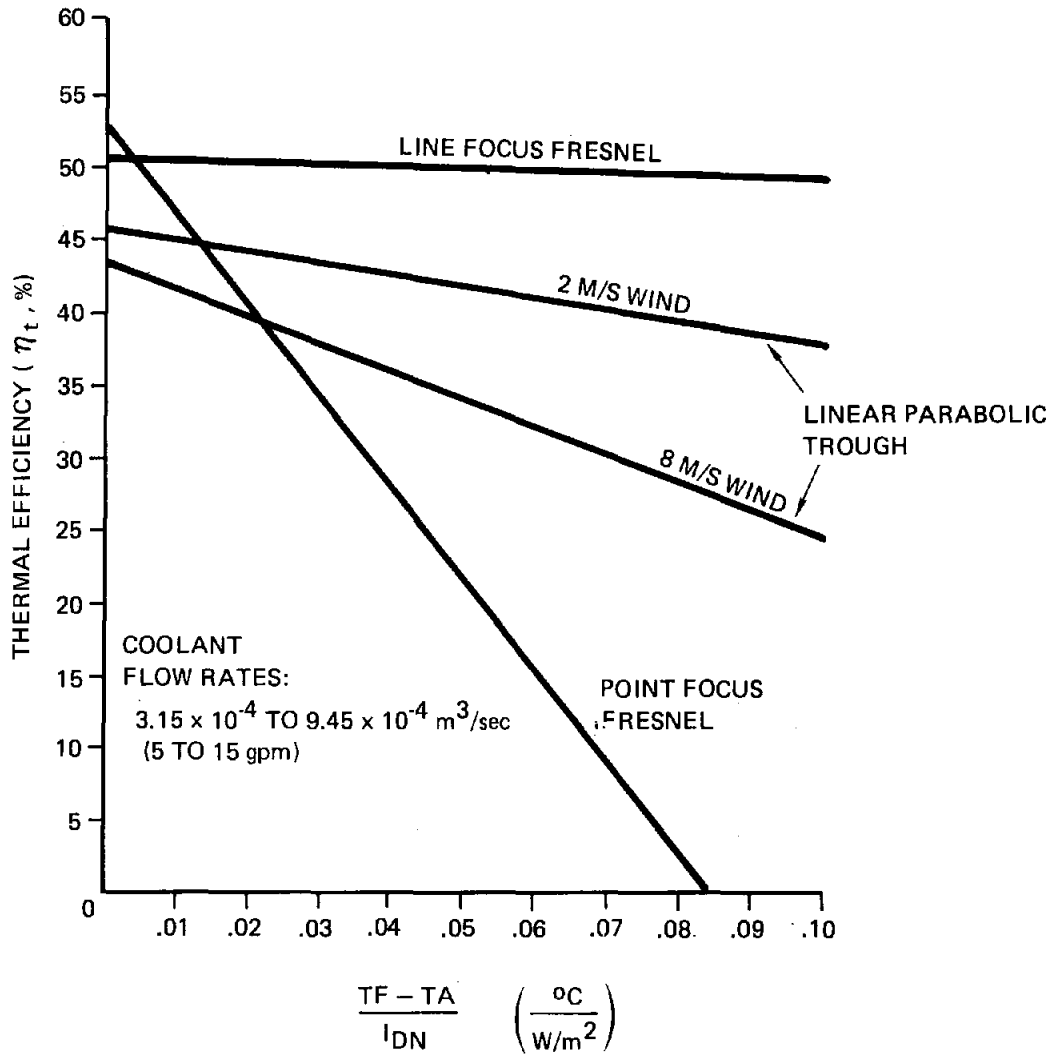

BDM/A-82-458-TR-R1

Figure II-7. Results of SOLCEL Thermal Performance Calculations for Concentrating PV-T Systems

TABLE II-3. EFFICIENCY PARAMETERS

COLLECTOR TYPE	CONDITIONS	η_{int}	η_o*	F_m	β	U_L
LFF	(ALL CASES)	0.51	0.66	0.77	0.25	0.32
LPT	(2 m/s WIND)	0.46	0.58	0.79	0.85	1.1
	(8 m/s WIND)	0.44	0.58	0.76	1.9	2.5
PFF	(TA = 15°C)	0.53	0.64	0.83	6.3	7.5

*SOLCEL-II INPUT

The significance of these parameters can be seen by performing a steady state thermal energy balance on the collector:

energy collected = energy absorbed - energy lost to ambient

$$\dot{q}_c = I\ \eta_o - U_L\ (T_S - T_a) \qquad \text{(Eq. II-6)}$$

where:

$\dot{q}_c$ = useful thermal energy absorbed per unit aperture area (W/m^2)
I = direct normal radiation on the collector plane (W/m^2)
η_o = optical efficiency of the collector
U_L = overall collector heat loss coefficient ($W/m^2\ {}^oC$)
T_S = average receiver tube surface temperature (^oC)
T_a = ambient temperature (^oC)

However, the surface temperature of the receiver section is usually not known. To express the energy collected in terms of the collector average fluid temperature, a collector heat removal efficiency factor, F_m, is introduced where:

$$F_m = \frac{\text{Energy Collected}}{\text{Energy collected if entire receiver were at fluid temperature}} \qquad \text{(Eq. II-7)}$$

Thus, the collector energy balance can be expressed as:

$$\dot{q}_c = F_m \left[I \ \eta_o - U_L \ (T_f - T_a) \right] \qquad \text{(Eq. II-8)}$$

where T_f is the average fluid temperature. The instantaneous thermal efficiency is given by:

$$\eta_{th} = \frac{\dot{q}_c}{I} = F_m \left[\eta_o - U_L \frac{T_f - T_a}{I} \right] \qquad \text{(Eq. II-9)}$$

where U_L is assumed constant.

As seen in table II-3, U_L depends on the environmental condition, such as wind velocity, for the LPT. This is to be expected since the receiver section is exposed to the wind. For the LFF, with an enclosed and insulated receiver, the heat loss coefficient is independent of environmental conditions. This is also evident for the PFF system.

The electrical efficiency results are presented versus TF and I_{DN} in figure II-8.

3) Annual Efficiencies

The annual performance of each collector type was simulated using TMY weather data for seven typical days in each of the four seasons in Albuquerque, New Mexico. The coolant fluid was water flowing at 0.622 kg/s (10 gpm) with a constant inlet temperature of 55°C (130°F). The LPT and LFF receivers were oriented in a north-south direction, and incident angle effects ($R_b < 1$) were included for the single-axis tracking LPT. The simulation was for only one module (or LFF array), so there were no row or module shading effects. The results are shown in table II-4.

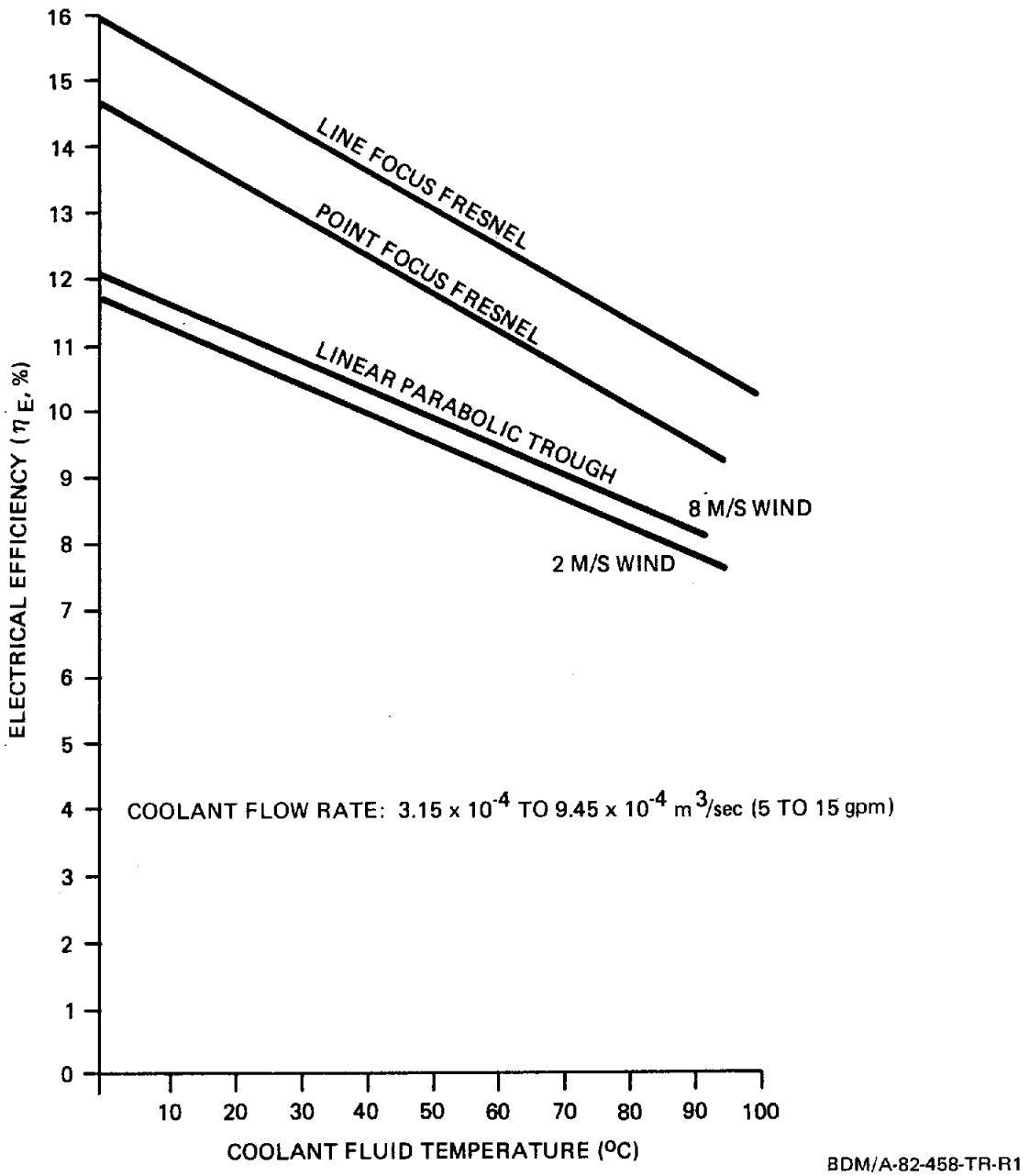

Figure II-8. Results of SOLCEL Electrical Performance Calculation for Concentrating PV-T Systems

TABLE II-4. ANNUAL EFFICIENCIES (%)*

	ELECTRICAL	THERMAL
LFF:	12.7	50
LPT:	8.5	29
PFF:	11.4	22

*Efficiencies for a single LPT collector, a PFF array, and a four-module LFF array

h. Collector Costs

A study of PV concentrator array costs was completed by the General Electric Space Division for SNLA in 1980 (ref. II-26). The study included actively cooled LPT, LFF, and PFF technologies and assumed manufacturing levels of 100,000 m^2 of aperture area per year (1.076×10^6 ft^2/yr). The components included the optical and receiver assemblies, and the tracking control and drive systems. The method of analysis used was a price factor approach based on surveys of existing cell price mark-up methodologies. Shipping and installation costs were based on array areas large enough to produce 400 kW (peak). The resulting capital costs are shown in table II-5. An economic analysis was also performed to obtain levelized annual costs, shown in table II-6. The assumptions in that analysis were as follows: 30-year evaluation period and system life, a fixed charge rate of 18 percent, a 6 percent inflation rate, and a 10 percent cost of capital.

Another cost study was performed by General Electric Advanced Energy Programs Department, in 1981-1982 (ref. II-27). In this study three 1980 vintage concentrator hardware designs were analyzed to determine their production and installation cost potential based on a 100,000 m^2/yr production rate. The three design studies were:

1. E-Systems' second generation linear Fresnel--actively cooled
2. Sandia's TR-80 point-focus Fresnel--passively cooled
3. Sandia's sheet metal parabolic trough--actively cooled.

Table II-5. CAPITAL COST SUMMARY IN $\$/m^2$ ($\$/FT^2$)*

COST	LPT		LFF		PFF	
DIRECT MATERIAL	113.6	(10.55)	123.2	(11.45)	126.1	(11.71)
APPLIED LABOR	8.1	(0.75)	12.3	(1.14)	14.7	(1.37)
SELL PRICE	192.8	(17.91)	209.1	(19.43)	222.9	(20.71)
SHIPPING	16.3	(1.51)	15.3	(1.42)	17.2	(1.60)
INSTALLATION	84.9	(7.89)	149.2	(13.86)	107.8	(10.01)
INTEREST DURING CONSTRUCTION (10%)	25.0	(2.32)	27.8	(2.58)	29.4	(2.73)
TOTAL COST	319.0	(29.64)	401.4	(37.29)	377.3	(35.05)

*ESTIMATED 1980 COSTS BASED ON 1979 ACTUAL COSTS.

Table II-6. LEVELIZED ANNUAL COSTS IN $\$/m^2$ ($\$/FT^2$)*

COST	LPT		LFF		PFF	
CAPITAL	30.50	(2.83)	34.30	(3.19)	36.10	(3.35)
OPERATION AND MAINTENANCE	3.30	(0.31)	3.30	(0.31)	3.30	(0.31)
COMPONENT REPLACEMENT**	3.10	(0.29)	-	-	-	-
TOTAL	36.90	(3.43)	37.60	(3.49)	39.40	(3.66)

*ESTIMATED 1980 COSTS BASED ON 1979 ACTUAL COSTS.
**REPLACE REFLECTIVE SURFACE EVERY 10 YEARS AT $\$35/m^2$ ($\$3.25/FT^2$)

The results of the GE study are projected collector costs based on prototype hardware which has been tested and analyzed for performance and reliability. These results differ significantly from the results of the previous study (ref. II-26) which looked at current costs of existing technologies. The results of the latter study indicated that the installed costs for the linear Fresnel and LPT ($367.9/m^2 and $357.6/m^2, respectively) could be much less than even a passively cooled PFF ($444/m^2).

i. Expected Life, Reliability, and Maintenance

PV-T collectors are typically designed for 20 to 40-year life expectancies, with less than 10 percent degradation. The demands placed on all system components are severe, and include exposure to harsh ultraviolet rays from the sun, wind and snow loads, rain and humidity, air-born dust and pollution, and temperature cycling. Potential problem areas include reflector or lens degradation, failure of the flexible hoses between modules, cell or cover glass breakage due to thermal stresses, optical degradation of encapsulant due to ultraviolet radiation and/or overheating, and open or short circuits in flexed wiring. Most of these problems have been solved by careful design, material selection, and cycle testing by manufacturers as well as independent contractors and agencies of the government. However, PV-T installations have not been in operation for more than a few months, so field experience is not extensive. Actual lifetimes will certainly depend on site conditions as well as the quality of maintenance services.

Typical maintenance requirements and costs are shown in table II-7 (ref. II-26). In addition to those requirements, the reflective materials currently used on LPTs must typically be replaced every 10 years, and perhaps even more frequently in severe environments.

2. Other System Components

In addition to the collectors, the following major components are required for a completely operational PV-T system:

(1) Power conversion system for AC electrical loads.

(2) Electrical circuits and wiring.

TABLE II-7. OPERATION AND MAINTENANCE COST SUMMARY

MAINTENANCE ITEM	FREQUENCY TIMES/YEAR	MAN HR/ OCCURRENCE	$/M^2-YEAR	RATIONALE
CLEAN REFLECTIVE SURFACE/ LENS	6	–	.24	SANDIA EST. $.04/m^2/CLEAN
CHECK GEAR BOX OIL LEVEL	2	7	.050	30 G.B. X 10 MIN/x 1.33*
CHECK AND REPAIR INSULA-TION	2	16	.115	ESTIMATE
REBUILD COOLANT PUMP	1	16	.058	ESTIMATE
PAINTING	.5	40	.072	SPOT FIX-UP-SAND & PAINT
LUBRICATE BEARING	2	27	.194	500 BEAR X 2.5 MIN/X 1.33
INSPECT & RETIGHTEN FOUNDATION BOLTS	1	52	.187	480 LOC X 5 MIN/X 1.33
INSPECT & REPAIR DRIVE LINKAGES	2	24	.173	ESTIMATE
CLEAN & INSPECT TRACKING MOTORS	1	20	.072	20 MOTORS X 1 HR (CHECK R)
CLEAN & INSPECT COOLANT PUMP MOTOR	1	8	.029	PULL COVER, CLEAN, ETC.
CLEAN & INSPECT SOLAR SENSORS	4	20	.288	30 SEN. X 30 MIN/X 1.33
INSPECT & REPAIR VALVES	2	13	.094	60 VAL. X 10 MIN/X 1.33
SITE STERILIZATION	1	–	0.327	$3.00/1000 FT^2 EST. X 10 ACRE
FENCE MAINTENANCE	1	32	.115	2700' OF FENCE
COOLANT WATER ANALYSIS	2	1	.004	1 SAMPLE, PACKED, & SHIPPED
TOTAL			2.018	

LOADED LABOR RATE = 30,000/YR = $14.40/HR.
APERTURE AREA = 4,000 M^2
*LABOR EFFICIENCY = 75%

BDM/A-82-458-TR-R1

(3) Heat exchanger to supply the thermal load.

(4) Back-up heat rejection system.

(5) Fluid flow system.

(6) Monitoring and control system.

Electrical storage, which is quite costly, is generally not considered because either the PV power is small compared to the daytime load or excess power can be sold to the local utility company. The need for thermal storage depends on the application and site climate.

Each of the subsystems mentioned above is discussed briefly in the following sections and in more detail in Volume III.

a. Power Conversion System

The most commonly specified configuration for a PV electrical system is a DC to AC inverter with a maximum power tracker supplying an AC load, using the utility as a backup. The power controls and conditioning hardware are designed for various operating modes, based on load and utility requirements. The modes of operation most often provided are start-up, steady-state operation with maximum power tracking, normal shutdown, emergency shutdown, and maintenance and diagnostic modes. The major design consideration is minimizing electrical losses. Typical conversion efficiencies range from 85 to 95 percent. Other hardware characteristics are as follows:

(1) Internal logic to synchronize the inverter phase to the utility phase.

(2) Internal logic for maximum power tracking and to regulate the inverter voltage to match the utility voltage at the load.

(3) Internal logic to start the inverter automatically or manually, sense inverter status, shutdown the inverter, and provide alarms for abnormal conditions.

(4) Motorized manual/automatic circuit breakers for protection, isolation, and diagnostics for maintenance, safety, and emergency power purposes.

(5) Step-up and step-down transformers.

(6) Filters for EMI and RF suppression.

(7) Control of waveform deviation, power factor, steady-state and transient peaks, and inverter cooling.

(8) Inverter redundancy.

(9) Manual over-ride of maximum power tracker.

Some of the major manufacturers of inverters include Windworks, Helionetics (DECC), Westinghouse, Abacus, Power Control Systems, and American Power Conversion. Inverter costs are approximately $500/kW (ref. II-28). Moreover, inverters as small as 65 kW can be very large and heavy, which is an important consideration in the design of a control center.

b. Electrical Circuits and Wiring

A PV cell module resembles a battery in that the voltages add when the modules are placed in series, and the DC currents add when they are connected in parallel. The number of modules placed in series (typically using #12 wire) depends on the collector field layout and the desired output voltage and current. An effort is made to keep the current low to reduce power losses, and the voltage must match the inverter range, which depends on the size of the inverter. Typically, the wire size is increased (e.g., #8) at the end of a series string, and the individual lines are run to a junction box at the inverter. An intermediate junction box is often included at the edge of the field to facilitate checkout and wire handling.

Electrical wiring and connectors exposed to sunlight must be insulated with an ultraviolet-resistant material (such as Teflon), or covered with a metal sheathing, or ultraviolet-resistant plastic (such as polyolefin shrink tubing). Quick-connectors (such as A-mode by AMP) between cell modules facilitate installation and removal. Each series string is protected against lightning by a spark gap and varistor circuit, and against static electricity buildup by a bleed resistor. Each line also contains a safety fuse and diode to prevent reverse current through the modules. Switches are included on both sides of this safety package, since both sides can be electrically hot.

On the AC side of the inverter, several switches are conveniently located outside the building, at the inverter, and at the utility junction box inside the building for safety reasons. If sell-back to the utility is not allowed, a reverse power sensor and breaker is used to prevent feed into the utility lines. All circuitry is designed to meet local electrical codes.

c. Heat Exchangers

The transfer of heat from the collector fluid (usually ethylene glycol and water) to the load is accomplished by a standard industrial heat exchanger. If the demand is for hot air, then a liquid-to-air heat exchanger is used. For liquid-to-liquid heat transfer, several units are available, including the shell-and-tube type, plate-and-frame, and the spiral-heat exchangers. If the energy system includes a thermal storage tank, then a coil-in-tank or tank-in-tank heat exchanger may be used.

The selection of a heat exchanger depends on the overall system configuration and the temperatures and flow rates involved. In some applications, particularly food processing, a double wall (or extra-thick wall, depending on local code) must separate the fluids to ensure that mixing does not occur, and there are several designs that meet this requirement. Manufacturers usually provide the information required for proper sizing.

A list of major manufacturers of heat exchangers includes Patterson-Kelley, Frick, Ace Bueller, Alfa-Laval, Tranter, and American Heat Reclaiming. Costs for shell-and-tube type heat exchangers generally range from \$97 to \$161 per square meter of surface area (\$9 to \$15/ft^2) for large units (40 to 100 m^2) (ref. II-29). Compact heat exchangers run higher, but the reduced size and higher heat transfer coefficients make them attractive (ref. II-30).

d. Fluid Flow System

The fluid flow system consists of the following components:

(1) Pumps: Centrifugal type, constant or variable flow, with seals appropriate for the working fluid; insulated.

(2) Piping: Carbon steel or copper which may be less expensive, depending on the particular installation.

(3) Automatic antifreeze makeup system: Monitors concentration and adds antifreeze as needed.

(4) Expansion tank: Takes up volume increase due to temperature rise.

(5) Fluid cooler: Dry or wet heat rejection unit to ensure PV cell cooling in absence of thermal load.

(6) Automatic control valves: These direct flow through different loops depending on operating modes. Three-way valves are generally avoided due to inadequate close-off.

(7) Balancing and service valves: Manual valves (constant flow mode only) used to achieve balanced flow and uniform output temperatures in all collector delta-T strings, as well as for isolation for maintenance purposes.

(8) Pressure relief valves: Open automatically for safety purposes at predetermined pressure limits.

(9) Control logic and actuators: Differential thermostats and small computers to control operating modes.

(10) Pipe strainers: Filter out fine particles to protect valve seats and pump seals.

Another important component is pipe insulation. The selection of insulation materials is based on cost, thermal resistance value, and resistance to moisture and weathering. There are a variety of compositions, including closed-cell types that will not absorb moisture from leaking pipes or rain, which can severely degrade the performance of loose-fill types such as fiberglass. Metal insulation jackets are generally used to prolong the life of the installation, particularly to protect against ultraviolet degradation and moisture.

Determining the optimum insulation thickness for a given pipe size involves finding the minimum value of the sum of the cost of

the insulation, and the value of the energy lost through the insulation. Heat loss coefficients for use in that analysis are provided in references II-25 and II-31. Algorithms for calculating the economic thickness of insulation are available from several sources, including those given in reference II-31, and from the Thermal Insulation Manufacturers Association (TIMA) in Mt. Kisco, New York, which offers an analysis on magnetic tape for computer execution.

The importance of insulating pumps and valves--significant sources of heat loss--has been investigated by SNLA (ref. II-32).

e. Monitoring and Control System

In a concentrating PV-T collector, adequate coolant flow must be maintained during operation to prevent irreversible damage to the costly PV cell modules. A major portion of the monitoring and control system is dedicated to this responsibility (in addition to serving other functions). Usually, all of the following sensors are employed to alert the control center to a condition requiring immediate defocusing of the collectors involved:

(1) A pressure transducer in the main line, and flow switches in each delta-T string (collectors thermally in series) and in the main line.

(2) Fluid temperature sensors at the outlet of each delta-T string.

(3) Temperature sensors imbedded in the receiver heat sinks at the outlet of each delta-T string to directly monitor sudden increases in cell temperature.

The thermal performance of each delta-T string is measured, based on flow meter and inlet and outlet fluid temperature readings. The thermal gain for the entire field is measured via a main line flow meter and temperature sensors on each side of the heat exchanger.

The electrical performance of each series string, as well as the entire field, is measured by sensing DC currents and voltages. The instantaneous AC current and voltage from the inverter is monitored for each phase, and the total power output is monitored as the ultimate measure of PV system performance.

PV-T systems to date have been experimental installations, and therefore, have included extensive monitoring capabilities that would not be required in a commercial installation. For example, a weather station is generally installed at the site to advise the tracking systems of inclement weather, and to provide solar intensity readings for efficiency calculations. The tracking status of each individual collector is usually monitored at the central station, and the status is often recorded for diagnostic purposes. Another useful tool for monitoring the entire field is a closed circuit television camera with zoom capability.

Data recording and compilation varies in sophistication. Experimental installations have generally had extensive computerized data reduction capability, although the essential control, diagnostic, and performance monitoring functions can be accomplished by a small computer or with relay logic. The primary design criteria are: (1) instantaneous availability of diagnostic data, (2) near-instantaneous availability of performance data, and (3) a convenient form for data storage. Another valuable aid to system operation (as well as public relations) is a well-designed display panel showing the status of the system.

All instrumentation cables are isolated from power lines and shielded to eliminate interference, and all cable runs are lightning protected.

f. Thermal Energy Storage

The most common form of thermal energy storage for water-based solar collector systems is a steel tank. Other vessels can be used for low pressure applications, including fiberglass-reinforced plastic and concrete, and wood structures with liners. The collector heat transfer fluid can be used as the storage medium, providing its cost is not too high and the storage volume is not too large. The alternative is to use the water in the load fluid loop as the storage media. Other media can be used, including phase-change materials.

The possible system types include stratified tanks, multi-tank systems, variable volume systems, and multi-media systems. Modes of

operation, piping configurations, and sizing depend on the collector area, the load characteristics, the solar availability at the site, and costs. A solar energy system is generally more cost-effective if the load matches the solar availability and only minimal or no storage is required (ref. II-33).

g. Heat Rejection System

Provision must be made for dissipating the heat in the coolant fluid if there are periods when there is no thermal load, but the electrical load can be met by the PV system. This cooling is usually provided by a closed-loop evaporation cooler or air cooler; such systems will be discussed in more detail in Volume III.

C. SYSTEM DESIGN ISSUES

1. Array Field Layout

Assuming that sufficient space is available for the desired collector area, the arrangement of the collector arrays in the field involves the following issues: layout pattern, delta-T string length, row spacing, and collector type. The choices in each of these areas involve advantages and disadvantages that can only be resolved by a life cycle cost analysis. Such an analysis compares the alternatives based on the energy produced and the total cost of that energy over a period of time. Each of the above issues is discussed in the following subsections. The trade-offs are described in general in table II-8.

a. Layout Patterns

The primary layout patterns--direct return, reverse return, and center feed--are illustrated in figure II-9. As noted in table II-8, there are significant advantages and disadvantages for each, and the best choice is not obvious.

It should be noted that for linear collectors, the resulting field is rectangular. Packing them into irregularly-shaped fields would require breaking the delta-T strings (as is done in the center field pattern). Arrays that occupy circular land patterns (such as the PFF) are more flexible in regard to field packing.

Table II-8. FIELD LAYOUT TRADE-OFFS

ISSUE	ADVANTAGES	DISADVANTAGES
LAYOUT PATTERN		
DIRECT RETURN:	SIMPLE; LESS MANIFOLD PIPING.	BALANCING VALVES PRODUCE SIGNIFICANT PRESSURE LOSS.
REVERSE RETURN:	MORE BALANCED FLOW, BALANCING VALVES PRODUCE LOWER PRESSURE LOSS.	MORE MANIFOLD PIPING.
CENTER FEED:	LESS MANIFOLD PIPING IF LOAD IS NEAR CENTER OF FIELD. BETTER ACCESS.	BALANCING VALVES PRODUCE SIGNIFICANT PRESSURE LOSS. SLIGHTLY MORE LAND REQUIRED. MORE FITTINGS.
SHORT DELTA-T STRINGS:	INCREASED THERMAL EFFICIENCY DUE TO LOWER AVERAGE TEMPERATURE. LESS VOLTAGE MISMATCH.	MORE MANIFOLD PIPING. MAY DIVIDE DRIVE TRAIN. MAY INCREASE PRESSURE LOSS.
CLOSER ROW SPACING:	LOWER LAND COSTS; LESS MANIFOLD PIPING AND LOWER PUMP POWER REQUIREMENTS; LESS WIRING AND POWER LINE LOSSES.	PERFORMANCE LOSS DUE TO ROW SHADING; DECREASED ACCESS.
COLLECTOR TYPE		
LPT:	SMALL LAND AREA PER POWER OUTPUT; SHORT PIPING AND WIRE LENGTHS.	
LFF:	SMALL LAND AREA PER POWER OUTPUT.	EXTENSIVE PIPE AND WIRE LENGTHS.
PFF:	FLEXIBLE FIELD LAYOUT.	LARGE LAND AREA PER POWER OUTPUT; VERY EXTENSIVE PIPE AND WIRE LENGTHS.

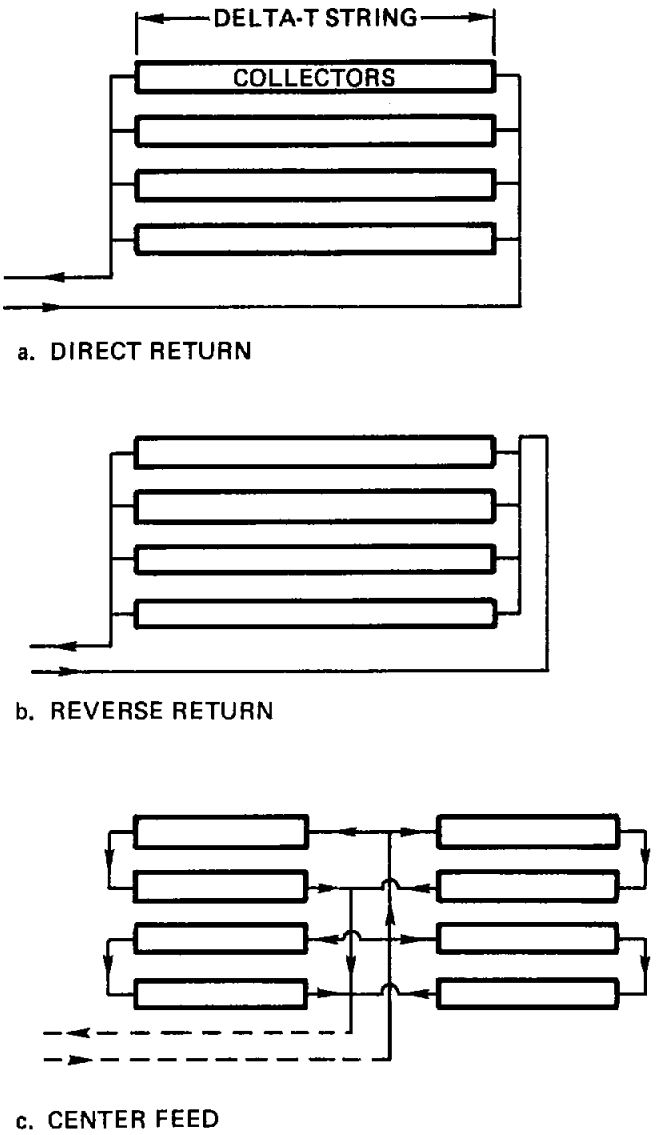

BDM/A-82-458-TR-R1

Figure II-9. Collector Field Layout Patterns

b. Delta-T and Voltage String Lengths

The number of collectors thermally in series determines the temperature rise and delta-T for the array field. A performance and cost trade-off study must be conducted to determine the best delta-T string length, since the operating temperatures are also affected by the collector flow rate, the characteristics of the load, and the heat exchanger. The relationships between these parameters are quite complex.

The number of cells electrically wired in series determines the output voltage of the array field, and should match the voltage range of standard power inverters. The temperature rise per collector and the delta-T string length also affects the design of the voltage string length. If the voltage string length is less than the delta-T string length, then voltage strings have different average temperatures, and a voltage mismatch problem results. Since each voltage string is in parallel with the others, and all must operate at the same voltage, each will operate off peak power. This will degrade the electrical output depending on the temperature difference. This effect is discussed in detail in chapter III, Volume III.

If the voltage string length is equal to the delta-T string length, there is no significant mismatch problem. The cell voltages are different within a string due to temperature, and each must operate at the same current, but the individual peak power points are not far from the average (actual) peak power for the string.

The design of the electrical strings must also include consideration of current levels and the increasing hardware costs for circuits carrying higher current.

The electrical wiring and delta-T string length should be compatible with the standard access provided by the collectors. For the SKI T-700, for example, the standard drive-train length is six troughs, or 38 m (125 ft, which is also the flow length), and the standard gap between troughs is only about 20 cm (8 in). There is a 41-cm (16-in) space at the center of the string where the drive pylon is located, but even that is not sufficient for an insulated coolant hose that must flex

without snagging as the collectors rotate. The MMC active-cooled prototype array can accommodate piping for two delta-T strings, each with 136 cell modules and a flow length of about 46.6 m (153 ft). The E-Systems LFF roll-axis drive length consists of four modules in a 6.1-m (20-ft) long frame. The flow length is about 22.3 m (73 ft). As many as 18 of these arrays can be coupled in one tilt-axis drive-train.

c. LPT Orientation, Row Shading, and Tracking Threshold

Table II-8 shows that one of the parameters involved in determining the best row spacing is the impact of row shading. For linear parabolic troughs with single axis tracking, the effect of row shading depends on whether the trough axis is oriented north-south or east-west. Orientation is determined by comparing the hourly and annual load profiles to the solar energy available for each orientation. Appendix H of reference II-34, an LPT handbook by R. W. Harrigan of SNLA, provides solar availability profiles for 26 locations, based on data for a typical year (SOLMET TMY). These profiles (which are for unshaded collectors and neglect end effects) show the effect of variations in the incident angle of the sun (the cosine factor), which can be regarded as reducing either the available radiation or the effective collector area. Sample profiles (Albuquerque, New Mexico) are reproduced in figure II-10. This graph illustrates that collectors oriented east-west intercept more energy in the winter months than collectors oriented north-south. In more northern latitudes an east-west orientation may provide additional energy for as long as 6 months, although a north-south orientation can provide more energy to a summer load (33 percent more in Albuquerque in June). The north-south orientation provides more energy on an annual basis in most regions of the United States as indicated by the average annual availability, which is also shown on the Harrigan graphs for each site. Thus, if the annual load profile is relatively flat or summer-dominant, then the north-south orientation is preferred.

The effect of row spacing on collector shading for each orientation is also described in reference II-34, which provides graphs of the annual shading factor versus land-to-collector area ratio

(spacing) for the SOLMET locations. The graph for Albuquerque is reproduced in figure II-11. The shading factor is defined as the ratio of the radiation incident when there is shading to the available radiation for a single row without shading. It should be emphasized that these shading factors can only be applied on an annual basis since they are not uniform throughout the year. Monthly shading effects are illustrated in reference II-34 for only one location (Albuquerque), shown in figure II-12. Shading is more pronounced in the winter months as indicated by the spread between the curves relative to the incident solar energy. Table II-9 shows the difference between shading factors for summer and winter and the annual value. A system designed to meet a summer-dominant load in the south may have a somewhat closer row spacing than a system designed for a winter-dominant load in the far north.

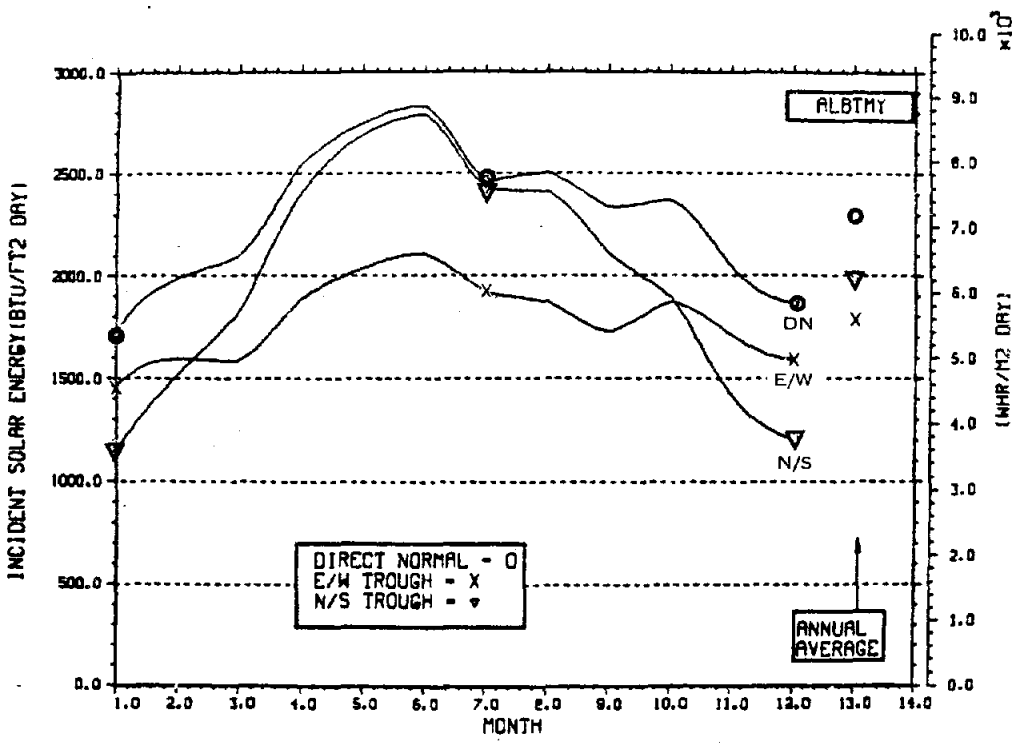

BDM/A-82-458-TR-R1

Figure II-10. Energy Incident on Collector Aperture (LPT)

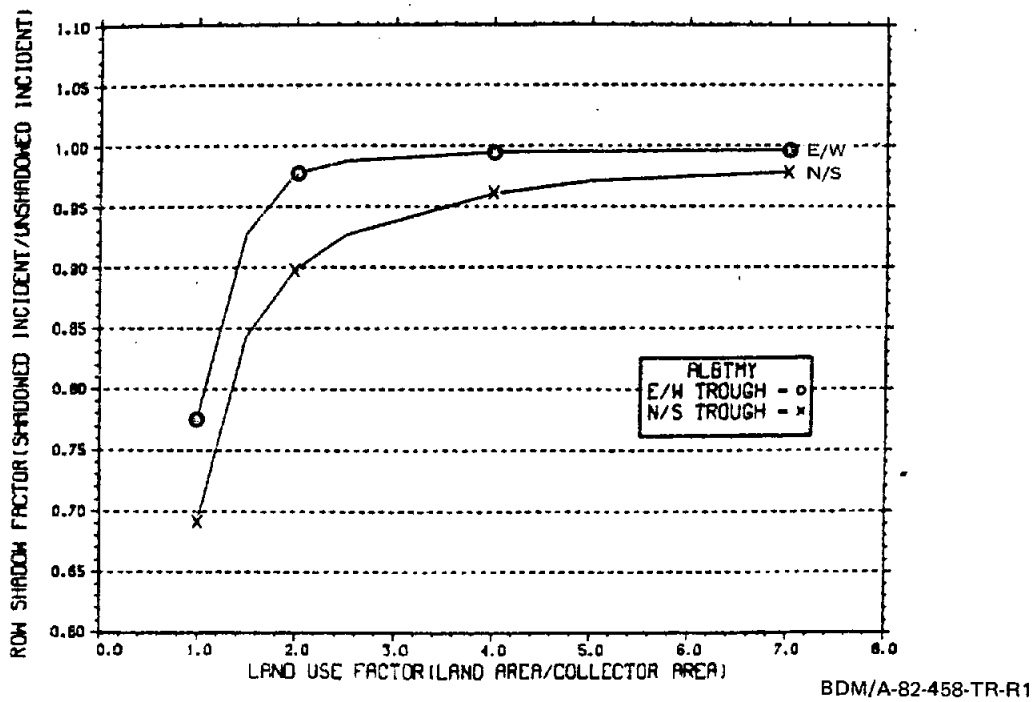

Figure II-11. Annual Nonfirst Row Shading

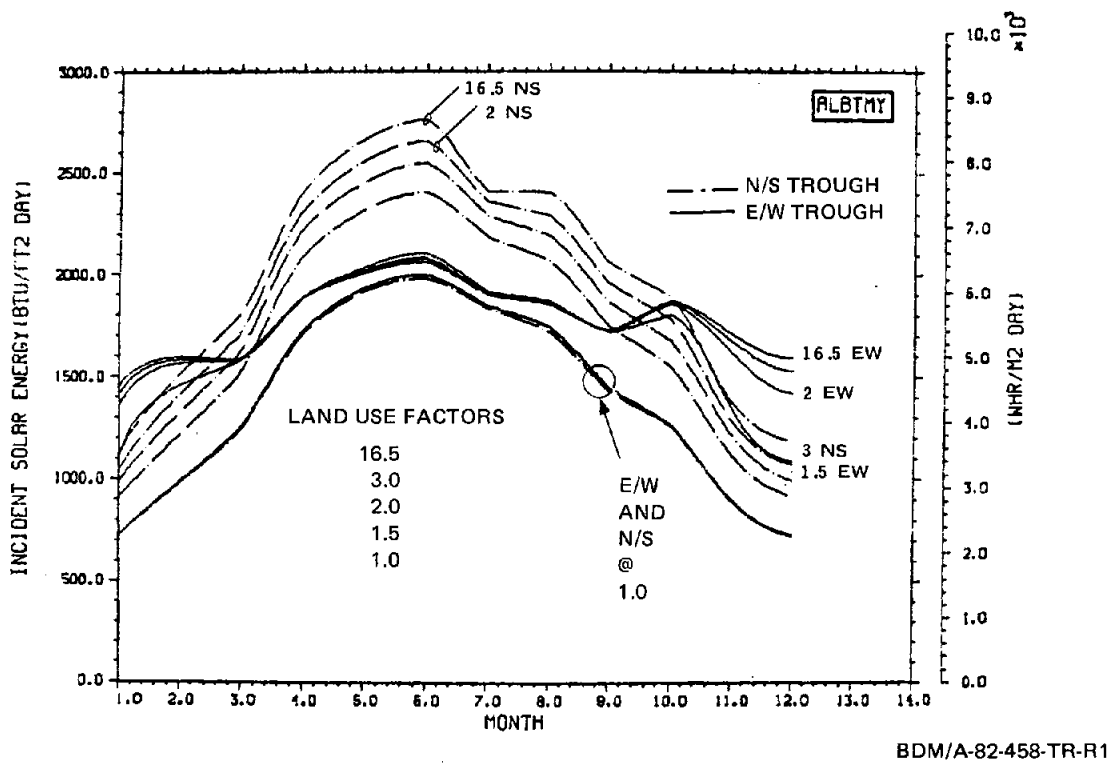

Figure II-12. Monthly Shadowing of E/W and N/S Parabolic Troughs

From SNL "Handbook for the Conceptual Design of Parabolic Trough Solar Energy Systems — Process Heat Application" (Ref. II-34)

TABLE II-9. SEASONAL VARIATIONS IN SHADING FACTORS (ALBUQUERQUE, LAND/COLLECTOR AREA=2.0)

PERIOD	SHADING FACTOR N-S	SHADING FACTOR E-W
AUGUST	0.91	1.00
ANNUAL	0.90	0.96
DECEMBER	0.84	0.90

Since one row of an array field is always fully sunlit (either the south row or the east row in the morning, and the west row in the afternoon), the shading factor for an entire field is given by:

$$\frac{1.0 + (N - 1)\ (\text{Row Shading Factor})}{N} \qquad \text{(Eq. II-10)}$$

where N is the number of rows.

Other factors affecting array performance are the minimum radiation and the minimum solar altitude required for tracking. These thresholds can totally mask the effects of shading. The shadow-band tracking system currently used by SKI will not initiate operation unless the available radiation exceeds 350 W/m^2 (111 Btu/hr ft^2). This threshold was established to prevent the trackers from following low-intensity reflections off clouds and other objects. The altitude threshold is set at 15° to keep the trackers from locking onto reflected sunlight from the back of a neighboring trough in the early morning and late afternoon. Figure II-13 shows the effects of these tracking thresholds, the cosine factor, and row shading for collectors oriented north-south for the worst case--spring and fall in far northern latitudes. The shading band was estimated from geometric constructions based on the "profile" angle of the sun (ref. II-35) throughout the day. The time, t, at which the altitude reaches 15°, was measured from noon and was determined from the following equations (ref. II-36):

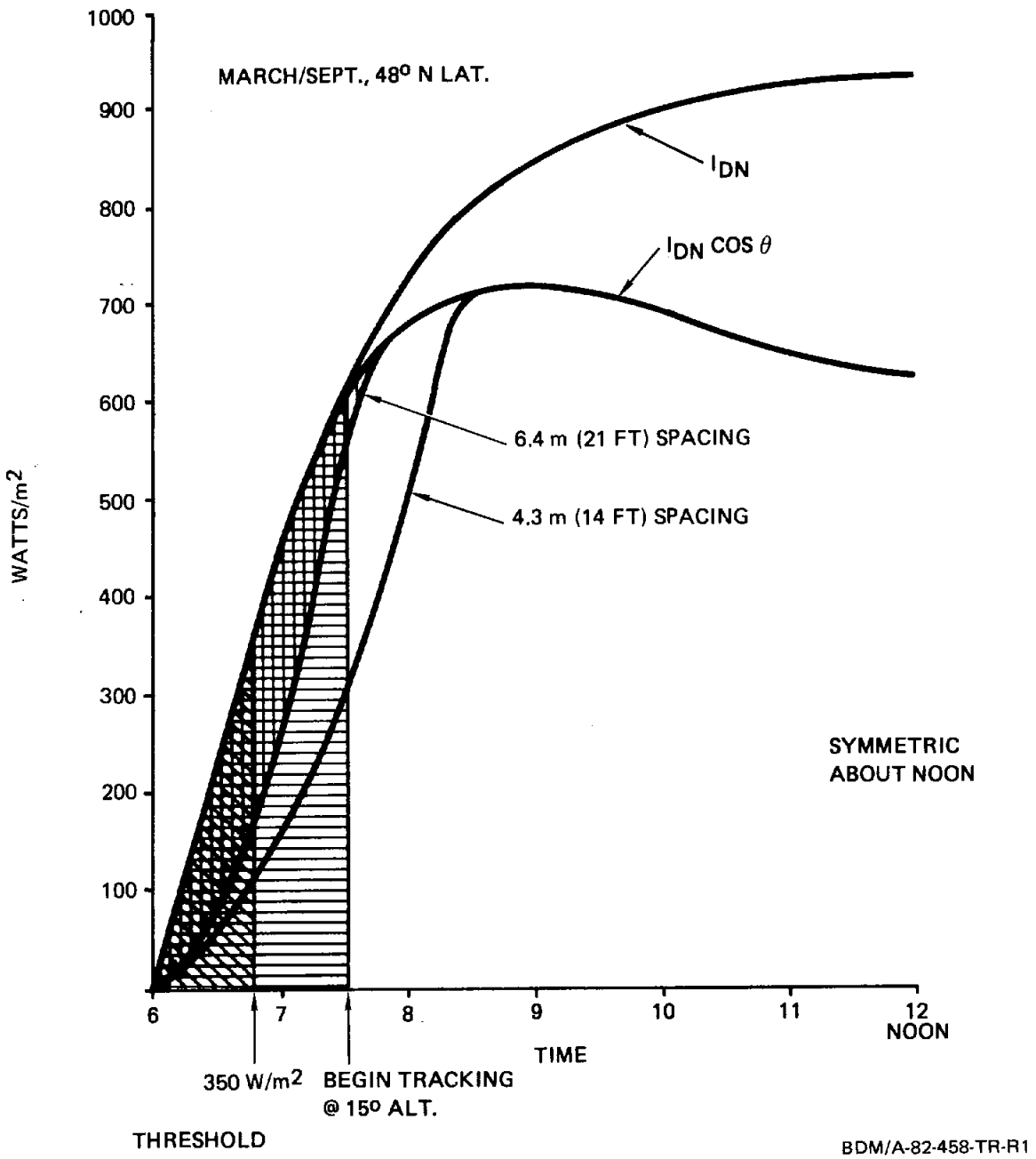

Figure II-13. Maximum Effect of Tracking Thresholds, Cosine Factor, and Row Shading for a N/S LPT

$$t = \frac{h}{15^{o}} \qquad \text{(Eq. II-11)}$$

where:

$$h = \cos^{-1}\left[\frac{\cos 75^{o} - \sin(DEC)\sin(L)}{\cos(DEC)\cos(L)}\right] \qquad \text{(Eq. II-12)}$$

and h is the hour angle, DEC is the seasonal solar declination, L is the latitude, and 75° is the zenith angle corresponding to the 15° altitude. The cosine factor was found from this equation (ref. II-36):

$$\cos i = \left[(\sin L \sin DEC + \cos L \cos DEC \cos h)^{2} + \cos^{2} L \sin^{2} h\right]^{\frac{1}{2}} \qquad \text{(Eq. II-13)}$$

It is evident from figure II-13 that when the tracking altitude threshold is 15°, shading and the effects of row spacing become less important.

d. LFF Row Shading and Tracking Thresholds

The orientation of the E-Systems array is fixed by its tracking design. The arrays are arranged in east-west rows and tilt about the east-west axis. The 0.915-m by 3.05-m (3-ft by 10-ft) modules rotate about a tilted north-south axis. The modules are shaded by adjacent modules in the array and by the neighboring array row. E-Systems has studied the impact of shading on the annual electrical efficiency of their passively cooled PV array (ref. II-37). The annual shading factor can be found by taking the ratio of the efficiency at a particular row spacing, to that at an infinite spacing, regardless of whether the array is passively or actively cooled. These shading factors are presented versus row spacing for eight locations in table II-10. These results take into account a roll-axis tracking threshold of 15° in the (tilted) plane of the array. There is no threshold for the tilt axis, and essentially no intensity threshold for the E-Systems tracker.

Thus, these shading factors can be applied directly to annual performance estimates.

TABLE II-10. LFF SHADING

LOCATION	LATITUDE (DEGREES)	ANNUAL I_{DN} KW hr/m^{2}yr	SHADING FACTOR ROW SPACING IN METERS (FT) 4.6 (15)	6.1 (20)	7.6 (25)	9.1 (30)	10.7 (35)
LAKE CHARLES, LA	30.1	1283	0.95	0.99	1.00	1.00	1.00
EL PASO, TX	31.8	2670	0.95	0.98	1.00	1.00	1.00
FORT WORTH, TX	32.8	1763	0.93	0.98	0.99	1.00	1.00
ALBUQUERQUE, NM	35.0	2613	0.91	0.97	0.99	1.00	1.00
NASHVILLE, TN	36.1	1290	0.93	0.98	0.99	0.99	1.00
DODGE CITY, KS	37.8	2132	0.90	0.97	0.98	0.99	1.00
MADISON, WI	43.1	1316	0.89	0.95	0.98	1.00	1.00
CARIBOU, ME	46.9	1199	0.87	0.94	0.97	0.99	1.00

e. PFF Row Shading

Martin Marietta conducted a shading study on their first generation passive array, which is the same size as their active-cooled prototype. The study (ref. II-38) considered two spacings corresponding to areas of 13.4 m by 13.4 m (44 ft by 44 ft), and 19.2 m by 16.2 m (63 ft by 53 ft) per array. The results, presented for the solstices and equinoxes in Albuquerque, New Mexico, are shown in table II-11.

TABLE II-11. PFF SHADING IN ALBUQUERQUE

AREA PER ARRAY	SHADING FACTOR MAR 21	JUN 21	SEP 21	DEC 21
13.4 x 13.4 m	0.82	0.92	0.80	0.88
19.2 x 16.2 m	0.99	0.99	0.99	0.96

BDM/A-82-458-TR-R1

f. Collector Comparisons

The three collector types considered here are different not only in terms of cost, and thermal and electrical efficiency (see section B), but also in terms of array field layout. The issues involved include land use, manifold piping, voltage string length, and delta-T string length. The advantages and disadvantages of each type are summarized in table II-8.

Consider the land required for each array type. Assuming a 2.5-aperture spacing for a 2.1-m by 6.3-m (7-ft by 20.8-ft) LPT, the land required is 37.8 m^2 (385 ft^2) per trough. For a four-module LFF like the E-Systems array (3.05 m by 6.1 m), a preliminary study by Battelle-Columbus Laboratories (BCL) (ref. II-39) recommends a 2.5 aperture spacing, which results in a land area of 46.5 m^2 (500 ft^2). A pedestal-mounted PFF like the MMC active-cooled prototype will sweep out a circle 11 m (36 ft) in diameter. Based on the relative spacing recommended by BCL (ref. II-39), an area of approximately 11.6 m by 14.6 m (38 ft by 48 ft) or 169 m^2 (1824 ft^2) is required. These figures alone are not conclusive, however, since efficiencies must also be considered. Table II-12 provides a comparison based on an array field producing 204 kW of electrical power. Each array electrical output was based on SOLCEL II annual efficiencies and an average solar radiation of 900 W/m^2.

TABLE II-12. COMPARISON OF LAND USE

	COLLECTOR TYPE		
LAND USE	PFF	LFF	LPT
ELECTRICAL EFFICIENCY (ANNUAL)	0.114	0.127	0.085
SAMPLE FIELD OUTPUT (kW)	204	204	204
ELECTRICAL OUTPUT PER ARRAY (kW)	2.59	1.27	0.995
ARRAYS PER FIELD	79	160	205
LAND AREA (k m^2)	13.3	7.4	7.3
LAND AREA PER POWER (m^2/kW)	65	36.4	35.8

2. Constant Versus Variable Fluid Flow Rate

Constant flow rate systems must be sized so the cells will remain below a predetermined temperature limit. On the other hand, when the ambient conditions provide significant cooling and the solar intensity is moderately low, then the fluid outlet temperature may be too low for the thermal energy to be useful. It may be desirable to decrease the flow rate under such conditions to maintain the output temperature. The flow rate can be varied by using a variable speed pump, throttling a constant speed pump, or by using pumps in parallel. However, a major problem arises when the flow is varied in that the flow balance in the collector rows is lost. A variable flow system then, would require extensive controls to operate the balancing valves, which otherwise are adjusted only on installation. Calculations also indicate a 10 percent annual improvement in thermal gain compared to a variable flow system. Therefore, the constant flow system is generally recommended.

3. Freeze Protection and Fluid Selection

Based on heat transfer properties, water would be the best working fluid for solar energy systems. Water, however, exerts high pressures at high temperatures and freezing temperatures. Current state-of-the-art PV-T receivers must be maintained at low cell temperatures at all times, so high temperatures are not a major concern. The maximum operating fluid temperature of current PV-T technologies is about 120°C (248°F; E-Systems LFF), which produces a water vapor pressure of only 200 k Pa (29 psia). Freezing temperatures, on the other hand, occur in most regions of the United States. If water is used, it must be completely drained from all exposed piping (or warm water circulated) when temperatures approach freezing. Mechanical freeze-protection methods are described in detail in references II-40 and II-41. In PV-T systems, these methods are generally not feasible because the collector piping includes many elevation changes that would make it difficult to ensure complete draining and complete air evacuation upon refilling. Other disadvantages include the difficulty of achieving the required elevation gradients in large ground-mounted fields, pipe scaling,

corrosion of mild steel in the presence of water and fresh air, water consumption or containment costs, and parasitic power consumption.

Most PV-T systems achieve more reliable freeze-protection by using an antifreeze fluid. This alternative involves significant design, installation, and maintenance considerations, however, in addition to system cost and performance penalties. The fluid must be compatible with the metals used in the system, and the critical properties of the fluid must be monitored and maintained. A heat exchanger is usually required to separate the collector fluid from the load thermal medium, which imposes a system efficiency penalty. Furthermore, some fluids are toxic, so the heat exchanger may have to be double-walled, and special handling and disposal may be required. Antifreeze fluids also have less efficient heat transfer properties than water. Advantages and disadvantages of various freeze protection techniques are summarized in table II-13.

Antifreeze fluids include water-glycol solutions, refrigerants, silicones, and hydrocarbons. Comparisons of these fluids and tables of properties are provided in references II-42 through II-46. Ethylene and propylene glycol solutions are usually used in PV-T systems because they are readily available, relatively low in cost, and have more favorable heat transfer properties. They have been widely used in collector systems with considerable success. Solutions can be obtained with freezing points below -45°C (-50°F), and boiling points at atmospheric pressure of about 108°C (225°F), which is sufficient for most hot water applications.

Somewhere above the boiling point (depending on the product), glycols will decompose into organic acids if exposed to air, which can cause corrosion problems. Since PV-T systems are maintained at low temperatures for cell protection and are normally not vented, such corrosion problems should not occur. However, added protection is usually obtained by the addition of a corrosion inhibitor, which may be specially designed for the metals used in the piping system. Different manufacturers use different inhibitors, so it is important to verify that a proposed combination of materials will provide adequate protection.

TABLE II-13. METHODS OF FREEZE PROTECTION FOR PV-T SYSTEMS

METHOD	ADVANTAGES	DISADVANTAGES
CHEMICAL (ANTIFREEZE):	RELIABLE FREEZE PROTECTION: NO CONTROLS.	COMPARED TO WATER, MORE EXPENSIVE, TOXIC, REACTIVE WITH ROOFING MATERIALS, SHORT LIFE, POORER HEAT TRANSFER PROPERTIES SO REQUIRES HIGHER FLOW RATE, HIGHER VISCOSITY SO REQUIRES LARGER PUMP AND PIPE SIZES. ADDED HEAT EXCHANGER EXPENSE AND PERFORMANCE PENALTY. THERMOSYPHONING HEAT LOSS.
MECHANICAL:		
DRAIN DOWN -	NO INVENTORY STORAGE SYSTEM.	WATER WASTED EACH TIME.
DRAIN BACK -	NO LARGE WATER LOSS; LINE WATER STORED IN INSULATED TANK, WHICH MAY BE PART OF VARIABLE-VOLUME THERMAL STORAGE SYSTEM.	PARASITIC POWER AND CONTROL SYSTEM REQUIRED TO REFILL LINES. EXTRA EXPENSE FOR HOLDING TANK. POSSIBILITY OF THERMAL SHOCK DURING REFILL.
FOR BOTH DD & DB -	WATER HAS FAVORABLE PROPERTIES AND IS CHEAP. NO THERMOSYPHON EFFECT WHEN DRAINED.	MORE COMPLICATED CONTROLS. HISTORY OF RELIABILITY PROBLEMS. BACKUP POWER REQUIRED. AIR INTRODUCED ACCELERATES CORROSION.
WARM WATER CIRCULATION:	SIMPLE; FEW CONTROLS; NO HOLDING TANK.	PRACTICAL ONLY WHEN FREEZING IS VERY INFREQUENT. PARASITIC POWER REQUIRED AND HEAT LOST.

Distilled or deionized water should be used in glycol solutions where aluminum piping is present (PV-T receivers), and glycols should not be used with galvanized steel (ref. II-44). NALCO 2755 is one inhibitor used with ethylene glycol that prevents corrosion in systems where steel, copper, and aluminum are present. Annual checks of the PH (acid concentration) and specific gravity (glycol concentration) are generally recommended.

Regarding heat transfer and pumping power (viscosity), glycol solutions are more efficient than the other antifreeze fluids, as indicated by the discussion of heat transfer efficiency factor in reference II-42. Actual tests have shown (ref. II-46) that flat plate collector efficiencies drop 4 to 8 percent when glycol is used, as compared to water, while the other fluids result in 9 to 15 percent efficiency penalties (ref. II-44). In these tests, all flow rates were the same, and no heat exchanger was included in the system.

Ethylene glycol is less viscous and has better heat transfer properties than propylene glycol, but ethylene glycol is toxic when ingested (less than one pint can be fatal), whereas propylene glycol is not. Additives and products of decomposition, however, can make a nontoxic fluid toxic. It is recommended that disposal of glycols be coordinated with local health agencies.

D. SUMMARY OF PV-T APPLICATIONS

1. The DOE Program

In 1973 the U.S. Department of Energy (DOE) initiated a National Photovoltaics Program for the purpose of stimulating the development of economically competitive, commercially available photovoltaic systems, to provide safe and reliable electric energy for a wide range of applications. One of the prime application areas for these systems is the intermediate load center (ILC) sector, i.e., intermediate-sized service, commercial, institutional, and industrial loads. In support of the national program objectives and to provide initial experimental data

on photovoltaic system performance in the ILC sector, the DOE Albuquerque Operations Office, with technical support from Sandia Laboratories, issued two Program Research and Development Announcements (PRDA) inviting proposals to conduct design studies leading to the fabrication, installation, operation, and evaluation of on-site experiments in the range of 20 to 500 kW peak output. The resulting program was designed to be a phased effort in which preliminary and detailed designs were generated in Phase I, selected systems were installed in Phase II, and the installed systems were operated and evaluated in Phase III.

Following a competitive evaluation, 29 designer/user teams were chosen to participate in the Phase I activity. Twelve of these teams were selected to work on flat panel array designs (PRDA-38), and 17 on concentrator array designs (PRDA-35). The design activity was begun in June 1978 and completed in February 1979 (ref. II-47).

Three of the concentrator array designs that were selected for the Phase III activity were active-cooled. They were the BDM Office Building CAPVC Project in Albuquerque, the Dallas-Fort Worth Airport building lighting project, and the Wilcox Memorial Hospital Project in Hawaii. All of these projects have only recently completed the major portion of the installation phase, and are now beginning operation and system testing. Although the DOE goals described above have certainly been met, the full benefits of the work have not become generally available because none of the final reports on Phase II and Phase III have yet been published. When completed, these reports will certainly complement the results presented in the remainder of this report. The following sections of this chapter present highlights of the three DOE PV-T projects mentioned above, plus the DOE grant project at Mississippi Community College, which represent the extent of PV-T system development in the United States to date.

2. <u>The BDM CAPVC Project</u>

This experimental installation was designed to supply electricity and thermal energy to a new 6691-m^2 (72,000-ft^2) office building in Albuquerque, New Mexico. The building, which includes a small

auditorium, computer center, and print shop, is owned by the Craddock Development Corporation and is leased by the The BDM Corporation, the PV-T project leader.

The system uses 54 Solar Kinetics T-700 linear parabolic troughs oriented north-south on the roof of the building. The PV cell modules and collector receiver tube designs were developed by BDM with the aid of computer modeling and extensive prototype testing. The cell modules were fabricated by Applied Solar Energy Corporation.

The collector field consists of nine rows with six 6.1-m (20-ft) collectors per row. There is one drive train and one electrical series string per row. Each row is divided into two delta-T strings that provide two side-by-side direct-return patterns with a common return line. Each electrical series string is designed to provide 240 V at 22 amps, at a peak power of 5.22 kW. The inverter is a Westinghouse unit designed for a peak efficiency of 93 percent between 200 and 300 VDC.

The electrical load is primarily daytime lighting and summer cooling. A major portion of the winter heating load is also furnished by electrical systems. The peak electrical load (summer) is about 250 kW. The project goal is to provide 47 kW of electrical power at a solar intensity of 1000 W/m^2. There is no requirement for electrical storage or utility sell-back, although feed-back to the utility is planned on an experimental basis. The 47 kW peak power capability is expected to provide 12 percent of the annual electrical load. Since April 1982, three rows have been tested; the electrical output was approximately 15.3 kW at about 975 W/m^2 solar intensity, which matches the performance goal for that much of the field.

The delta-T strings in the thermal system have produced a temperature rise of 6°C (10°F) at a constant flow rate of 6.9×10^{-4} m^3/sec (11 gpm). A centrifugal pump with a 7.46-kW (10-hp) motor is used to propel the coolant fluid. The thermal energy is presently being dissipated by a Marley closed-loop evaporative cooler, in addition to the natural heat loss from the manifold piping, which is not presently insulated.

Important lessons learned on this project include the following:

(1) Roof structures should be carefully evaluated. In this case, the structure was not as strong as early estimates indicated, particularly in regard to torsion. An external mounting structure had to be built above the roof deck.

(2) Unusual wind loadings must be anticipated. One collector row was severely damaged by high winds shortly after installation. In the stow position one rim of the SKI trough is higher than the other, and the collectors in the last row had been oriented so the upper rim was pointed into the air currents coming over the roof parapet. When the row was replaced, its stow position was reversed in relation to the other rows, and winds now flow harmlessly over the smooth back surfaces.

(3) Installing electrical wiring can be very time consuming. Quick-connect leads and factory-installed wiring can reduce field installation time and expense. Many sensors require non-standard fittings and connectors.

(4) Copper piping may be less expensive than steel, particularly for short runs, due to relative ease of installation.

(5) Parasitic losses for operating cooling towers can be severe and may include significant water consumption.

(6) Initial estimates for electrical junction box sizes should probably be doubled to facilitate wire installation and accommodate unexpected additions.

(7) Flexible-hose lengths are critical. If they are too long, they will kink and snag on near-by hardware. If they are too short, they will break after extended use.

3. <u>The E-Systems Dallas-Fort Worth Airport Project</u>

This PV-T system is designed to meet 100 percent of the continuous 25 kW lighting load at the central power plant for the Dallas-Fort Worth Airport. The thermal output will preheat low temperature boiler feed water that is continually recirculated within the plant.

The system uses 110 linear fresnel concentrator modules 0.915-m (3-ft) wide by 2.44-m (8-ft) long. They are first-generation collectors designed and manufactured by E-Systems, Inc., of Dallas, Texas. There are 10 modules per array mounted individually on two different roof levels of the power plant building. The array tilt adjustment is manually activated every few days. Each array consists of one roll-axis drive train, one electrical series string, and one delta-T string. The field piping will be arranged in a direct-return layout. The voltage output per string will be 260 V at 9.4 amps, and the temperature rise across a delta-T string will be about 22°C (40°F) at a constant flow rate of 1.6×10^{-4} m^3/sec (2.5 gpm). A centrifugal pump with a 746-watt (1-hp) motor will be used.

The fully-transistorized inverter, which was custom made (Jim Ross, consultant) is designed to operate with a 97 percent efficiency at a fixed 26 kW load. The lighting load is invariant, and the backup utility power is rectified to DC and routed through the inverter. With this arrangement there are no electrical storage or sell back requirements.

The thermal energy is transferred to the boiler feedwater line via two Bell & Gossett counterflow shell-and-tube heat exchangers that have a total UA of 12,000 W/°C. The boiler supplies a Rankine cycle system that drives centrifugal chillers for the airport air conditioning system. An emergency system will divert the PV coolant fluid to an alternate load (a 41.6 m^3 (11,000 gal) make-up water storage tank) in the event that the boiler feedwater flow is interrupted. The peak thermal output is expected to be 140 kW for a total of 280,000 kWH for a typical year.

The arrays were being installed at the airport at the time of this writing. Each module built for the installation had already received extensive testing, however, and all results indicate that the 25 kW goal will be met as planned.

4. The Acurex Hawaiian Hospital Project

The Acurex Corporation of Mountain View, California, designed and built the LPT collectors they have installed at the Wilcox Memorial Hospital in Kauii, Hawaii (latitude 22° N). The system supplies electricity and hot water to the 165 bed hospital. The Acurex collectors are oriented north-south on 9 acres of land. The PV-T receiver was designed by Acurex, and the cell modules were fabricated by Applied Solar Energy Corporation.

The collector field consists of 10 rows with eight 3.05-m (10-ft) collectors per row. There is one drive train per row (24.4 m, 80 ft), and all the rows are connected in one continuous delta-T string (244 m, 800 ft). The delta-T is about 50°C (90°F) with the fluid temperature maintained below 82°C (180°F) by a finned heat rejection unit (Aerofin, 321 kw (1.1×10^6 Btu/hr) nominal capacity). A flow rate of 1.1×10^{-3} m^3/sec (17 gpm) per row is maintained by a 2.24 kw (3-hp) pump. The thermal system includes a vented 11.4 m^3 (3000 gal) water storage tank with an internal tube heat exchanger having an area of about 6.0 m^2 (65 ft^2). The thermal load of 83.3 m^3 (22,000 gal) per year at 82°C is about 20 percent of the expected thermal output; therefore, about 80 percent of the array thermal output must be rejected, decreasing the overall system efficiency.

The electrical series string is one row long each at 240 V above or below ground and having a current of 29 amps for a peak field power of 35 kW at 1000 W/m^2 and 29°C (84°F) ambient air temperature. The inverter is a Westinghouse unit with an operating efficiency of 92 percent. The annual electrical load is typically 2.7×10^6 kWH. About 60 percent of that is summer air conditioning and 28 percent is lighting. The 35 kW power output represents about 6 percent of the electrical load, so there are no storage or utility feed back requirements.

The system has been fully operational since December 1981. The output was initially as expected, but has recently degraded. Possible causes are currently being investigated. Some of the problems encountered include electrical shorting from cell to receiver, cover glass

breakage, and cell overheating due to uneven application of thermal grease (ref. II-48). In addition, moisture absorbed in cell encapsulant (PVB) produces bubbles upon being heated in the presence of ultraviolet radiation.

5. The BDM/SKI MCC College Project

This large installation was designed by The BDM Corporation and Solar Kinetics, Inc. in 1978. It provides energy to a new 5,000-m^2 (53,440 ft^2) building that houses Mississippi County Community College in Blytheville, Arkansas. The system employs 270 ground-mounted T-700 collectors oriented in a north-south direction and arranged in four direct-return patterns. The two patterns in the north half of the field are joined by a common return line, as are the two patterns in the south section. The delta-T string length corresponds to SKI's standard six-collector drive train length. The delta-T is presently averaging about 12°C (22°F) at a flow rate of 6.3×10^{-4} m^3/sec (10 gpm). The field flow is driven by a 22.4-kw (30-hp) pump.

Each electrical series string consists of six collectors, and provides 370 VDC at 14.4 amps for a peak field power of 240 kW at 845 W/m^2 and 30°C design conditions. The inverter, which was built by the Delta Electronic Control Corporation, has a rated efficiency of 92 percent. The cell modules were fabricated by the Solarex Corporation, and the one-piece receiver was designed by SKI.

The project goal was to meet 100 percent of the thermal and electrical loads. The electrical load includes lighting and summer air conditioning. Any excess electricity is supplied to the utility network. The thermal load, which averages about 8,000 kWH per day, consists of the domestic hot water and the space heating requirements. A thermal storage system consisting of two 151.4 m^3 (40,000 gallon) water tanks enables the system to meet night-time loads. The thermal system also includes two Marley closed circuit evaporative coolers for heat rejection and a 240-plate Chester-Jensen heat exchanger. The full collector field was operational in April 1981, but as of April 1982, the electrical output was less than 50 percent of the design value. This is believed to be a

result of reflector defects and tracking errors, although the problem is still under investigation. Other problems that have been encountered include cell module electrical insulation breakdown, optical alignment errors, corrosion in the plumbing (pure water was run in the system for a period of time), and excessive settling of the collector foundations (ref. II-49).

E. REFERENCES

II-1. H. S. Rauschenbach, Solar Cell Array Design Handbook, Van Nostrand Reinhold Co, 1981.

II-2. E. R. Hoover, SOLCEL-II, An Improved Photovoltaic System Analysis Program, SNL, SAND 79-1785, 1980.

II-3. R. M. Turfler, T. J. Lambarski, R. W. Grant, Design Guidelines For Large Photovoltaic Arrays, Sandia National Laboratories, SAND 79-7001, by The BDM Corporation, January 1979.

II-4. H. J. Gerwin, "Photovoltaic Concentrator Test Results and Interpretations," IEEE, 1981.

II-5. B. Y. H. Liu and R. C. Jordan, The Long-Term Average Performance of Flat-Plate Solar Energy Collectors, (Solar Energy, 7, 53, 1963).

II-6. H. C. Hottel and A. Whillier, "Evaluation of Flat Plate Solar Collector Performance," (Trans. Conference on the Use of Solar Energy, 2, 74, University of Arizona Press, 1958).

II-7. G. O. G. Lof and J. A. Duffie, Optimization of Focusing Solar-Collector Design, (Journal Engr. Power, Trans. ASME, 87, 1-12, 1965).

II-8. S. A. Klein, et. al., TRNSYS, A Transient Simulation Program, (Engineering Experiment Station Report #38, Version 10, 1979, The University of Wisconsin, Madison).

II-9. M. E. Fewell and N. R. Grandjean, User's Manual for Computer Code SOLTES-1, (Sandia National Laboratories, SAND 78-1315, Revised, 1981).

II-10. Ed Lumsdaine, The Production of Industrial Process Heat by Solar Energy, Proceedings of the Solar Technology Assessment Conference, Orlando, Florida, January 29, 1981.

II-11. C. F. Kutscher, et. al., Design Approaches for Solar Industrial Process Heat Systems, Solar Energy Research Institute, SERI/TR-253-1356, Golden, Colorado, 1981.

II-12. W. E. Schwinkendorf, Development of New Cell-Substrate Bonding Systems, Sandia National Laboratories, Albuquerque, SAND 83-7036, by The BDM Corporation, to be published.

II-13. J. A. Peterka, J. J. Lou, and J. E. Cermak, Wind Tunnel Test of a Photovoltaic Concentrator Array, by Colorado State University, for Martin Marietta, CER78-79 JAP-JJL-JEC62, June 1979, 34 pages.

II-14. J. A. Peterka, J. M. Sinou, and J. E. Cermak, Mean Wind Forces on Parabolic--Trough Solar Collectors, Sandia National Laboratories, SAND 80-7023, May 1980, 109 pages.

II-15. M. Poreh, J. A. Peterka, and J. E. Cermak, Wind-Tunnel Study of Wind Loads on Photovoltaic Structures--Phase II (Draft), by Colorado State University for Bechtel National, Inc., Fort Collins, Colorado, 1981, 47 pages.

II-16. D. E. Randall, "Wind Load Definition for Line-Focus Concentrating Solar Collectors," pp. 231-246, in Proceedings of the Line-Focus Solar Thermal Energy Technology Development, Sandia National Laboratories, Albuquerque, September 1980.

II-17. D. E. Randall, D. D. McBride, and R. E. Tate, "Mean Wind Loading on Parabolic Trough Solar Collectors," Journal of Solar Energy Engineering, Volume 103, November 1981, pp. 313-322.

II-18. H. E. Auld, "Foundations for Line Focusing Solar Collectors," pages 247-254 in Proceedings of the Line-Focus Solar Thermal Energy Technology Development Seminar Laboratories, Albuquerque, September 9-11, 1980.

II-19. H. E. Auld and P. F. Lodde, Study of Low-Cost Foundations/Anchor Designs for Single-Axis-Tracking Solar Collector Systems, Sandia National Laboratories, SAND 78-7048, Albuquerque, January 1979.

II-20. H. E. Auld and P. F. Lodde, Study of Foundation Designs for Single-Axis-Tracking Solar Collector Systems Under Reduced Loading Conditions, Sandia National Laboratories, SAND 79-7016, May 1979, 21 pages.

II-21. D. H. Merkle, Full Scale Load Tests of Experimental Solar Collector Foundations, Sandia National Laboratories, SAND 80-7076, June 1981, 109 pages.

II-22. V. D. Dunder, "Analysis and Design Modification of Second Generation Heliostat Foundations Using Program PADLL (Pier Analysis and Design for Lateral Loads)," Memorandum, Sandia National Laboratories, Livermore, California, February 9, 1982.

II-23. V. D. Dunder, "Potential Cost Savings for Heliostat Foundations Designed With PADLL (Pier Analysis and Design for Lateral Loads)," Memorandum, Sandia National Laboratories, Livermore, California, March 11, 1982.

II-24. P. J. Lunde, Solar Thermal Engineering, (New York: John Wiley and Sons, 1980).

II-25. C. F. Kutscher, et. al., Design Approaches for Solar Industrial Process Heat Systems, (Draft), Solar Energy Research Institute, SERI/TR-253-1356, November 1981.

II-26. R. C. Hodge, et. al., Photovoltaic Concentrator Array Production Process Study: Final Report, Volumes I and II, Sandia National Laboratories, Albuquerque, SAND 79-7055, by General Electric Space Division, January 1981.

II-27. J. Chan, Manufacturing Cost Analysis of 1980 Vintage Photovoltaic Array, Sandia National Laboratories, Albuquerque, SAND 81-7010, April 1982.

II-28. D. J. Anderson, et. al., Commercial Application of a Photovoltaic Concentrator System, Phase I, Final Report, The BDM Corporation, DOE/CS/05313-1, April 1980, p. II-139.

II-29. R. S. Hall, J. Matley, and K. J. McNaughton, "Current Costs of Process Equipment," Chemical Engineering, Volume 89, No. 7, April 5, 1982, p. 80.

II-30. K. S. N. Raju and J. Chand, "Consider the Plate Heat Exchanger," Chemical Engineering, August 11, 1980, p. 133.

II-31. D. A. Dougherty, "Heat Loss Coefficients for Insulated Pipes in Solar IPH Systems," Proceedings from the Fourth Annaul Conference of the ASME Solar Energy Division, April 1982, Albuquerque, New Mexico, p. 277.

II-32. M. A. Quintana and L. E. Torkelson, Pump Heat Loss Test Report, Sandia National Laboratories, Albuquerque, SAND 80-2526, January 1981.

II-33. S. M. Hock and M. E. Karpuk, "The Value of Thermal Storage in Solar IPH Systems," Proceedings from the Third Annual Conference of the ASME Solar Energy Division, April 1981, Reno, Nevada, p. 696.

II-34. R. W. Harrigan, Handbook for the Conceptual Design of Parabolic Trough Solar Energy Systems--Process Heat Applications, Sandia National Laboratories, Albuquerque, SAND 81-8763, July, 1981.

II-35. ASHRAE HANDBOOK OF FUNDAMENTALS, American Society of Heating, Refrigerating, and Air-Conditioning Engineers, New York, New York, 1977, p. 26.7.

II-36. F. Kreith and J. F. Kreider, Principles of Solar Engineering, Hemisphere Publishing Co., 1978.

II-37. E-Systems Contract Review Meeting, Sandia National Laboratories, Albuquerque, March 1982.

II-38. J. A. Sanders, R. L. Donovan, S. Broadbent, 10-Kilowatt Photovoltaic Concentrator Array Fabrication, Sandia National Laboratories, Albuquerque, SAND 80-7062, December 1980, p. 33.

II-39. Battelle-Columbus Laboratories, "Photovoltaic Concentrator Array Field Optimization and Modularity Study," Third Project Integration Meeting on Photovoltaic Systems and Applications, Sandia National Laboratories, Albuquerque, SAND 82-0309, February 1982, p. 257.

II-40. G. F. Tully, "Drainback Space Heating Systems: Simple, Reliable and Easy to Repair," Solar Engineering, January 1981, p. 16.

II-41. S. R. Schiller, "Freeze Protection," Solar Age, August 1981, p. 26.

II-42. C. F. Kutscher, et. al., Design Approaches for Solar Industrial Process Heat Systems (Draft), Solar Energy Research Institute, SERI/TR-253-1356, November 1981, Section 7.2.

II-43. T. Sullivan, "Solar Heat Transfer Fluids," Solar Age, December 1980, p. 33.

II-44. J. G. Avery and J. J. Krall, "Corrosion Prevention and Fluid Maintenance in Active Solar Systems: The State-of-the-Art," a 3-part series, Solar Engineering and Contracting, February, March, and April 1982.

II-45. C. F. Cheng, C. P. Chen, R. M. Wolosewicz, "Corrosion Problems Associated with Solar Fluid and Components."

II-46. R. Barber, W. Schultz, and W. W. Youngblood, Solar Collector Fluid Parameter Study, Wyle Laboratories, July 1979, funded by DOE Contract No. EG-77-C-01-4050.

II-47. E. L. Burgess, E. A. Walker, editors, Summary of Photovoltaic Applications Experiments Designs, ALO-71, U.S. Department of Energy, October 1979.

II-48. B. Spencer, "Operational Experience with a 35-KWP Concentrating Photovoltaic System," European Photovoltaic Conference Proceedings, May 1982.

II-49. S. I. Kaplan, "Startup Experience with a Concentrating Photovoltaic Power System," Proceedings of the AIAA 20 the Aerospace Sciences Meeting, Orlando, Florida, January 1982.

CHAPTER III

SITE/APPLICATION PAIR SELECTION, LOAD PROFILE DEVELOPMENT, AND ECONOMIC ANALYSIS

A. INTRODUCTION

The second part of Task I was to propose 10 site/application pairs for further analysis, to determine the feasibility of using a PV-T system to displace a fraction of the required electrical and thermal energy. Five of these site/application pairs were to be selected from the commercial sector and five from the industrial sector. In order to specify five site/application pairs which have the potential for PV-T application, a ranking of the myriad of applications and sites was required in order to choose only the most promising pairs. Such a ranking was performed for both the commercial and industrial sectors.

An extensive study of potential PV-T applications for the commercial sector was performed by Research Triangle, Inc. (RTI) for Sandia National Laboratories (SNLA) (ref. III-1). This RTI report is the basis for the present ranking of commercial site/application pairs. Very little has been done to rank the various industrial applications. One of the major problems lies in the diversity of electrical and thermal energy requirements for the various industrial processes. Drexel University performed an energy analysis of 108 industrial processes (ref. III-2); this report, and several other industrial processes heat studies, and the RTI ranking methodology, provide the basis for selecting five industrial site/application pairs. Near the end of this study it was felt that a laundromat would be a good PV-T application. Thus, a total of six industrial site application pairs were analyzed.

Once the 11 site/application pairs were identified, electrical and thermal load profiles were required for further analysis. Energy usage and load profiles are extremely process and site-dependent. Load profiles for three of the top ranked industrial site/application pairs

were available from previous total solar energy studies. Trade organizations and plant managers provided load profiles for three additional industrial applications. Load profiles for the commercial sector were more difficult to obtain since they are more site and climate-dependent than industrial loads, which are primarily process-dependent. The development of the commercial load profiles will be described in a later section.

After obtaining load profiles for the 11 site/application pairs, a systems analysis was performed to determine the economics of using a PV-T system to meet all or part of the load. The conceptual systems design is shown in figure III-1, and consists of the PV-T array, inverter, piping and pumping system, heat exchanger, cooling tower, auxiliary heater, and the load. A modified version of SOLCEL II (ref. II-2) was used to perform an electrical and thermal analysis to determine the energy delivered to the load on an annual basis, the life cycle cost of the PV-T system, and the life cycle cost of backup energy provided by the auxiliary heater and utility. A life-cycle cost ratio, defined in equation III-1, was calculated:

$$\text{LCCR} = \frac{\text{LCC of the PV-T system} + \text{LCC of fossil fuel and utility backup}}{\text{LCC of conventional energy without a solar system}} \qquad \text{(Eq. III-1)}$$

The LCCR is calculated using the methodology developed by Perino (ref. III-3). This methodology takes into account both the initial costs of purchasing a system and the recurring costs associated with operating the system through its lifetime. Financial parameters reflecting the state of the economy in general, and the economic position of the systems owner, are used in the analysis. These include fuel costs, escalation rates and general inflation, discount rate, etc. The result of the analysis is the life-cycle cost (LCC) of the solar system, which may then be compared to the LCC of a conventional energy system to determine economic feasibility. For the systems considered in this program, a

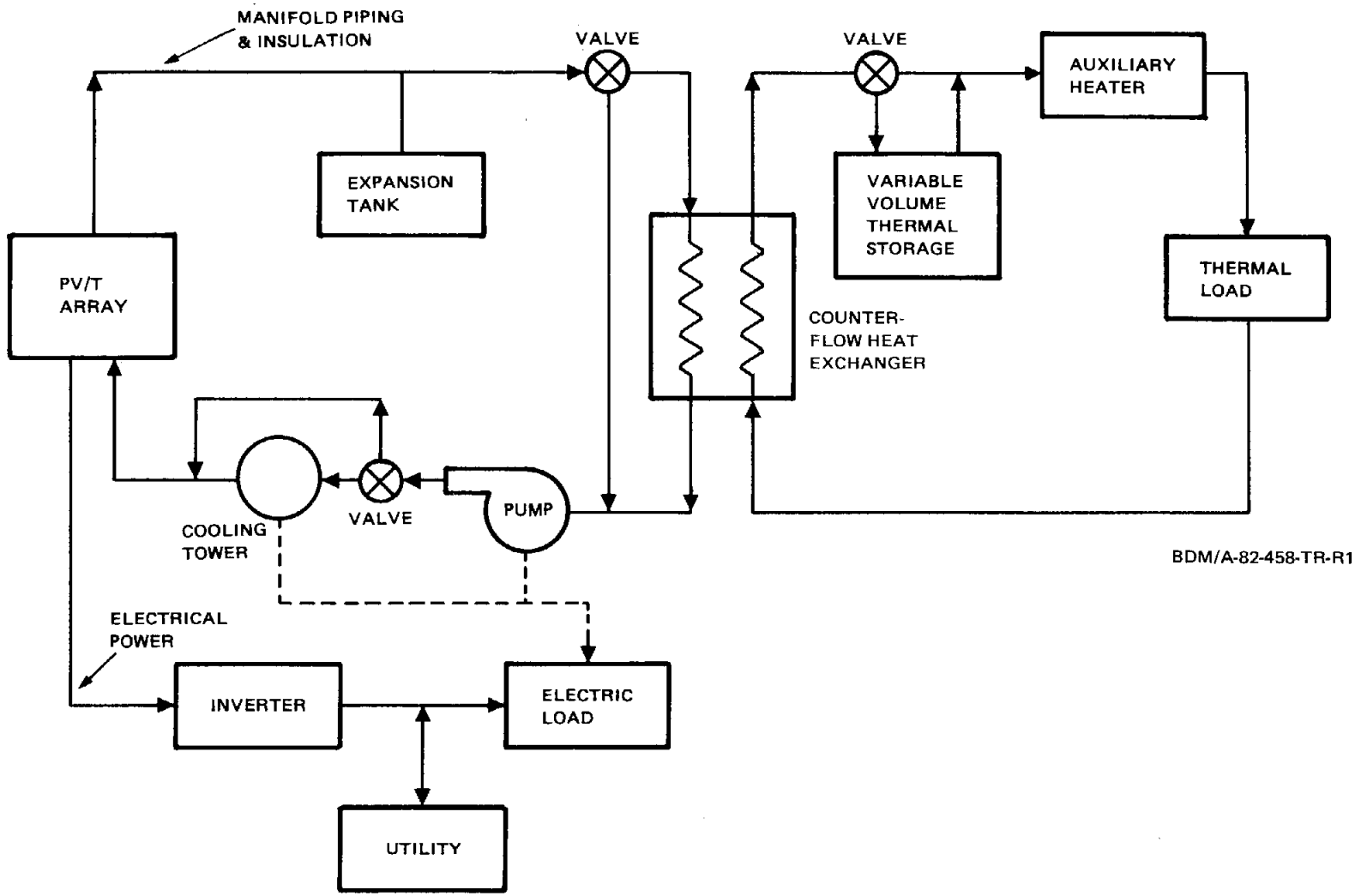

Figure III-1. Conceptual PV-T System for Preliminary Analysis and Sizing

conventional energy system is considered to already be in existence, and this system is capable of providing the backup energy required. Therefore, the LCC of the backup and conventional systems does not include any capital expenditure and only includes the cost of fuel or electricity used.

If the LCCR is less than one, then the cost of the solar system plus the cost of backup energy is less than the annual cost of conventional energy, and the PV-T system would be economically feasible. Based on this system's analysis, three of the 11 site/application pairs will be chosen for detailed analysis and design.

A description of the systems analysis and results is contained in section D. In section B, the ranking of the commercial section is described, along with the method for developing the commercial load profiles. Section C contains a description of the industrial sector ranking method and industrial applications.

B. COMMERCIAL SECTOR ANALYSIS

1. Ranking of Commercial Site/Application Pairs

Research Triangle, Inc. (RTI) performed a study of potential PV-T applications in the commercial sector based on a ranking factor defined in equation III-2 (ref. III-1). The higher the ranking factor, the more appropriate (relatively speaking) the application is for a PV-T system.

$$R = \frac{\text{annual value of electrical energy supplied} + \text{annual value of thermal energy supplied}}{\text{annualized cost of the PV-T array}} \qquad \text{(Eq. III-2)}$$

Through various manipulations, described in detail in section C, equation III-2 can be reduced to equation III-3:

$$R = K\ (P_e + Q_s\ P_q/E_L)\ \eta_e d I_a \qquad \text{(Eq. III-3)}$$

where:

Q_s = supplied thermal energy
E_L = electrical load
P_q = price of thermal energy
P_e = price of electrical energy
η_e = array electrical efficiency at operating temperature
d = number of operating days per year
I_a = annual average daily solar insolation
K = constant containing the fixed charge rate, electrical efficiency at reference temperature, and capital PV-T costs.

The ranking developed by RTI used national average fuel and electricity costs and national average daily insolation. The price of fuel for a particular application was based on the national average consumption of each type of fuel, and the national average cost for those fuels. This is illustrated in table III-1 (from reference III-1). The results of this analysis by RTI for electric cooling is shown in table III-2. As indicated in reference III-1, this ranking may improve for some applications if thermal cooling (absorption chillers) replaced vapor compression cooling.

As indicated in table III-2, hospitals, public administration buildings, and schools ranked the highest for PV-T application, and also consume 49 percent of the total energy used by the commercial sector. Although FIRES and retail ranked low nationally, they consume 41 percent of the total energy used. A ranking of these five application sectors was developed for 11 energy regions in order to select five site/application pairs.

First, the annual average daily direct normal insolation in kWh/m^2 for each census division was determined from SOLMET data. This data and the regional averages are given in table III-3. The Mountain and Pacific census regions have been divided into South and North Mountain and South and North Pacific due to the large variation in insolation between the southern and northern sites. The amount of each type

TABLE III-1. ILLUSTRATIVE COMPUTATION OF Pq FOR HOSPITALS BASED ON TOTAL NATIONAL ENERGY CONSUMPTION

FUEL	ANNUAL USE* (10^9 Btu)	FRACTION OF TOTAL THERMAL FUELS	Pq' (¢/kWh)
COAL	5370	0.011	0.45
DISTILLED FUEL OIL	91885	0.182	2.49
RESIDUAL FUEL OIL	54367	0.108	1.58
LPG	446	0.001	1.54
NATURAL GAS	322779	0.640	1.24
STEAM	29231	0.058	1.02
SUBTOTAL	504078		
ELECTRICITY	87715		
TOTAL	591793		

$$Pq = (0.011)(0.45) + (0.182)(2.49) + \cdots (0.058)(1.02)$$
$$= 1.483 \text{ ¢/kWh}$$

*ENERGY DATA ARE FROM THE ECDB, REFERENCE III-4.

BDM/A-82-458-TR-R1

TABLE III-2. RTI RANKING FACTORS FOR PV-T APPLICATIONS IN THE COMMERCIAL SECTOR

APPLICATION SECTOR	R	Q_S/E_L	η_e	OPERATING DAYS	PERCENT OF COMMERCIAL SECTOR TOTAL ENERGY
HOSPITAL	0.41	4.6	0.11	365	11
PUBLIC ADMINISTRATION	0.29	4.5	0.12	252	22
SCHOOLS	0.25	4.2	0.12	225	16
UTILITIES	0.25	1.9	0.12	330	3
WHOLESALE	0.22	1.0	0.12	330	5
COMMUNICATION	0.20	0.7	0.12	330	1
FIRES*	0.17	1.3	0.12	252	19
RETAIL	0.13	0.9	0.08	300	22

*FINANCIAL, INSURANCE, REAL ESTATE, SERVICE

TABLE III-3. REGIONS FOR INSOLATION DATA FOR FULLY TRACKING COLLECTORS

Census Region	SOLMET Site	AVERAGE DIRECT NORMAL INSULATION (kWh/m^2) Site	Region
New England	Blue Hill, MA	3.3	3.8
	Boston, MA	3.3	
	Caribou, ME	4.8	
Middle Atlantic	New York, NY	3.0	3.0
South Atlantic	Apalachicola, FL	4.3	3.9
	Cape Hatteras, NC	4.2	
	Charleston, SC	3.8	
	Miami, FL	3.8	
	Washington, D.C.	3.5	
East North Central	Madison, WI	3.8	3.8
East South Central	Nashville, TN	3.6	3.6
West North Central	Bismarck, ND	4.5	
	Columbia, MO	4.3	5.1
	Dodge City, KS	5.8	
	Omaha, NE	4.5	
South Mountain	Albuquerque, NM	7.1	7.0
	Ely, NV	6.6	
	El Paso, TX	7.3	
	Phoenix, AZ	6.9	
North Mountain	Great Falls, MT	4.4	4.4
South Pacific	Santa Maria, CA	5.5	5.5
North Pacific	Medford, OR	4.3	4.3
	Seattle, WA	4.2	

of fuel and the amount of electricity used, was determined for each application sector, and within each census division, from the Energy Consumption Data Base (ref. III-4). The cost of electricity and the cost of each type of fuel within each census region was found in references III-5 and III-6. These costs were escalated to 1982 price levels so all energy costs had a common basis. Using the technique shown in table III-1 to obtain the cost of thermal energy for each application and within each census division, and using equation III-3 with values of η_e, d and Q_s/E_L, obtained from table III-2, the ranking factor for each application and for each census region was determined as shown in table III-4.

In general, the highest ranking application is hospitals, with schools and public administration buildings ranking next, depending on region. The 10 top ranked site/application pairs are listed in table III-5. In keeping with the intent of the program to select a broad variety of applications and geographic locations for more detailed analysis, those site/application pairs marked with * were selected.

Participants in the National Energy Conservation Policy Act (NECPA) grant program were determined, and several were contacted to obtain energy audits of these facilities. These facilities, and those for which load profiles will be developed, include hospitals in Fresno, California and Seattle, Washington; schools in Albuquerque, New Mexico and Boston, Massachussetts; and a public administration building in Phoenix, Arizona.

2. Development of Commercial Load Profiles

a. Introduction

Based on an initial screening process of commercial loads, the following site/application pairs were selected for further evaluation:

- Hospital, Fresno, California
- Hospital, Seattle, Washington
- School, Albuquerque, New Mexico
- School, Boston, Massachussetts
- Public Administration Building, Phoenix, Arizona

TABLE III-4. RANKING OF THE COMMERCIAL SECTOR BY REGION

Region	HOSPITAL r	HOSPITAL E/T	PUBLIC ADM. r	PUBLIC ADM. E/T	SCHOOLS r	SCHOOLS E/T	FIRES r	FIRES E/T	RETAIL STORES r	RETAIL STORES E/T
New England	.39	.109	.25	.158	.28	.210	.23	0.663	.13	1.155
Mid Atlantic	.30	.123	.21	.168	.22	.223	.21	0.692	.12	1.229
South Atlantic	.27	.263	.17	.333	.19	.310	.17	1.081	.07	2.130
East North Central	.28	.130	.20	.158	.20	.208	.20	0.562	.12	0.893
East South Central	.17	.320	.12	.337	.14	.237	.13	1.207	.07	1.895
West North Central	.28	.134	.21	.139	.21	.143	.23	0.401	.12	1.008
West South Central	.25	.276	.19	.239	.18	.264	.18	0.661	.10	1.427
Northern Mountains	.27	.139	.20	.220	.21	.181	.20	0.682	.12	1.473
Southern Mountains	.43	.139	.32	.220	.33	.181	.32	0.682	.19	1.473
Northern Pacific	.31	.217	.18	.292	.18	.362	.18	1.041	.10	1.343
Southern Pacific	.39	.217	.23	.292	.23	.362	.23	1.041	.13	1.343

TABLE III-5. TEN TOP RANKED SITE/APPLICATION PAIRS

Region	Application	Rank
Southern Mountains	Hospital	0.43
*South Pacific	Hospital	0.39
New England	Hospital	0.38
*Southern Mountains	School	0.33
*Southern Mountains	Public Admin Bldg.	0.32
Southern Mountains	FIRES	0.32
*North Pacific	Hospital	0.31
Mid Atlantic	Hospital	0.30
East North Central	Hospital	0.28
West North Central	Hospital	0.28
*New England	School	0.28

As shown in table III-6, the loads for these applications are space heating and cooling, water heating, lighting, and various electrical appliances and equipment. Hourly values of these loads were developed for the SOLCEL II PV-T performance simulations. All the loads, except heating and cooling, were developed from available data and then input to SOLCEL II. Since the heating and cooling loads depend on ambient conditions, which are available in SOLCEL II, it was convenient to calculate those loads during each simulation. It was assumed that cooling is provided by electrical equipment, and heating and hot water are provided by direct thermal energy (natural gas systems).

The heating and cooling load development was based primarily on standard ASHRAE (American Society of Heating, Refrigerating, and Air-Conditioning Engineers) methods (ref. III-7), and the Uniform Building Code (ref. III-8). The other loads were developed from data provided in two studies: a PV-T applications report by the Research Triangle Institute (RTI) (ref. III-1), and an energy consumption study by Jack Faucett Associates, Inc. (ref. III-4).

TABLE III-6. CLASSIFICATION OF COMMERCIAL LOADS

THERMAL	ELECTRIC
o BUILDING HEATING:	o BUILDING COOLING AND DEHUMIDIFICATION:
Skin heat losses and solar gains	Skin heat gains and solar gains
Sensible and latent heat gains from people	Sensible and latent heat gains from people
Ventilation heat loss	Sensible and latent heat gains from ventilation
Heat gain from lights	Heat gain from lights
o SERVICE HOT WATER	o LIGHTING
	o LOADS "NOT ELSEWHERE CLASSIFIED" AND REFRIGERATOR LOADS

b. Heating and Cooling Loads

In the calculation of the losses and gains through the building skin, the opaque surfaces were divided into those that are exposed to direct sunlight, and those that are shaded. For shaded surfaces, the heat transfer was calculated each hour from:

$$Q = U \times A \times (TR - TA) \qquad \text{(Eq. III-4)}$$

where U is the conductance, A is the surface area, and TR and TA are the indoor reference and ambient temperatures, respectively. For sunlit surfaces the ambient temperature was replaced by the outside surface temperature, which from the energy balance equation is:

$$TS = \frac{ALPHA \times I \times RBS + TA \times HO + U \times TR}{U + HO} \qquad \text{(Eq. III-5)}$$

where I is the direct normal radiation for the hour. The U values and areas for each building surface and ALPHA, RBS, and HO are defined in

table III-7, which also shows the values assumed in the SOLCEL II runs. Heat transfer through windows from the ambient air was calculated from the UAΔT, and the solar gain was calculated from the equation:

$$Q = GTA \times RBS \times ENT$$

where ENT is the total horizontal radiation and GTA and RBS are defined in table III-7.

The U values used in these calculations were based on the minimum requirements given in the Uniform Building Code. The values were site-specific based on the annual heating degree days for the location, as illustrated in figure III-2, which shows the maximum allowable U values for opaque walls.

The building surface areas were based on the typical building configurations shown in table III-8. The floor areas and number of stories are typical values, according to reference III-9. The window areas for schools and hospitals are the same as those assumed in the RTI report. For the public administration building, the window area was limited to 20 percent of the wall area to comply with the energy conservation code for cooling. To simplify the development, all buildings were assumed square in plan, with a flat roof and one wall facing directly south.

The heat lost in ventilation air was calculated from the following equation:

$$Q = VENT \times (TR - TA) \qquad \text{(Eq. III-7)}$$

where VENT is the product of the building volume, the number of air changes per hour, and the specific heat and density of air. The assumed number of air changes per hour for hospitals, schools, and public administration buildings were 2, 3, and 1, respectively, based on ASHRAE standards.

TABLE III-7. SOLCEL COMMERCIAL LOAD INPUT VALUES

Variable Description	Variable Name	Units	Hospitals Fresno	Hospitals Seattle	Schools Alb.	Schools Boston	Public Admin Phoenix
Solar radiation roof and wall absorptivity	ALPHA		0.60	0.60	0.60	0.60	0.60
Cooling system coefficient of performance	CCOP		2.5	2.5	2.5	2.5	2.5
Flow rate through space heating loop	FMDHL	kg/s	2.86	2.96	3.51	3.62	1.08
Flow rate through service hot water loop	FMDHWL	kg/s	0.35	0.35	2.22	1.34	0.074
Transmittance area product for window glass	GTA	m^2	169	169	54.4	54.4	25.8
Average heat transfer coefficient walls & roof surfaces to ambient	HO	W/m^2C	10.2	10.2	10.2	10.2	10.2
Peak electrical loads "not elsewhere classified"	PKENEC	W	31400	13740	36100	39100	24450
Peak service hot water load (delivered)	PKHWL	W	112900	112900	635600	394300	33210
Peak lighting load	PKLL	W	52800	52800	433000	394000	29240
Average beam radiation tilt factors* for east-facing surfaces in Spring (1), Summer (2), Fall (3), and Winter (4)	RBE (1)		0.99	1.15	0.99	1.15	0.99
	RBE (2)		0.92	0.87	0.92	0.87	0.92
	RBE (3)		0.99	1.15	0.99	1.15	0.99
	RBE (4)		1.08	0.68	1.08	0.68	1.08

*See reference III-12.

TABLE III-7. SOLCEL COMMERCIAL LOAD INPUT VALUE (Continued)

Variable Description	Variable Name	Units	Hospitals Fresno	Hospitals Seattle	Schools Alb.	Schools Boston	Public Admin Phoenix
Average beam radiation tilt factors for south-facing surfaces each season	RBS (1)		0.74	1.09	0.74	1.09	0.74
	RBS (2)		0.13	0.28	0.13	0.28	0.13
	RBS (3)		0.74	1.09	0.74	1.09	0.74
	RBS (4)		2.04	3.37	2.04	3.37	2.04
Ratio Carrier Corp. grand total to room total cooling loads	RGTRT		2.7	2.7	1.3	1.3	1.3
Sensible plus latent heat gain per person	SPLP	W/person	100	100	120	120	120
Temperature of water out of boiler (delivered to loads)	TLD	°C	101.7	101.7	101.7	101.7	101.7
Thermostat set points for cooling daytime (1) and nighttime (2) - Sundays all hours (2)	TRC (1)	°C	23.9	23.9	25	25	25
	TRC (2)		23.9	23.9	50	50	50
Thermostat set points for heating	TRH (1)	°C	23.9	23.9	21.1	21.1	21.1
	TRH (2)		23.9	23.9	13.9	13.9	13.9
Conductivity area product indoor space to outside surface of roof	UACR	W/C	1668	1357	1377	1208	350
UA from indoor space to outside surface of east (or west)-facing walls excluding glass	UAEW	W/C	291	158	161	95	42

TABLE III-7. SOLCEL COMMERCIAL LOAD INPUT VALUE (Concluded)

Variable Description	Variable Name	Units	Hospitals Fresno	Hospitals Seattle	Schools Alb.	Schools Boston	Public Admin Phoenix
UA for shaded wall areas (N & E or W) including glass	UASHWG	W/C	3083	2623	1114	1006	476
UA for sunlit glass (S & E or W)	UASLG	W/C	2519	2519	812	812	384
UA indoor space to outside surface of south-facing walls excluding glass	UASW	W/C	291	158	161	95	42
U value ceiling/roof consistent with UACR	UCR	W/m^2C	0.579	0.471	0.511	0.448	0.579
U value east (or west)-facing walls consistent with UAEW	UEW	W/m^2C	0.636	0.344	0.636	0.375	0.346
Perimeter UA to depth of 2 feet (0.61 m)	UPAS	W/C	280	173	192	156	170
U value south-facing walls consistent with UASW	USW	W/m^2C	0.636	0.344	0.636	0.375	0.346
Ventilation heat transfer coefficient (see text)	VENT	W/C	24880	24880	37320	37320	12440

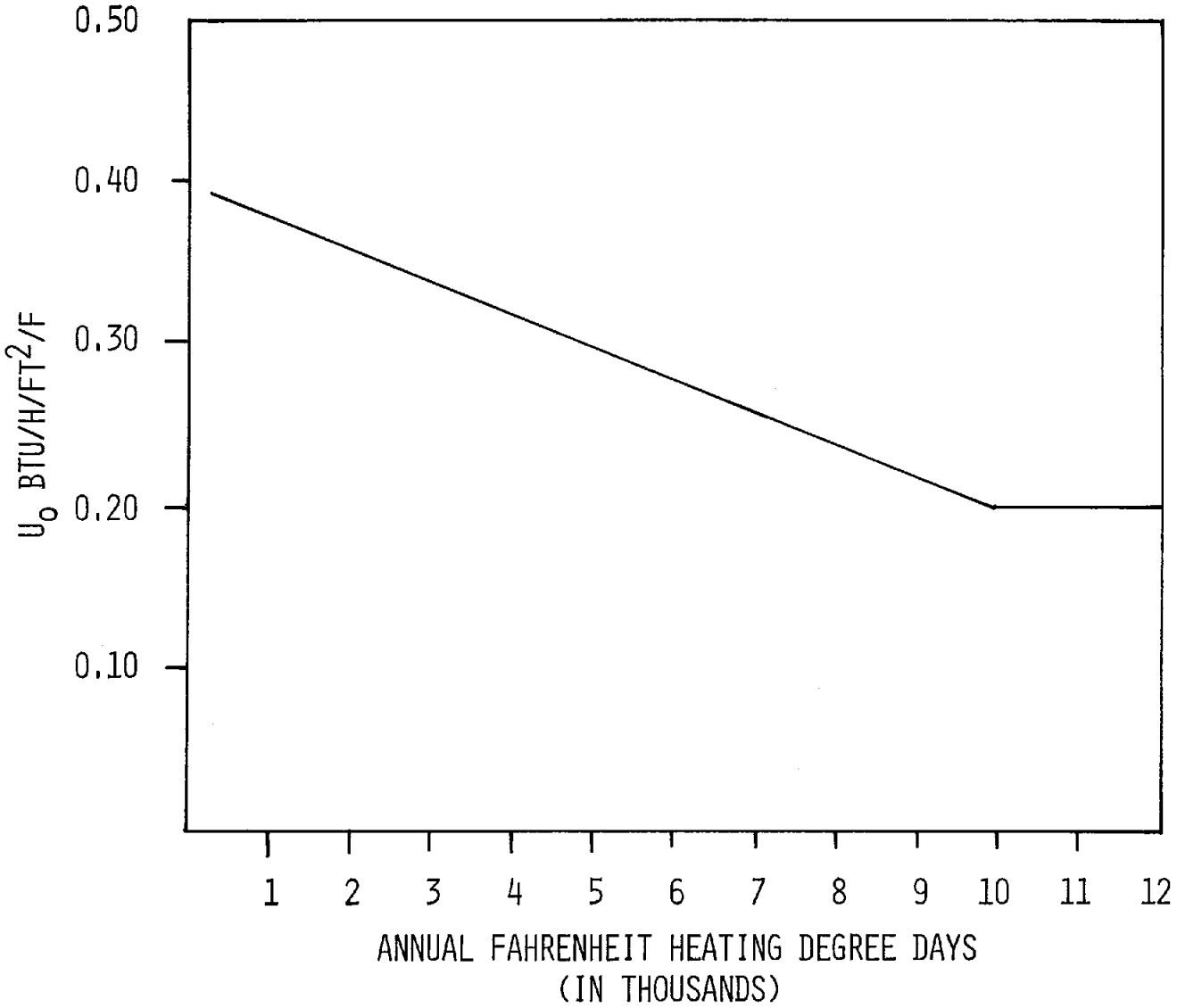

U_o WALLS - HEATING

FOR ALL BUILDINGS OTHER THAN RESIDENTIAL WHICH ARE THREE STORIES OR LESS

REPRODUCED FROM THE UNIFORM BUILDING CODE
1982 EDITION, COPYRIGHT 1982, WITH PERMISSION
OF THE PUBLISHER, THE INTERNATIONAL CONFERENCE
OF BUILDING OFFICIALS

BDM/A-82-458-TR-R1

Figure III-2. Uniform Building Code U Values for Walls

TABLE III-8. TYPICAL BUILDING STRUCTURES

Application	Floor Area in m^2 (sq ft)	Number of Stories	Window/Wall Area (%)
Hospitals	11524 (124,000)	4	30
Schools	5390 (58,000)	2	20
Public Administration	1208 (13,000)	2	20*

*Extreme climates (Phoenix, AZ)

When warm ventilation air is cooled by a refrigeration unit, the latent heat of the moisture in the air must be removed along with the sensible heat. The latent load depends on the ambient humidity, for which no hourly data were available. Therefore, in the cooling calculation a factor (RGTRT) was applied to the sum of the other cooling loads to account for the ventilation load. This factor was developed from typical cooling loads published by the Carrier Corporation (ref. III-10). The values assumed were 2.7, 1.3, and 1.3 for hospitals, schools, and public administration buildings, respectively.

The heat added to the space by the occupants also consists of sensible and latent components. Table III-7 shows the watts per person gains (SPLP) and the peak occupancies (PKOCC) that were assumed in this calculation. Both were obtained from the ASHRAE reference. Hourly occupancy profiles, in terms of peak percentage, were obtained from area-weighted averages of profiles given in the RTI report and reference III-11. The occupancy profiles used in the SOLCEL II simulations are shown in table III-9. The schools were assumed vacant in the summer.

The lighting load enters into the load calculations twice --first as an electrical load, and then as an internal heat gain affecting the heating and cooling loads.

c. Lighting, Service Hot Water, and NEC Loads

The peak values and profiles for lighting and service hot water loads for hospitals and schools were found in the RTI report. The

TABLE III-9. OCCUPANCY PROFILES (PERCENT OF PEAK)

Hour	HOSPITALS Weekdays	HOSPITALS Saturdays	HOSPITALS Sundays	SCHOOLS Weekdays	SCHOOLS Saturdays	SCHOOLS Sundays	PUBLIC ADMIN Weekdays	PUBLIC ADMIN Saturdays	PUBLIC ADMIN Sundays
1	51	51	51	3	0	0	0	0	0
2				0					
3									
4									
5									
6	51	51	51	0	0	0	0	0	0
7	57	58	57	0	0	0	10	10	5
8	61	61	57	5	0		20	10	
9	65	63	60	73	9		95	30	
10	76	63	60	100	9				
11	84	63	60	99	9				
12	84	63	60	96	9	0	95	30	5
13	83	63	60	96	9	0	50	10	5
14	84	64	60	95	0		95		
15	84	64	61	95					
16	84	60	61	62					
17	84	60	61	32			95	10	
18	80	60	60	17	0	0	30	5	5
19	59	58	58	17	0	0	10	5	0
20	52	52	52	22			10	0	
21	52	52	52	19			10		
22	51	51	51	10			10		
23	51	51	51	3			5		
24	51	51	51	3	0	0	5	0	0

peak values are given in table III-7, and the profiles are given in tables III-10 and III-11.

The RTI report also gives data for "other loads," which were assumed to be all-electric. However, the Faucett report indicates that for hospitals, the loads "not elsewhere classified" (NEC) include thermal as well as electrical energy consumption. A method for separating these energy loads was needed and was developed, based on other data in the Faucett report. According to that report, the electrical portion of the annual NEC load plus the refrigerating load for hospitals is 13 percent of the total annual electrical load. It follows that, together, these loads are 15 percent of the sum of the cooling and lighting loads. Since the RTI and Faucett consumption data do not specify the portion of the space conditioning load that is due to cooling, the annual cooling and lighting loads were determined from a SOLCEL II run. Then the annual NEC (and refrigerating) loads were calculated as 15 percent of those loads. The peak NEC electrical load was then obtained using the annual value divided by the percent-hours per year based on the hourly profiles as was done in the RTI report for the other peak values. The thermal portion of the NEC loads for hospitals includes cooking, and energy losses not pertinent to the PV-T analysis, so those loads were neglected. The NEC or "other load" data for schools and public administration buildings was totally electric, so the approach described above was not required for those applications. The peak NEC values assumed in the simulation are given in table III-7, and the NEC hourly profiles are included in tables III-10 and III-11.

The public administration building presented a unique problem because the number of facilities in each region of the country was not known. Therefore, the energy consumption per facility could not be found from the Faucett data, as was done by RTI for hospitals and schools. To circumvent this problem, annual usage values were obtained from an energy audit of a public administration building in Phoenix, Arizona (ref. III-12). The consumption summary from that audit is reproduced as table III-12. These values were scaled by floor area to correspond to the

TABLE III-10. HOSPITAL LOAD PROFILES (PERCENT OF PEAK)

Hour	LIGHTING Weekday	LIGHTING Saturday	LIGHTING Sunday	WATER HEATING Weekday	WATER HEATING Saturday	WATER HEATING Sunday	OTHER LOAD Weekday	OTHER LOAD Saturday	OTHER LOAD Sunday
1	19	19	19	12	12	12	79	79	79
2	19	19	19	12	12	12	79	79	79
3	19	19	19	12	12	12	79	79	79
4	19	19	19	12	12	12	79	79	79
5	19	19	19	14	14	14	79	79	79
6	19	19	19	17	17	17	79	79	79
7	26	26	25	45	44	44	84	84	84
8	67	67	63	69	56	56	91	87	86
9	76	75	74	67	59	61	90	89	88
10	88	75	74	52	66	66	92	90	88
11	100	75	74	63	57	55	95	92	90
12	100	75	74	68	58	56	95	91	90
13	100	75	74	72	63	61	94	91	90
14	100	75	74	75	72	70	95	91	90
15	100	75	74	66	59	58	95	91	90
16	100	75	74	49	41	40	97	93	91
17	100	75	74	51	42	41	96	91	90
18	91	65	65	51	43	39	96	91	91
19	90	65	65	63	55	53	91	91	91
20	58	57	57	41	37	35	90	90	89
21	58	57	57	22	18	18	90	88	87
22	57	56	56	16	16	14	83	83	82
23	56	56	56	14	7	5	82	82	82
24	19	19	19	14	7	5	83	83	81
% hours/day	1500	1257	1243	977	879	856	2113	2072	2056

TABLE III-11. HIGH SCHOOL LOAD PROFILES (PERCENT OF PEAK)

	LIGHTING			WATER HEATING			OTHER LOADS		
Hour	Weeday	Saturday	Sunday	Weekday	Saturday	Sunday	Weekday	Saturday	Sunday
1	7	3	3	5	3	3	0	0	0
2	7	3	3	5	3	3	0	0	0
3	7	3	3	5	3	3	0	0	0
4	7	3	3	5	3	3	0	0	0
5	7	3	3	5	3	3	0	0	0
6	7	3	3	5	3	3	0	0	0
7	7	3	3	5	3	3	0	0	0
8	25	6	3	10	3	3	100	0	0
9	78	13	6	34	3	5	100	0	0
10	86	13	6	60	5	5	100	0	0
11	86	13	6	63	5	5	100	0	0
12	91	13	6	72	5	5	100	0	0
13	79	13	6	79	5	5	100	0	0
14	74	6	6	83	3	5	100	0	0
15	78	6	6	61	3	3	100	0	0
16	71	6	6	65	3	3	100	0	0
17	56	3	3	10	3	3	100	0	0
18	47	3	3	10	3	3	0	0	0
19	28	3	3	19	3	3	0	0	0
20	28	3	3	25	3	3	0	0	0
21	24	3	3	22	3	3	0	0	0
22	24	3	3	22	3	3	0	0	0
23	9	3	3	12	3	3	0	0	0
24	5	3	3	3	9	3	0	0	0
% hours/day	938	134	96	691	80	84	1000	0	0

TABLE III-12. TABULATION OF SYSTEMS ENERGY CONSUMPTION FOR THE PHOENIX, ARIZONA PUBLIC ADMINISTRATION BUILDING

For Period: December, 1978 to November, 1979.

SYSTEM	ELECTRICAL (kW Hr)	NATURAL GAS (kW Hr Thermal)	PERCENT OF TOTAL ELECTRICAL	PERCENT OF TOTAL THERMAL	kW Hr USE PER M^2
HEATING		74,230		54.0	40
COOLING (1)	152,289		42.0		82.3
AIR DISTRIBUTION	48,225		13.3		26
WATER DISTRIBUTION	1,090		0.3		0.6
DOM. HOT WATER		63,300		46.0	34.2
LIGHTING	100,589		27.7		54.3
ELEVATORS					
MISC. USES & EQUIP.	60,450		16.7		32.7
ANNUAL CALCULATED TOTALS (2)	362,643	137,530	100	100	270.2
ANNUAL METERED TOTALS (2)	362,643	137,530	100	100	270.2

BUILDING GROSS AREA: 1851 m^2 (19920 ft^2)

(1) Includes refrigeration, cooling tower, air conditioning, water pumps and fans
(2) Annual calculated totals should equal annual metered totals by reconciling any degree day variations and by accounting for reheat, distribution losses, etc.

typical building in this study. Occupancy and energy use profiles were taken from reference III-11. The peak load values for lighting, water heating, and NEC loads are given in table III-7, and the corresponding profiles are shown in table III-13.

d. Indoor Reference Temperatures

As shown in table III-7, indoor reference temperatures were specified for both heating and cooling (TRH and TRC), and for day and night where appropriate. The logic used in SOLCEL II to calculate the heating or cooling load was designed to select the appropriate indoor reference temperature and the appropriate method of determining the ventilation load (see above) regardless of season. First, the heating load was calculated using TRH. If that load was negative, then the heating load was calculated again using TRC. If heating would be needed to raise the reference temperature to TRC then both the heating and cooling loads were set to zero. If heating was not needed--that is, the gains were high enough to raise the indoor temperature to TRC--then the cooling required to maintain the indoor space at TRC was determined (using the RGTRT method). Thus, both heating and cooling could occur during any day of any season depending on the ambient conditions and internal loads, and neither would be required if conditions were mild.

e. Thermal System Configuration and Flow Rates

A schematic of the thermal flow loops for a PV-T system applied to a commercial building is shown in figure III-3. The auxiliary boiler is typically a low pressure unit designed to deliver water at approximately 102°C (215°F) (TLD). The pump for the space heating system is usually designed to provide a constant flow rate FMDHL, sufficient to provide a minimum of 53°C (120°F) at the last heater in the line at peak load. At less than peak load, the space heaters are partially bypassed. The return temperature, T1, will therefore approach 53°C only near the peak heating load; at other times it will be higher.

Service or domestic hot water is drawn from a storage tank that is maintained at a set temperature. When the tank temperature drops below that point, water is circulated from the boiler through a heat

Table III-13. PUBLIC ADMINISTRATION BUILDING LOAD PROFILES (PERCENT OF PEAK)

	LIGHTING			WATER HEATING			NEC		
Hour	Weekdays	Saturdays	Sundays	Weekdays	Saturdays	Sundays	Weekdays	Saturdays	Sundays
1	5	5	5	5	5	4	0	0	0
2									
3									
4									
5	5			5	5	4			
6	10	5	5	8	8	7	0	0	0
7	10	10	5	7	7	4	50	0	0
8	30	10		19	11		100	50	
9	90	30		35	15				
10	90	30		38	21				
11	90	30		39	19	4			
12	90	30	5	47	23	6	100	50	0
13	80	15	5	57	20	6	100	50	0
14	90			54	19	9			
15	90			34	15	6			
16	90			33	12	4			
17	90	15		44	14	4		50	
18	50	5	5	26	7	4	100	0	0
19	30	5	5	21	7	4	100	0	0
20	30			15	7	4	0		
21	20			17	7	4			
22	20			8	9	7			
23	10			5	5	4			
24	5	5	5	5	5	4	0	0	0
% hours/day:	1040	280	120	537	256	113	1200	500	0

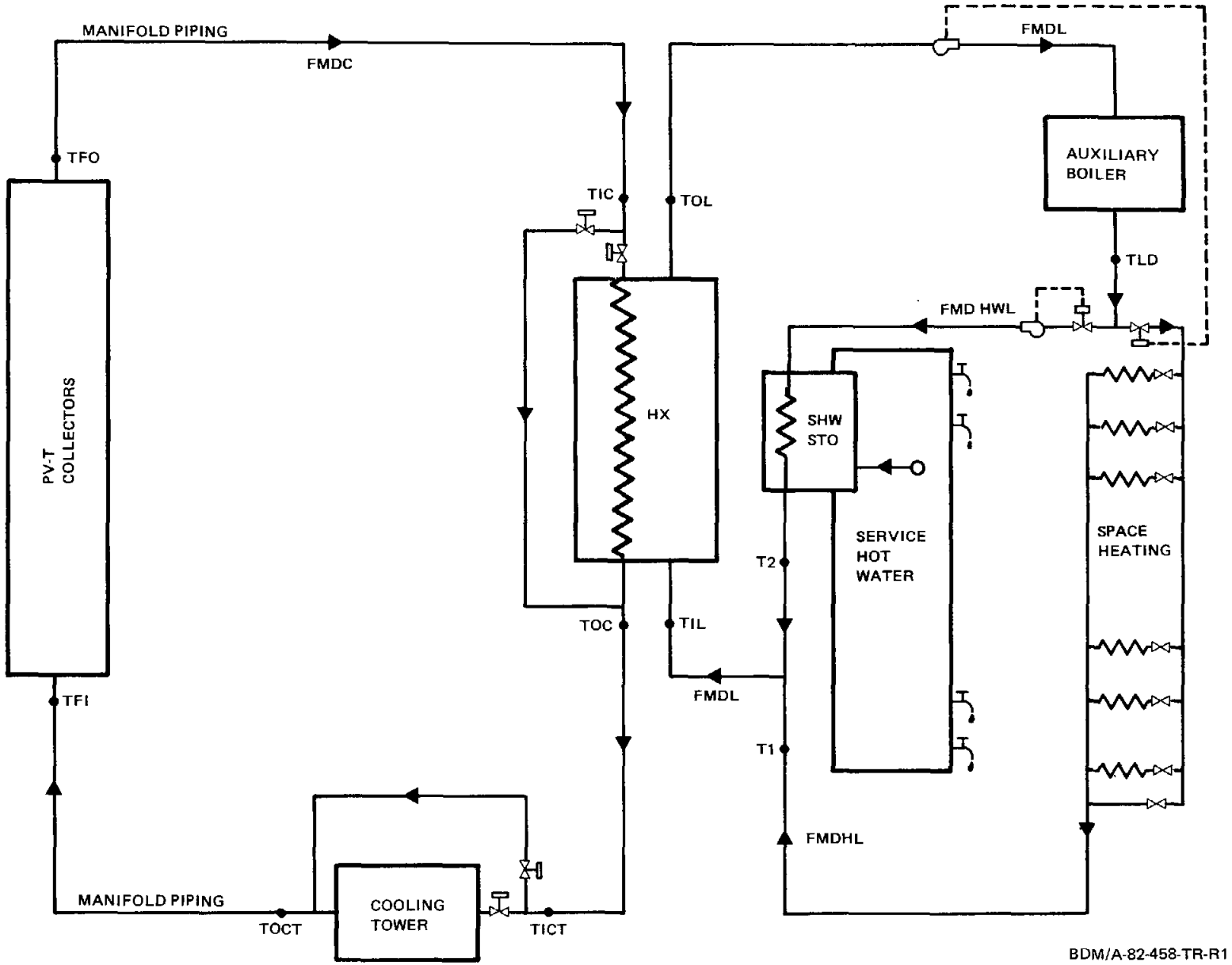

Figure III-3. Thermal System Configuration for PV-T Application to Commercial Buildings

exchanger in the tank. As in the case of the space heating system, the flow rate, FMDHWL, is constant and designed to meet the maximum load, in this case at a minimum temperature of about 44°C (110°F). Thus, the outlet from the heat exchanger, T2, depends on the service hot water load. According to the service hot water load profiles shown in tables III-10, III-11, and III-13, the service hot water loop operates at least for a short time each hour, probably just to make up heat losses from the tank.

To model the above modes of operation, the load flow rates used in the SOLCEL II program were calculated as follows:

$$FMDHL = \frac{HL\ max}{CFL \times (TLD - T1_{min}) \times 3600} \frac{(kg)}{(sec)}$$

$$FMDHWL = \frac{HWL\ max}{CFL \times (TLD - T2_{min}) \times 3600} \frac{(kg)}{(sec)} \qquad \text{(Eq. III-9)}$$

HL and HWL are the space heating and service hot water loads, respectively, and CFL is the specific heat of the fluid on the load side of the heat exchanger (the boiler water). The flow rates assumed for each commercial load application are given in table III-7 above. The return temperature to the collector heat exchanger, TIL, is calculated in SOLCEL II from:

$$TIL = TLD - \frac{HL + HWL}{CFL \times FMDL \times 3600} \qquad \text{(Eq. III-10)}$$

The total flow rate is:

$$FMDL = FMDHL + FMDHWL \qquad \text{(Eq. III-11)}$$

f. Results: Annual and Hourly Loads

Table III-14 shows the annual loads for each application as calculated by the SOLCEL II commercial load routine. Figures III-4

TABLE III-14. ANNUAL COMMERCIAL LOADS (MWh)

		THERMAL			ELECTRICAL			
APPLICATION	SITE	SPACE HEATING	SERVICE HOT WATER	TOTAL	COOLING	LIGHTS	NEC	TOTAL
HOSPITAL	FRESNO, CA	2342	520	2861	1246	275	241	1762
	SEATTLE, WA	3868	520	4388	426	275	105	807
SCHOOL	ALBUQUERQUE	2430	1225	3655	360	833	71	1264
	BOSTON	2964	739	3703	209	758	76	1044
PUBLIC ADMIN.	PHOENIX	293	71	363	85	85	92	262

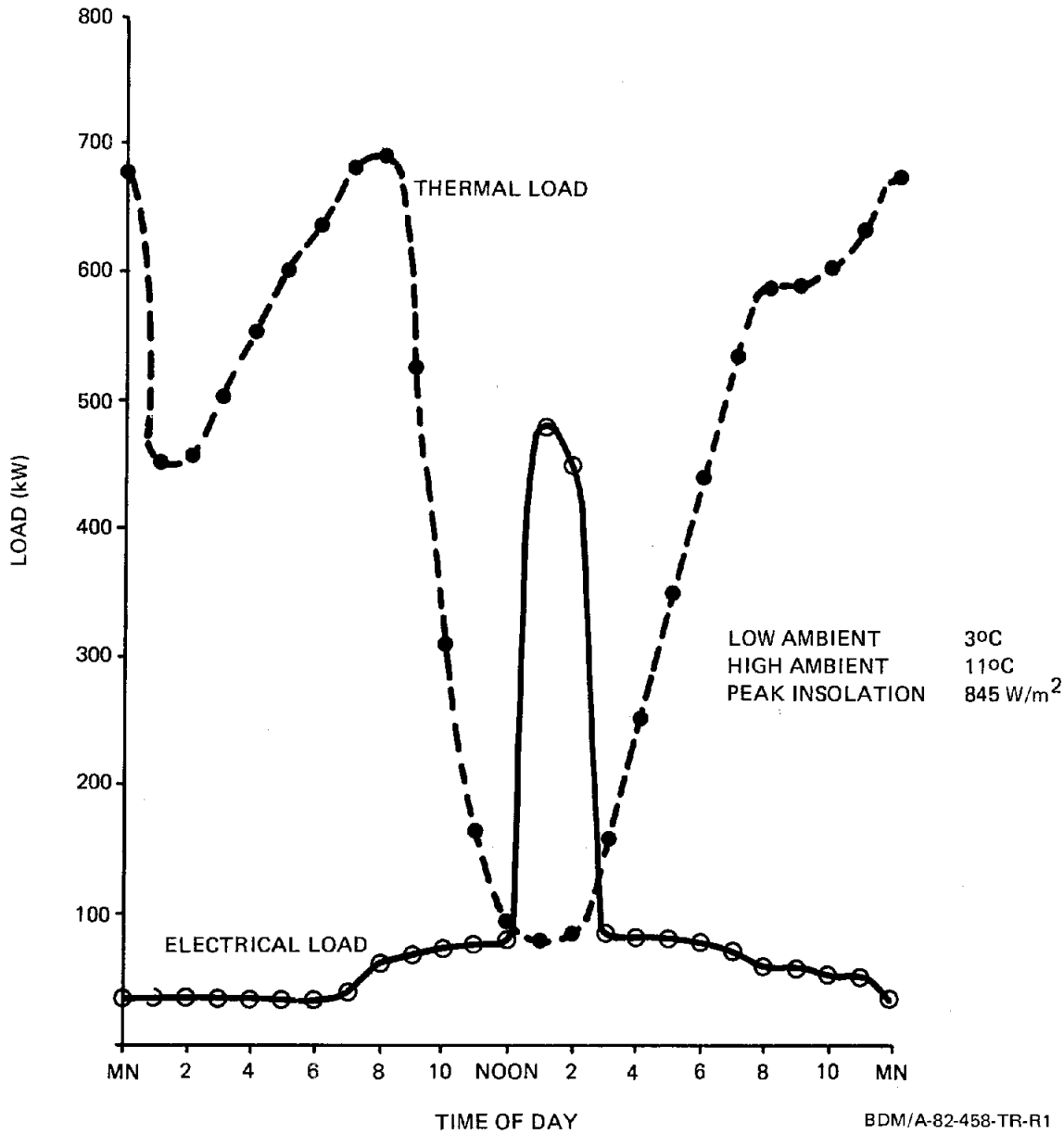

Figure III-4. Fresno, California Hospital Load Profile on a Cold, Clear Winter Day (350)

through III-13 show the electric and thermal load profiles for typical sunny days.

C. INDUSTRIAL SECTOR ANALYSIS

Energy use data from the Drexel Report (ref. III-2) provided the basis for ranking industrial processes for PV-T energy system application within each of 11 census regions. The Drexel report contains an energy analysis of 108 industrial processes which account for approximately 72 percent of U.S. industrial energy consumption. A process diagram is provided for each industrial process followed by a table listing process unit operations and characterizing each process stream by temperature, energy and mass flow. These data were supplemented by process information from the Inter Technology report (ref. III-13). Of the 108 industrial processes analyzed in the Drexel report, 71 were used in the PV-T ranking data base. Thirty-three processes were not considered because they either did not use electricity, or did not use a boiler to provide thermal energy. Four process energy use tables were incomplete in the published report, and one process was identified as being phased out in favor of an alternate process able to meet EPA clean water standards. Energy use data were complemented by production figures for 1977 from Census of Manufacturing reports (ref. III-14) and work schedule information obtained from process descriptions and consultants.

The second element needed to rank industrial processes was the cost of the energy used in each process. This information was obtained from the 1978 Annual Survey of Manufacturers, Fuels and Electric Energy Consumed report (ref. III-15). Data on the quantity of fuel and electricity consumed and the cost of that energy were collected by state for each three-digit SIC code identifying a particular industrial process in the PV-T data base. These data were aggregated by region. The 48 contiguous states were divided into 11 regions as shown in table III-15. These groupings reflect placement of SOLMET sites, geographic proximity, and average energy prices. Specifically, California was separated from

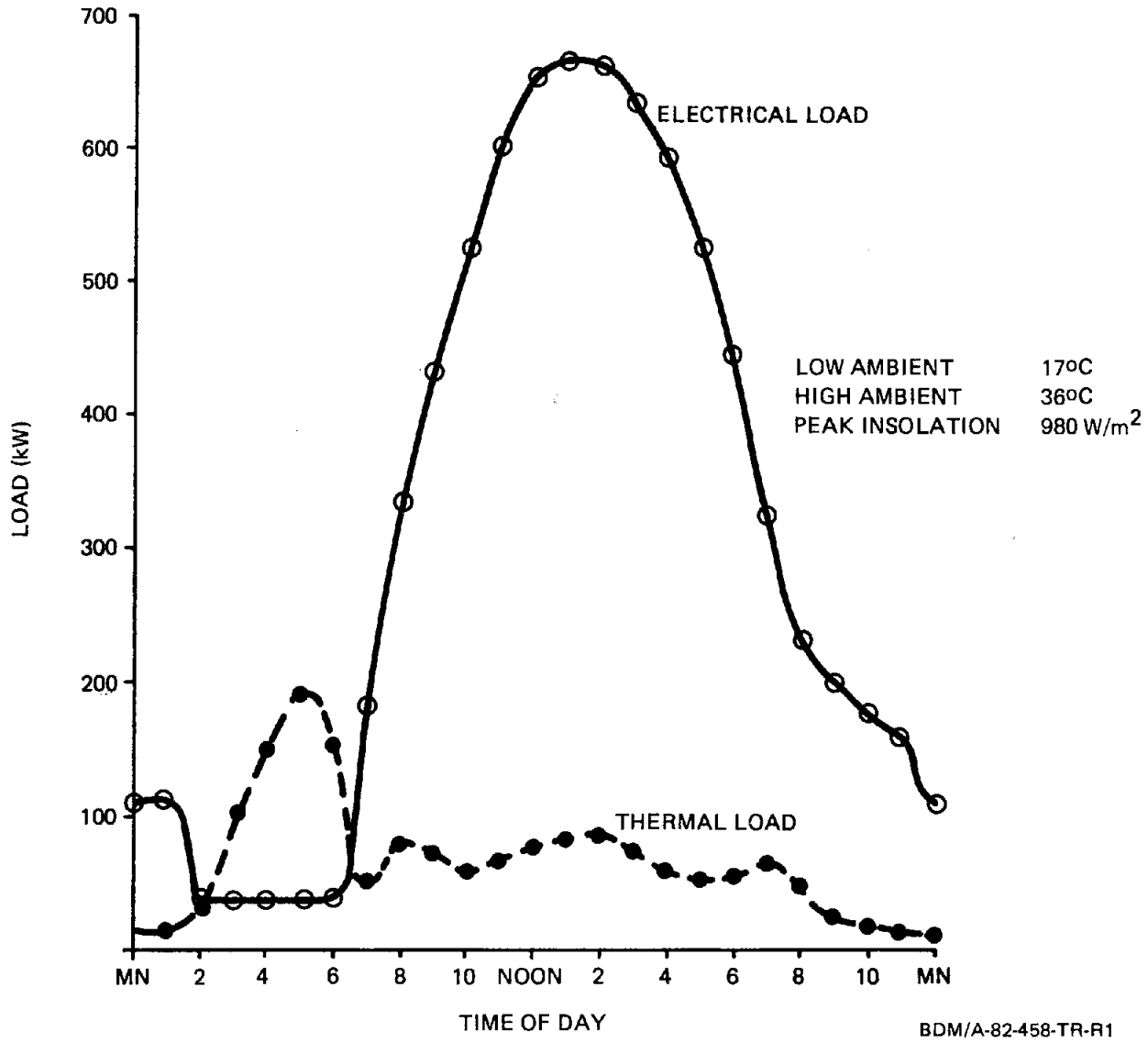

Figure III-5. Fresno, California Hospital Load Profile on a Warm, Clear Summer Day (160)

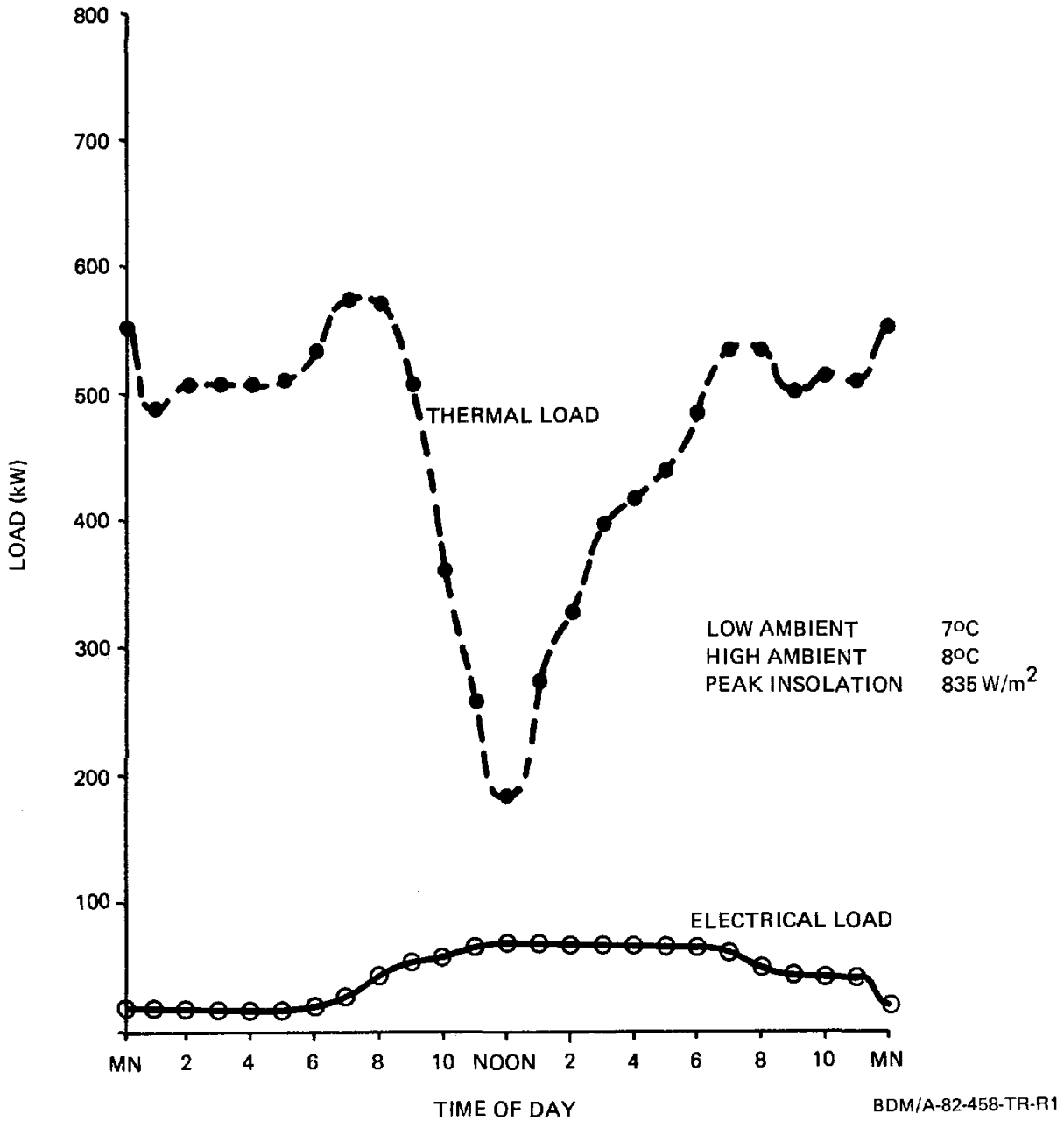

Figure III-6. Seattle, Washington Hospital Load Profile on a Cold, Clear Winter Day (350)

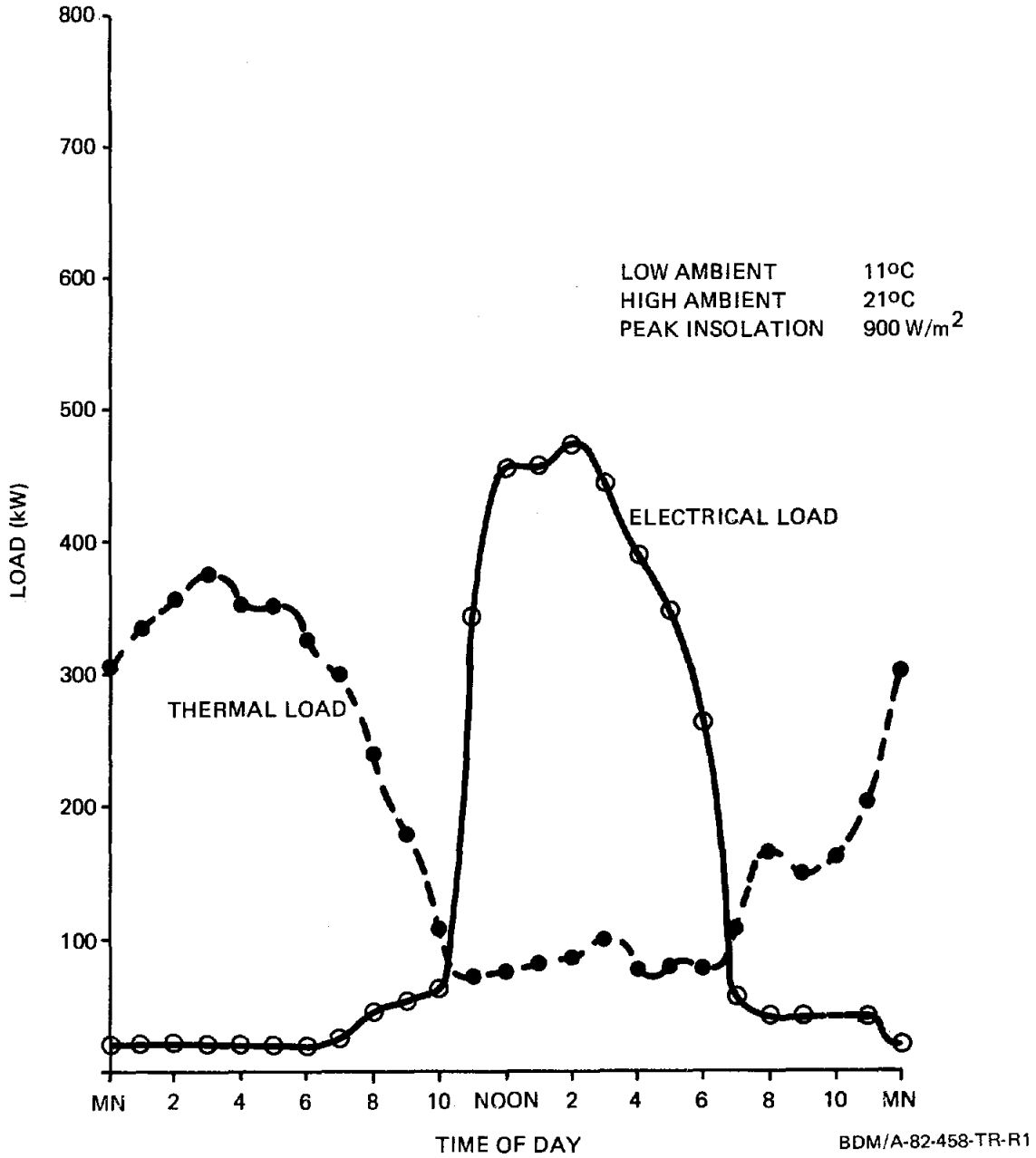

Figure III-7. Seattle, Washington Hospital Load Profile on a Warm, Clear Summer Day (173)

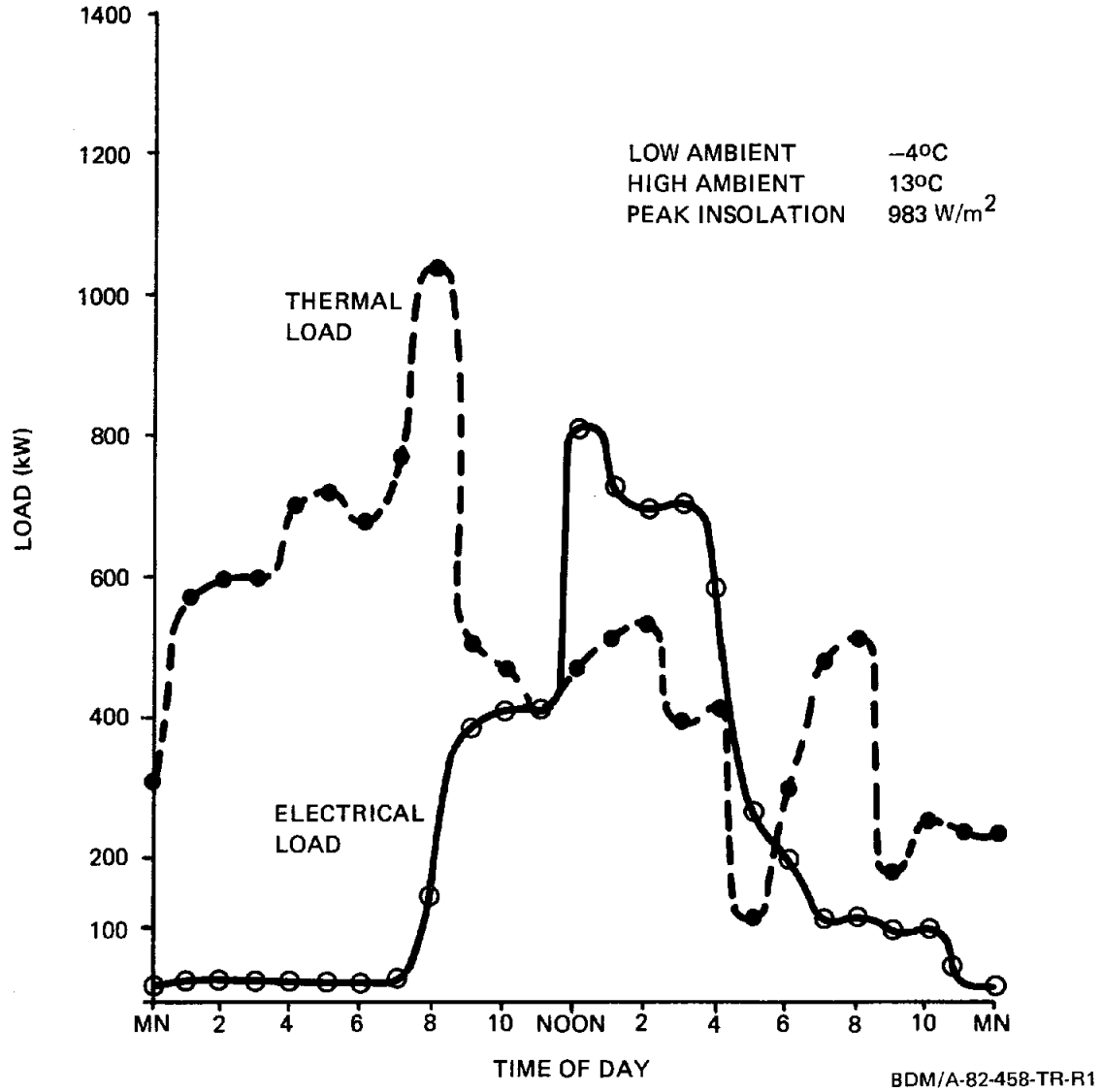

Figure III-8. Albuquerque, New Mexico School Load Profile on a Cool, Clear Winter Day (340)

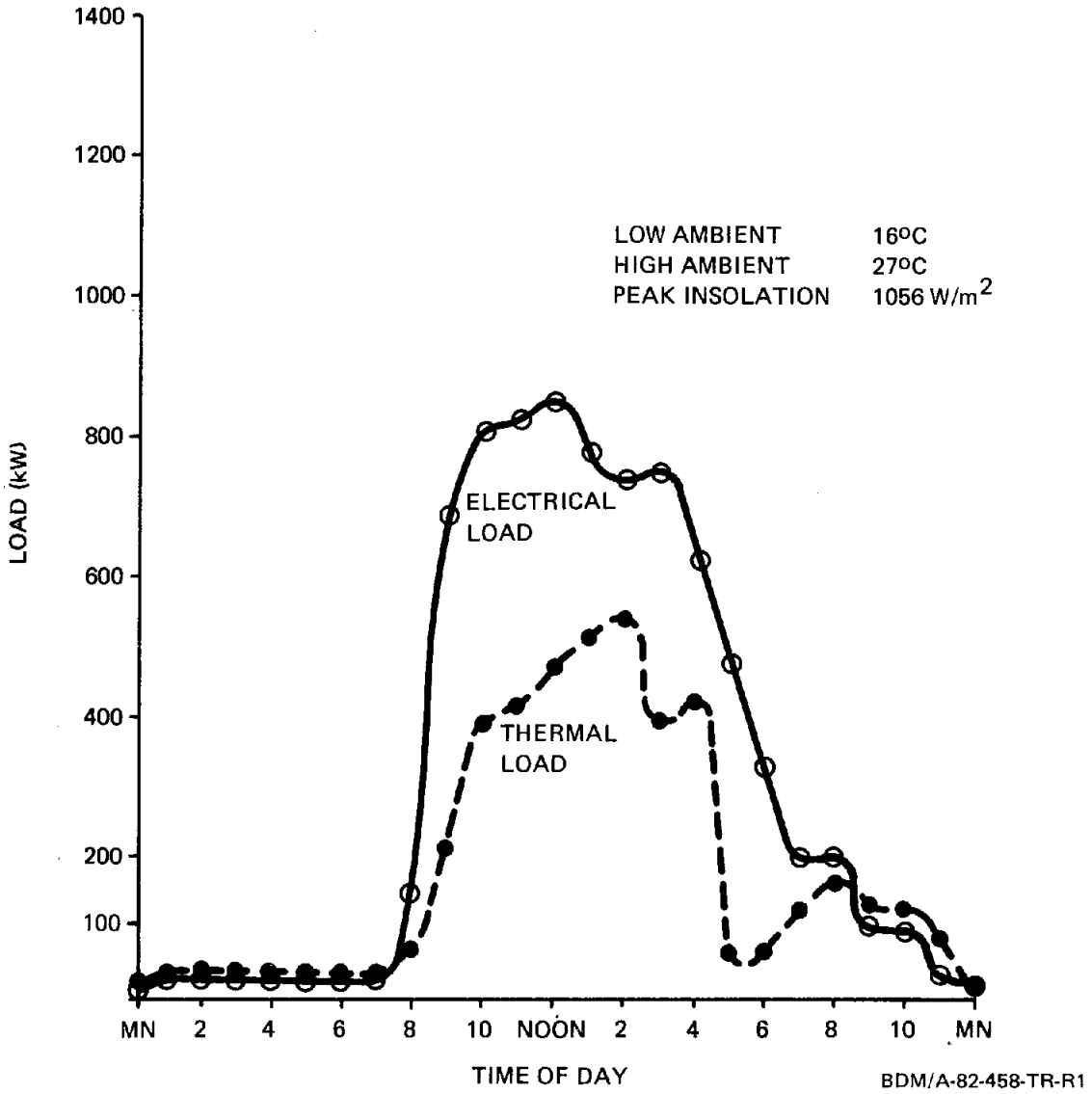

Figure III-9. Albuquerque, New Mexico School Load Profile on a Warm, Clear Fall Day (250)

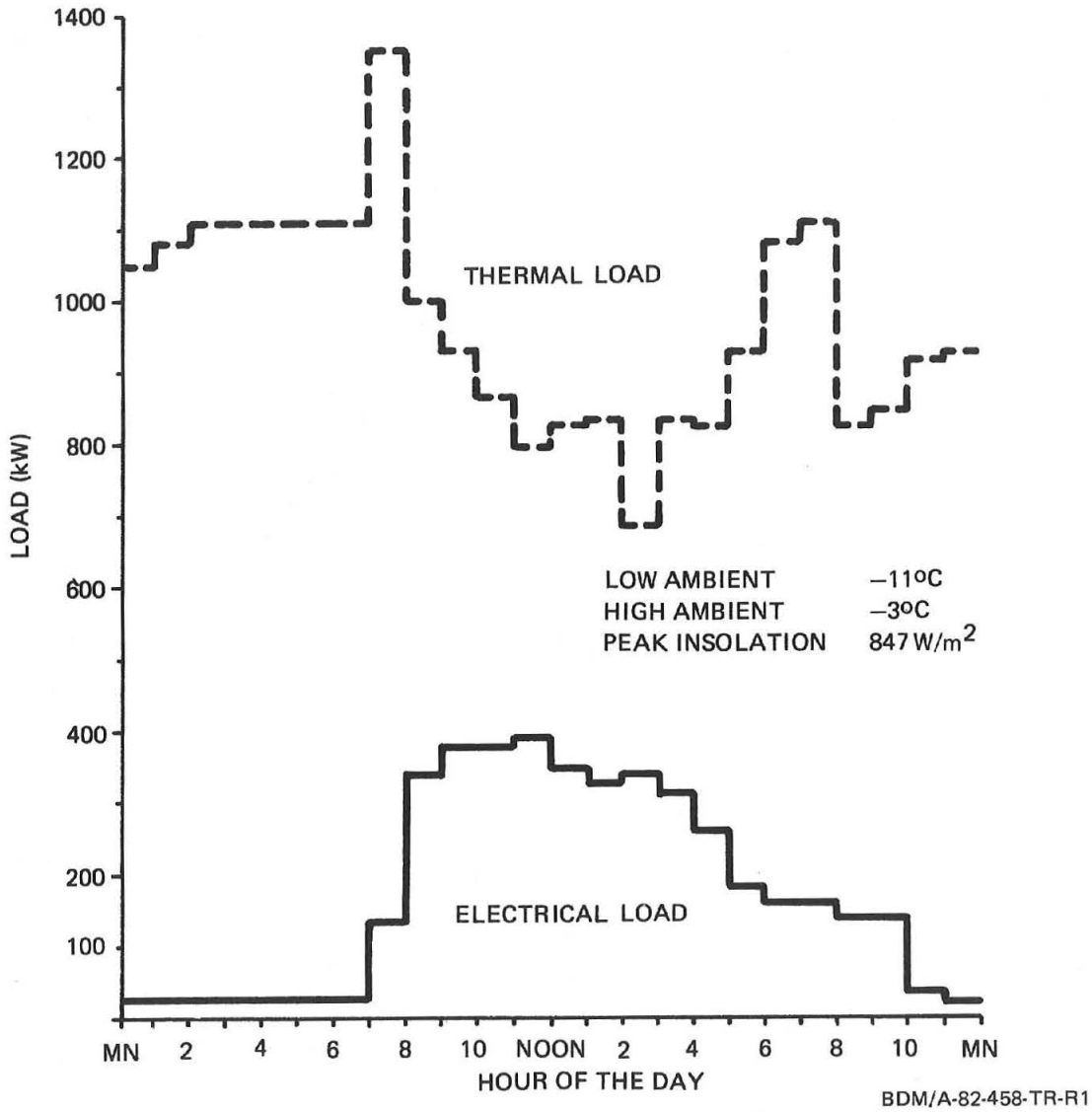

Figure III-10. Boston, Massachusetts School Load Profile on a Cold, Clear Winter Day (350)

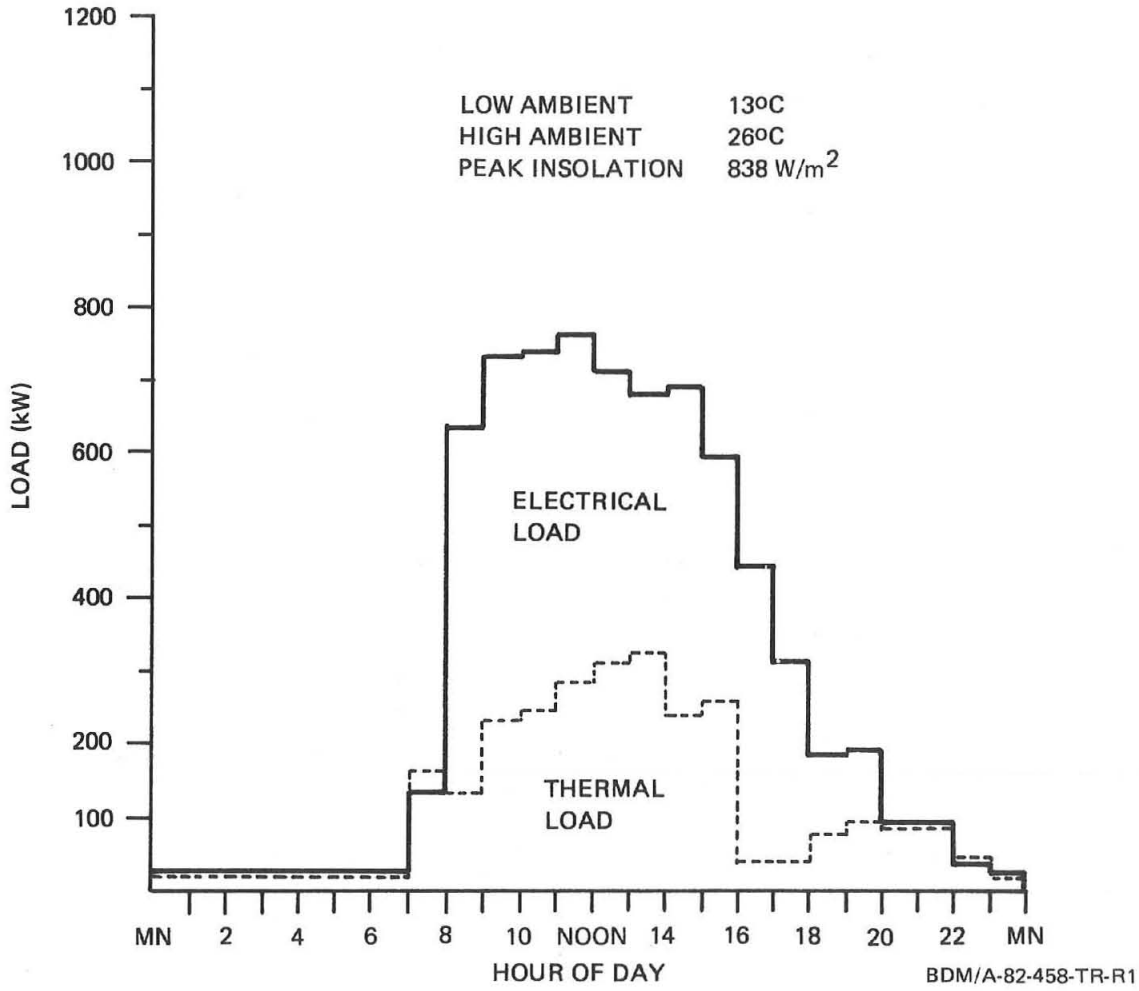

Figure III-11. Boston, Massachusetts School Load Profile on a Warm, Clear Fall Day (251)

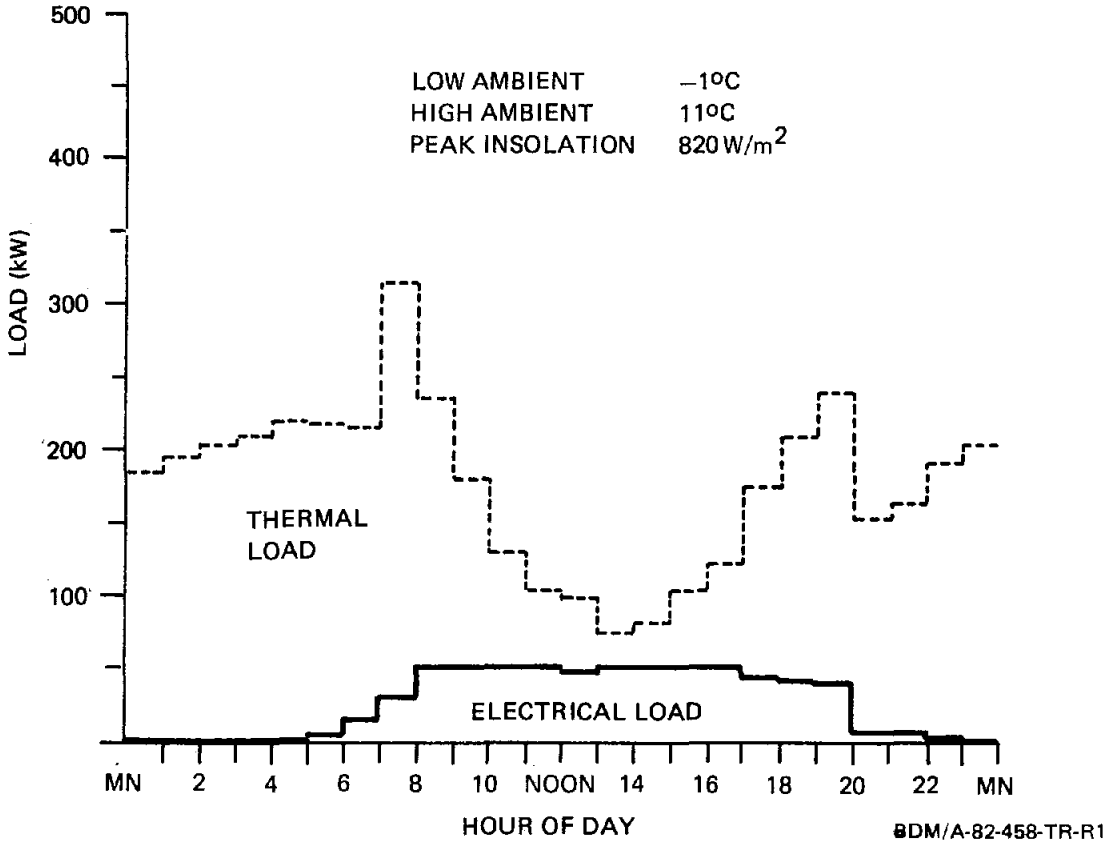

Figure III-12. Phoenix, Arizona Public Administration Building Load Profile on a Cool, Clear Winter Day (361)

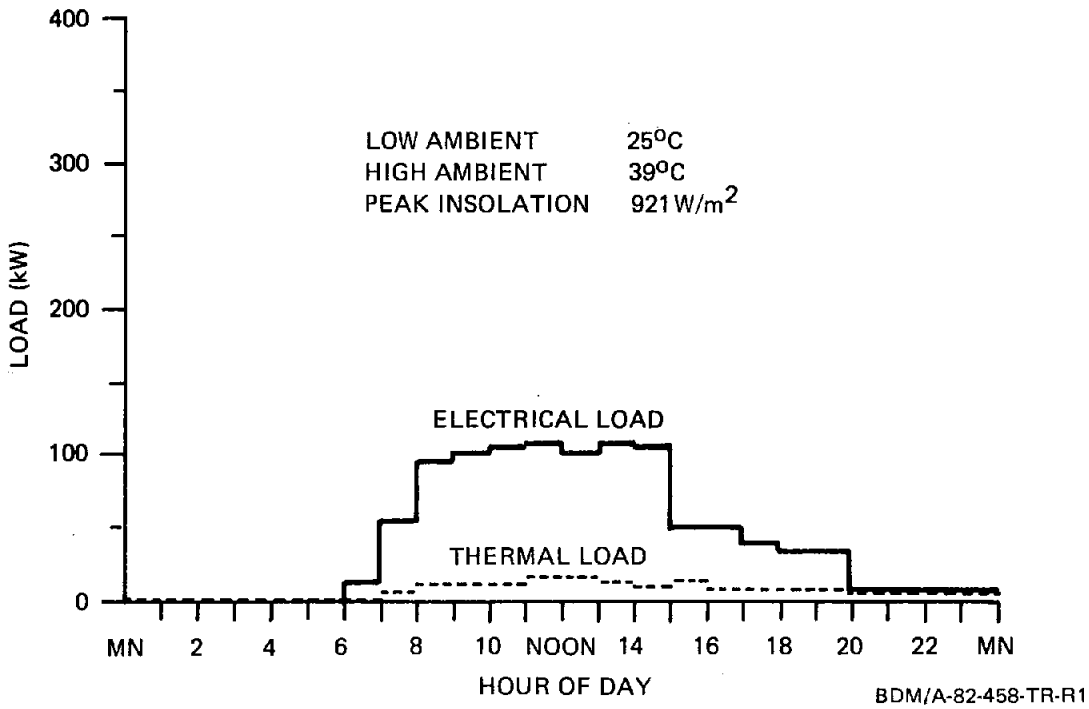

Figure III-13. Phoenix, Arizona Public Administration Building Load Profile on a Hot, Clear Summer Day (176)

TABLE III-15. INDUSTRIAL REGIONS

New England

Maine
New Hampshire
Vermont
Massachusetts
Rhode Island
Connecticut

Middle Atlantic

New York
New Jersey
Pennsylvania

South Atlantic

Delaware
Maryland
D.C.
Virginia
West Virginia
North Carolina
South Carolina
Georgia
Florida

East North Central

Ohio
Indiana
Illinois
Michigan
Wisconsin

East South Central

Kentucky
Tennessee
Alabama
Mississippi

West North Central

Minnesota
Iowa
Missouri
North Dakota
South Dakota
Kansas
Nebraska

West South Central

Arkansas
Louisiana
Oklahoma
Texas

North Mountain

Montana
Idaho
Wyoming
Colorado

South Mountain

New Mexico
Arizona
Utah
Nevada

North Pacific

Washington
Oregon

South Pacific

California

the other Pacific states to avoid averaging the low cost of electricity in Oregon and Washington with the high cost in California. An average price per kilowatt hour of electricity and fuel consumed were calculated for each region for each three-digit SIC code. A set of typical values is shown in table III-16.

The final element needed to rank industrial processes within regions was the amount of solar energy available to a PV-T system. An average annual insolation for a fully tracking collector was determined for each region using data from Solmet sites located within the region. These insolation values are shown in table III-3.

The energy use data, cost data, and regional insolation data were entered into a computerized data base. A calculation program, based on the RTI methodology (ref. III-1), was developed to determine a ranking factor for each industrial application and within each region. This ranking factor is defined in equation III-2.

To determine the annual energy supplied, the total annual electrical and thermal load requirements were determined from the data in the Drexel Report. The electrical load consisted of purchased electricity (E_1) and electricity generated on-site (E_2), using a specified quantity of fossil fuel (F_2). The thermal load was determined with and without recovery of heat from wastewater streams. In the case of no heat recovery, the thermal load was obtained by summing the energy required to heat the process stream from make-up water temperature or condensate temperature to the required load temperature. Thus:

$$Q_1 = \sum_{n=1}^{N} \dot{M}_n C_p (T_n - T_o) \qquad \text{(Eq. III-12)}$$

$$Q_2 = \sum_{j=1}^{J} \dot{M}_j C_p (212 - T_c) + \dot{M}_j (h_{s,j} - h_f) \qquad \text{(Eq. III-13)}$$

TABLE III-16. ENERGY COST - SIC 203 (FRUIT & VEGETABLE PROCESSING)

Census Region	State	FUEL Quantity (10^9 kWh)	FUEL Cost (10^6\$)	FUEL Unit Cost (¢/kWh)	ELECTRICITY Quantity (10^6 kWh)	ELECTRICITY Cost (10^6\$)	ELECTRICITY Unit Cost (¢/kWh)
New England							
	Maine	0.557	4.0		77.7	2.6	
	New Hampshire						
	Vermont						
	Massachusetts	0.117	1.0		24.1	1.0	
	Rhode Island						
	Connecticut						
		0.674	5.0	0.742	101.8	3.6	3.54
Middle Atlantic							
	New York	1.55	12.0		258.8	8.6	
	New Jersey	1.14	9.3		188.8	7.4	
	Pennsylvania	1.46	11.5		254.5	8.5	
		4.15	32.1	0.773	702.1	24.5	3.49
South Atlantic							
	Delaware	0.117	1.2		31.2	1.3	
	Maryland	0.264	2.1		52.0	2.0	
	D.C.						
	Virginia	0.264	1.8		58.8	1.9	
	West Virginia						
	North Carolina						
	South Carolina						
	Georgia	0.322	2.3		99.9	3.3	
	Florida	3.63	21.0		608.4	19.5	
		4.6	28.4	0.618	850.3	18.0	2.12
East North Central							
	Ohio	1.14	7.9		219.6	7.0	
	Indiana	0.762	5.1		79.6	2.4	
	Illinois	1.29	9.6		274.6	9.1	
	Michigan	0.967	6.7		177.7	6.1	
	Wisconsin	1.32	9.5		165.5	5.4	
		5.5	38.8	0.708	917.0	30.0	3.27
East South Central							
	Kentucky						
	Tennessee	0.352	2.7		81.4	2.0	
	Alabama	0.029	.3		18.3	.5	
	Mississippi						
		0.38	3.0	0.787	99.7	2.5	2.51

TABLE III-16. ENERGY COST - SIC 203 (FRUIT & VEGETABLE PROCESSING) (Concluded)

Census Region	State	FUEL Quantity (10^9 kWh)	FUEL Cost (10^6\$)	FUEL Unit Cost (¢/kWh)	ELECTRICITY Quantity (10^6 kWh)	ELECTRICITY Cost (10^6\$)	ELECTRICITY Unit Cost (¢/kWh)
West North Central							
	Minnesota	0.703	3.8		135.4	4.1	
	Iowa						
	Missouri						
	North Dakota	0.176	1.1		15.7	.5	
	South Dakota						
	Kansas						
	Nebraska						
		0.88	4.9	0.557	151.1	4.6	3.04
West South Central							
	Arkansas	0.645	3.2		102.9	2.7	
	Louisiana	0.088	.6		23.4	.6	
	Oklahoma	0.117	.7		42.7	1.0	
	Texas	0.938	6.6		145.7	4.5	
		1.8	11.1	0.633	314.7	8.8	2.80
North Mountain							
	Montana						
	Idaho	2.7	19.2		413.2	5.7	
	Wyoming						
	Colorado						
				0.711			1.38
South Mountain							
	New Mexico						
	Arizona	SIC DOES NOT APPEAR IN THESE STATES					
	Utah						
	Neveda						
North Pacific							
	Washington	1.46	12.1		296.7	1.9	
	Oregon	1.03	8.2		385.1	5.4	
		2.5	20.3	0.812	681.8	7.3	1.07
South Pacific							
	California	8.23	62.1	0.755	1031.9	36.7	3.56

where:

Q_1 = energy required for the hot water stream
Q_2 = energy required to produce steam
N = number of hot water streams
J = number of streams of process steam
$\dot{M}_n$ = flow rate of the nth hot water stream
T_n = the load temperature of the nth hot water stream
T_o = make-up water temperature
$\dot{M}_j$ = flow rate of the jth stream of process steam
$h_{s,j}$ = enthalpy of the process steam
T_c = temperature of condensate (< 100°C)
h_f = enthalpy of saturated water at 100°C

For the case of waste heat recovery, the make-up water was assumed to pass through a heat exchanger and to be heated by the waste water streams as specified in the Drexel Report.

Assuming an array size such that all the electrical load is provided, the annual value of displaced electricity is given by:

$$C_e = E_1 P_e + F_2 P_q \qquad \text{(Eq. III-14)}$$

where P_e = value of electricity, \$/kwh
P_q = value of thermal energy produced by fossil fuel, \$/kwh.

The electrical output of the array was calculated from equation III-15:

$$E_L = E_1 + E_2 = I_A A d \eta_e \qquad \text{(Eq. III-15)}$$

where E_L = annual total electrical demand, kwh/year
I_A = annual average daily solar insolation for a region, kwh/m^2 day
d = number of operating days per year

η_e = average array electrical efficiency
A = array area, m^2

Since the array capacity is such that the annual electrical demand is satisfied, the thermal output of the array may be determined from equation III-16:

$$Q_A = E_L \, {}^{\eta_a}/_{\eta_e} \qquad \text{(Eq. III-16)}$$

where Q_A = annual thermal output, kwh/year
η_a = average array thermal efficiency

Since credit can only be claimed for energy supplied to and used by the load, the supplied thermal energy is:

$$Q_S = Q_A \text{ if } Q_A < Q_L$$
$$Q_S = Q_L \text{ if } Q_A \geq Q_L \qquad \text{(Eq. III-17)}$$

where

$$Q_L = Q_1 + Q_2 \qquad \text{(Eq. III-18)}$$

The annualized capital cost of the PV-T array can be expressed by equation III-19:

$$C_A = C_p \cdot FCR \cdot E_p \qquad \text{(Eq. III-19)}$$

where C_p = cost per peak watt
FCR = fixed charge rate
E_p = peak array capacity at 28^oC

The peak electrical array capacity is:

$$E_p = I_p A \eta_{eo} \qquad \text{(Eq. III-20)}$$

where I_p = peak insolation, 1 kW/m^2
η_{eo} = peak array efficiency at 28°C

Solving for the area from equation III-13 and substituting into equations III-19 and III-20 gives:

$$C_A = \left[C_p \cdot FCR \cdot I_p \eta_{eo} \right] \frac{E_L}{I_A d\eta_e} \qquad \text{(Eq. III-21)}$$

where the term in brackets is assumed constant regardless of the region or application and, therefore, does not contribute to the relative ranking of the various site/application pairs. Setting this term equal to unity and substituting into equation III-2 gives the ranking factor as:

$$R = \frac{E_1 P_e + (F_2 + Q_S) P_q}{E_L / I_A d\eta_e} \qquad \text{(Eq. III-22)}$$

with Q_S given by equations III-16, III-17 and III-18.

In determining the ranking factor, the electrical and thermal efficiency of E-Systems line focus Fresnel module was assumed. These efficiencies were defined in a previous section. An average efficiency for the array was calculated based on the process temperatures required by a particular application. Thus:

$$\eta_e = \sum_i \eta_e' \cdot \text{(fraction of thermal load corresponding to } T_i\text{)}$$

(Eq. III-23)

$$\eta_q = \sum_i \eta'_q \quad . \quad \text{(fraction of thermal load corresponding to } T_i\text{)}$$

where η'_e and η'_q are the efficiencies corresponding to a specific energy end use temperature, T_i. For load temperatures greater than 120°C (250°F), the array efficiencies were calculated at 120°C (250°F) since it was assumed that although the array would not operate above 120°C, it could provide preheated water at that temperature.

The ranking factor, calculated for each industry and within each of the 11 regions, was stored in a second data base. This second data base, resulting from the calculations, was used by a separate program to rank the 71 input industries within each of the 11 regions. Two separate rankings were made; one considered conservation through application of usable waste hot water streams and the other without conservation. A listing was made of the 10 highest ranked industrial processes in each region. A comparison was made of the rankings with and without conservation. The same 27 industries were found on both sets of rankings. Within any region, ranking with conservation occasionally changed the placement of an industry, moving it up or down one position, but did not significantly change the ranking of any industry across regions. Since the rankings were so similar, the ranking without conservation was used to select industrial processes for further study.

A list was made of the 27 industrial processes which made the top ten in the various regions. A combined ranking was calculated by adding the rankings of each process in the various regions. The 27 industrial processes were then listed according to combined rankings (table III-17). Combined rankings ranged from 1.061 to .034. An analysis of the highly ranked industries was begun to eliminate those less suitable for PV-T system application and to match industrial processes to regions. Mineral wool production (3296), primary aluminum production (3334), pulp mills (2611-1, 2, 3), and petroleum refining (2911) were eliminated because the average thermal input temperatures of these processes are well above the

TABLE III-17. RANKING OF THE INDUSTRIAL SECTOR FOR POTENTIAL PV-T APPLICATION

Industry	SIC	Combined Rank	NE	MA	SA	ENC	ESC	WNC	WSC	NM	SM	NP	SP
Bread Baking	2051-1	1.061	.116	.089	.095	.094	.083	.114	.094	.071	.222	.083	
Acetylene	2813-3	.969	.129	.080	.101	.089	.090	.129	.088			.084	.179
Wet Corn Milling	2046	.961		.100	.138	.095	.095	.113	.125			.129	.166
Meat Packing	2011	.954	.113	.084	.101	.094	.080	.175		.076	.152	.079	
T_1O_2 by Sulfate Process	2816-2	.857	.124	.077	.098		.088	.126	.086			.084	.174
Man-Made Fiber Finishing	2262	.815	.107	.086		.097	.079		.091			.085	.144
Rayon	2823-1	.786	.120	.088	.101	.108	.078		.132				.159
Acetate	2823-2	.783	.119	.088	.101	.078		.132					.158
Synthetic Rubber (SBR)	2822-1	.777	.118	.091	.098	.106	.080		.115				.169
Paper Finishing	2621-1	.615			.089		.074	.119	.092			.092	.149
Cane Sugar	2062	.518	.112	.091	.107	.104			.104				
Cumene/Phenol	2865-2	.494	.110					.125				.098	.161
Cake & Pie Baking	2051-2	.239								.059	.180		
Primary Copper	3331	.219						.114			.105		
Sawmill	2421	.189								.061	.128		
Fluid Milk	2026	.173								.064	.109		
Potash	2819-4	.165						.100				.065	
Motor Vehicle	3711	.154								.080	.074		
Photographic Film	3861-1	.111				.111							
Dipped Latex	3069-1	.100											.100
LDPE Plastic	2821-3	.065										.065	
Mineral Wool	3296	.056								.056			
Primary Aluminum	3334	.054									.054		
Mechanical Pulp Mill	2611-3	.047								.047			
Sulfate Pulp Mill	2611-1	.044								.044			
Sulfite Pulp Mill	2611-2	.044								.044			
Petroleum Refining	2911	.034									.034		

thermal capabilities of PV-T collectors, and the fraction of thermal energy which could be provided by a PV-T system would be negligible. This fraction was calculated by the program and was part of the print-out, allowing for consideration at this stage. These industries all ranked in the top ten only in the Mountain regions. Fewer industries are located in these regions than in the rest of the country, and price data were often unavailable for industries known to operate there because the Survey of Manufacturers will not publish data traceable to a particular manufacturer.

The availability of energy price data was used to indicate the location of an industry within a region. Energy cost data were aggregated at the three-digit SIC code level. This led to some obvious discrepancies of industrial processes highly ranked in areas where they do not occur. There are 18 operating wet corn milling plants (2046) in the United States. These plants are located in the East North Central (Indiana and Illinois), West North Central (Iowa) and West South Central (Texas) regions. This process, however, was highly ranked in nine of the eleven regions and not just in the three where it actually occurs. The price data used for wet corn milling were aggregated under SIC code 204, which includes all grain milling. Grain milling of various types (wheat, corn, rice, etc.) occurs in nine regions leading to the misranking of wet corn milling in six regions where it does not occur. Plant location information from the Inter Technology report, addresses of manufacturers from Thomas' Register, and information supplied by contacted trade organizations were used to determine the actual locations of highly ranked industries. Wet corn milling was removed from further consideration because the Corn Refiners' Association reported that a sticky residue is released during the process and coats most plant equipment. This residue would coat solar collectors placed near the plant. The location of the industry and its current investment pattern were secondary considerations. Location was a prime reason for eliminating potash (2819-4) and cane sugar (2062). Potash production by the flotation process is located in New Mexico and Utah within the South Mountain region. The process was

not highly ranked in that region. Cane sugar is produced in California, Hawaii and along the South Atlantic Coast. Its high ranking in other regions reflects the production of beet sugar. Both processes are included in SIC 206 energy cost data. There is a solar industrial process heat application at a cane sugar operation in Hawaii. A PV-T application study might be appropriate after the effects of process pollution on the Hawaiian collectors have been analyzed.

Information from Thomas' Register, and telephone conversations with the manufacturers listed there, eliminated acetylene (2813-3), acetate (2833-2), and SBR synthetic rubber production (2822-1). Acetylene is produced by only three companies, although there are 131 production units scattered nationwide. None of these companies were interested in supporting a PV-T study by providing load profiles. The raw material used in acetylene production is natural gas. Production units are located close to supplies and are usually part of larger petro-chemical complexes. Cellulose acetate fiber production occurs in only five plants located in the Mid-Atlantic region. Its production process is similar to rayon production, which takes place in a significantly larger number of plants located in the South Atlantic, which has a higher average insolation. Thus, acetate was eliminated in favor of rayon. Styrene butadiene rubber (SBR) is made by two companies with 30 production units. Goodrich is the largest supplier. Discussions with the manufacturers indicated that production energy figures could not be separated from other processing steps involved in making SBR parts.

Review of processes eliminated production of titanium oxide by the sulfate process (2816-2) and cumene/phenol production (2865-2). There are several methods of producing titanium dioxide. Only the sulfate process was favorably ranked; however, the environment around a sulfate process plant is too corrosive for solar collector operation. Propylene is the raw material for cumene/phenol co-production. The production flow is complicated and involves the products of one process step being recycled to earlier stages. The heat released by exothermic reactions is used to heat other steps. All manufacturers are major oil companies and

the production units appear to be located near petroleum refining units. Both the plant environment and the complex mixture of thermal sources made this application less attractive.

Cake and pie baking (2051-2) was eliminated because the process is very similar to bread baking, which was more highly ranked in more regions. Primary copper production (3331) is being considered for a central receiver solar application in New Mexico. Sawmills (2421) were eliminated because solar applications cannot presently compete with several developing waste-wood technologies. Motor vehicle and automobile production (3711) was eliminated on the basis of perceived unwillingness of the industry in the Mountain regions to invest in PV-T retrofits considering the present economic state of the automobile industry. Dipped latex (3069-1), LDPE plastic (2821-3), and photographic film (3861-1) ranked high in one region each. The former two industries were tenth in their regions. Film manufacturing, while it ranked first in the East North Central region, is undergoing rapid changes in production techniques.

After reviewing the more highly-ranked industrial processes, six industries seemed to merit more intensive study to develop specific electrical and thermal load profiles. These were bread baking (2051-1), meat packing (2011), man-made fiber finishing (2262), rayon production (2823-1), paper finishing (2621-1), and fluid milk production (2026). To this list concrete block manufacturing was added. This industrial process was not included in the Drexel study, but it has a very favorable E/T ratio and was suggested for solar application in an Industry Notes article (ref. III-16).

Bread baking had the highest combined ranking. Bakeries are located in all regions of the country and are numerous. The 3,323 U.S. bakeries, which reported a total production in 1977 of 7.13×10^9 kg ($15,700 \times 10^6$ pounds) of baked goods, vary in size from small facilities employing less than five people (44 percent of the total), to large facilities employing over 1000. There are over 1100 bakeries in the medium size range employing 10 to 200 people in two shift operations. Bakeries have

been considered in several solar industrial processes heat studies (ref. III-2, 13, 17, 18). Review of these studies showed a consistent ratio between electrical and thermal use (.217), and a close correlation between energy use and plant production regardless of plant size or location. However, as will be seen shortly, the bread baking plant in Denver for which a load profile was available, has an E/T ratio of 0.962, which indicates a common problem in attempting to characterize the industrial section; indicating there is no "average" or typical plant. Several trends were noted that may increase PV-T application potential. Bakery production and plant size are increasing. Continuous mixing of dough is replacing the sponge dough process. This will lead to a reduction in steam requirements while increasing the electrical load. Demand for frozen bakery products is also increasing, and the addition of refrigeration capacity to a bakery may represent a logical capital investment, thereby increasing the electrical or thermal load depending on the type of refrigeration installed. Electrical and thermal load profiles were developed for a large bread and bun bakery located in Denver, Colorado (figures III-14 and III-15).

The bakery consists of two bread lines and one bun line (ref. III-18) Dough is loaded onto trays and placed in the proof box where the dough rises for about 1 hour. It is then taken to the oven and baked. Baked bread is placed in the cooler through which room air is drawn and exhausted to the atmosphere. Buns are cooled at ambient temperature without the aid of a cooler. The baskets used for transporting bread are washed and dried at the bakery. The bakery operates 5 days a week. One bread line operates 8 hours per day with a nominal capacity of 2700 kg/h. The second bread line operates 12 hours per day at 4100 kg/h. The bun line usually operates 8 hours per day but may run 24 hours per day during the summer demand peak. Its capacity is 1300 kg/h. Energy is presently supplied to the process via steam from a low temperature boiler. Steam is used to heat water to 66°C for space heating, to maintain the sugar room at 49°C, and to heat water for basket washing (82°C) and clean-up (71°C). Steam coils maintain the proof boxes at 30°C. Live steam

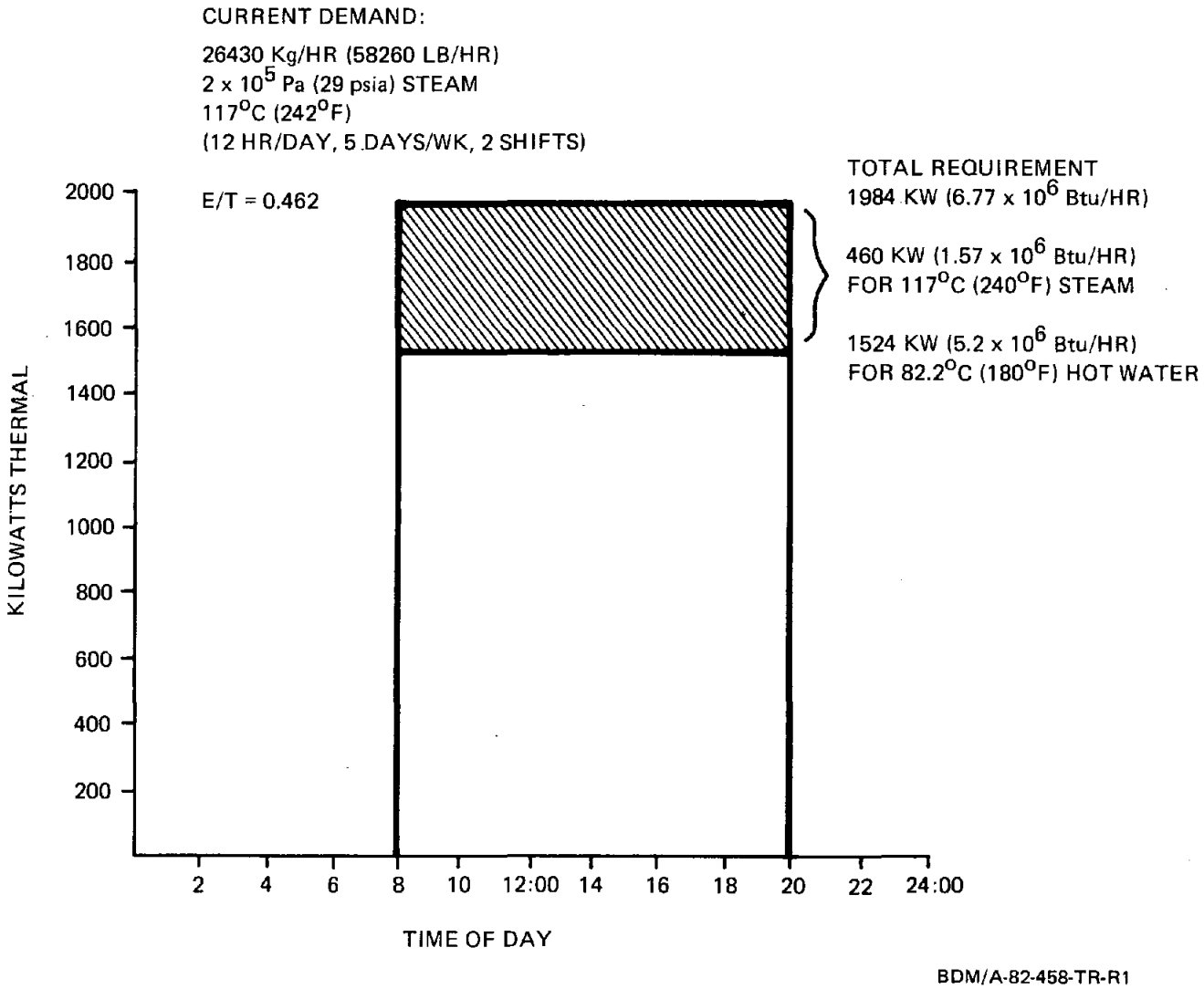

Figure III-14. Denver, Colorado Bread Bakery Thermal Load Profile

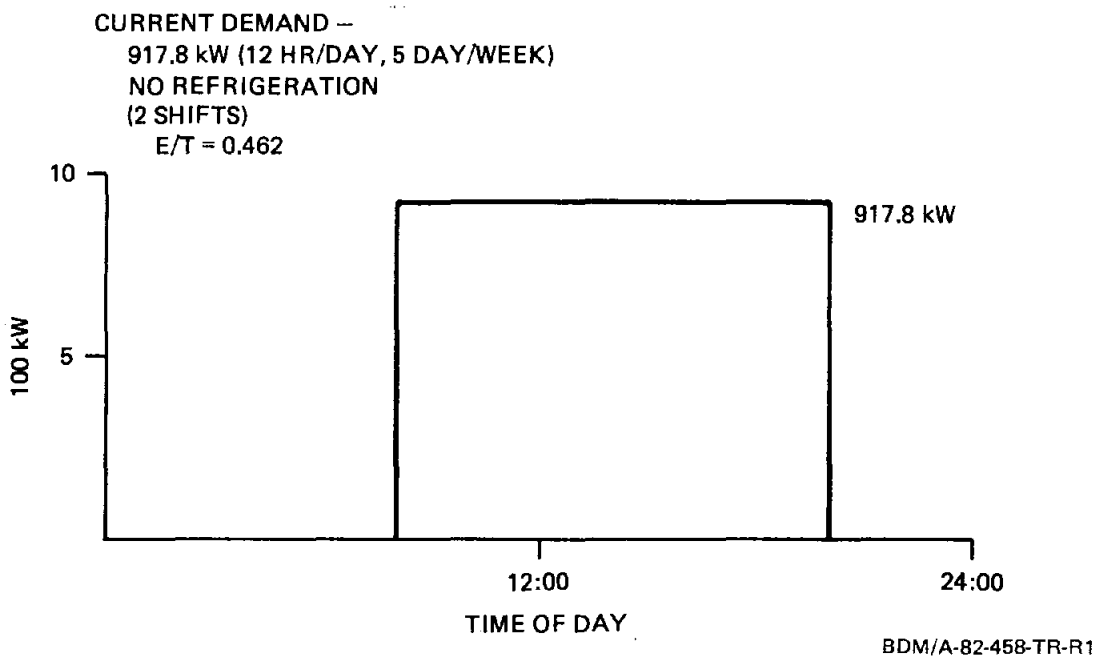

Figure III-15. Denver, Colorado Bread Bakery Electrical Load Profile

injection maintains those units at 90 percent relative humidity. The ovens and basket dryer are heated by direct-firing of natural gas. It appears that a PV-T system could provide most, if not all, of the hot water requirements for this process at 89.5°C (180°F) thereby replacing the boiler. The required humidity in the proof box could also be produced by aerated hot water. The process diagram indicates that most of the hot water goes to waste, so that in subsequent analyses it will be assumed that the return from the process is at make-up water temperature of 21.1°C (70°F).

Meat packing (2011) had the fourth highest combined ranking. Meat packing plants are found in all regions, but are not common in New England. There were 2490 plants operating in 1972 with a total production of 14 x 10^9 kg (31 x 10^9 pounds). Plant size varies widely. Over 50 percent of all plants are single shift operations employing less than 10 people, but 50 percent of all meat is processed in large plants with 100-500 people, and 30 percent of all meat is processed in the 22 plants with 1000 employees. Like bread baking, meat packing has been studied for solar industrial process heat and solar total energy applications (ref. III-2, 17, 18, 19, 20, 21). Sanitation requirements necessitate large quantities of hot water for clean-up, which is often a separate shift. The refrigerated meat storage capacity of a plant often determines plant throughput, but the amount of hot water necessary for clean-up is largely independent of throughput. Electrical and thermal load profiles were developed for a plant in Dixon, California (figures III-16 and III-17). The plant is intermediate in size and lamb and beef are processed (ref. III-20). The plant operates 5 days a week with a full shift from 8:00 a.m. to 4:00 p.m., a reduced shift from 4:00 p.m. to midnight, and clean-up from midnight to 7:00 a.m. The current demand for electricity includes a substantial amount (150 kW) to power vapor compression refrigeration (130 tons) for carcass cooling and cold storage. Storage demand is 24 hours a day, 365 days per year. Steam generated at the site is used to provide large amounts of 60°C (140°F) hot water used primarily for clean-up. We have assumed that a PV-T

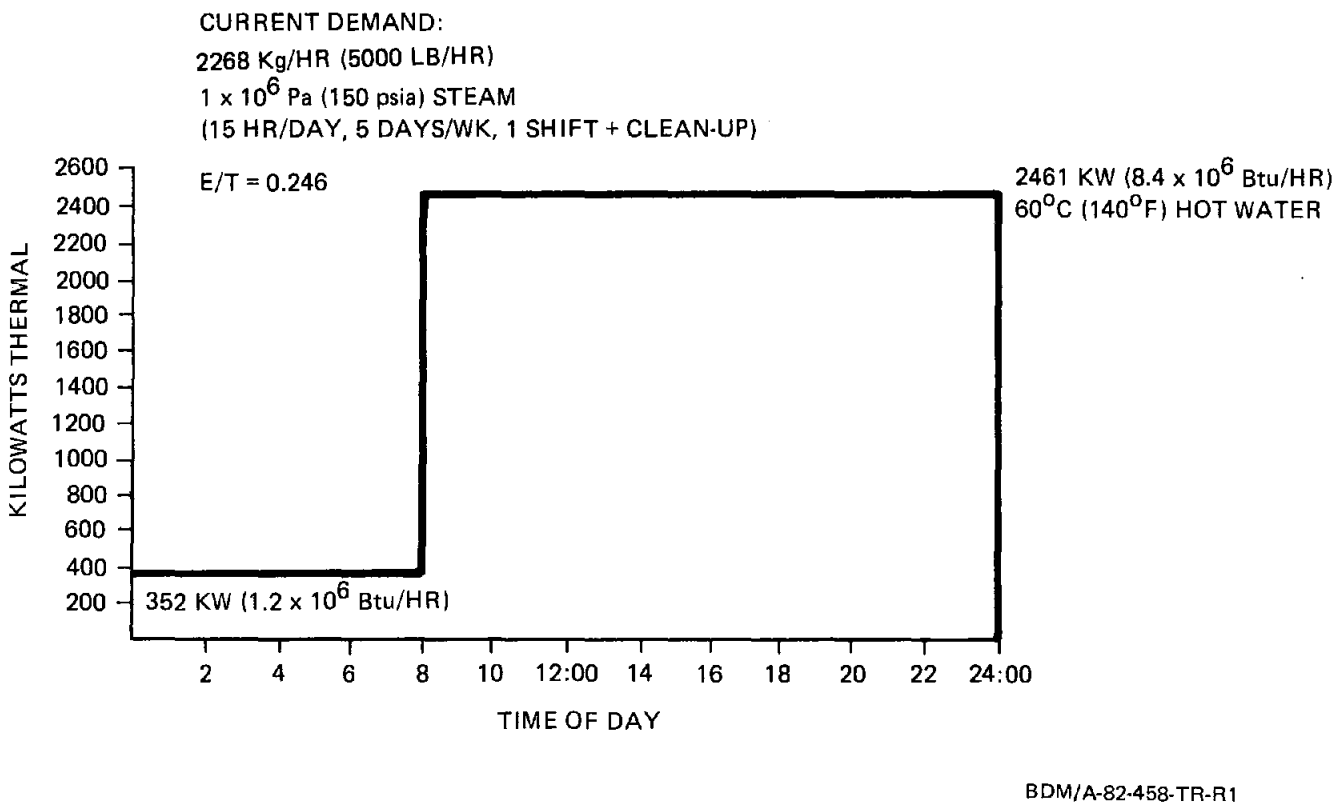

BDM/A-82-458-TR-R1

Figure III-16. Dixon, California Meat Packing Plant Thermal Load Profile

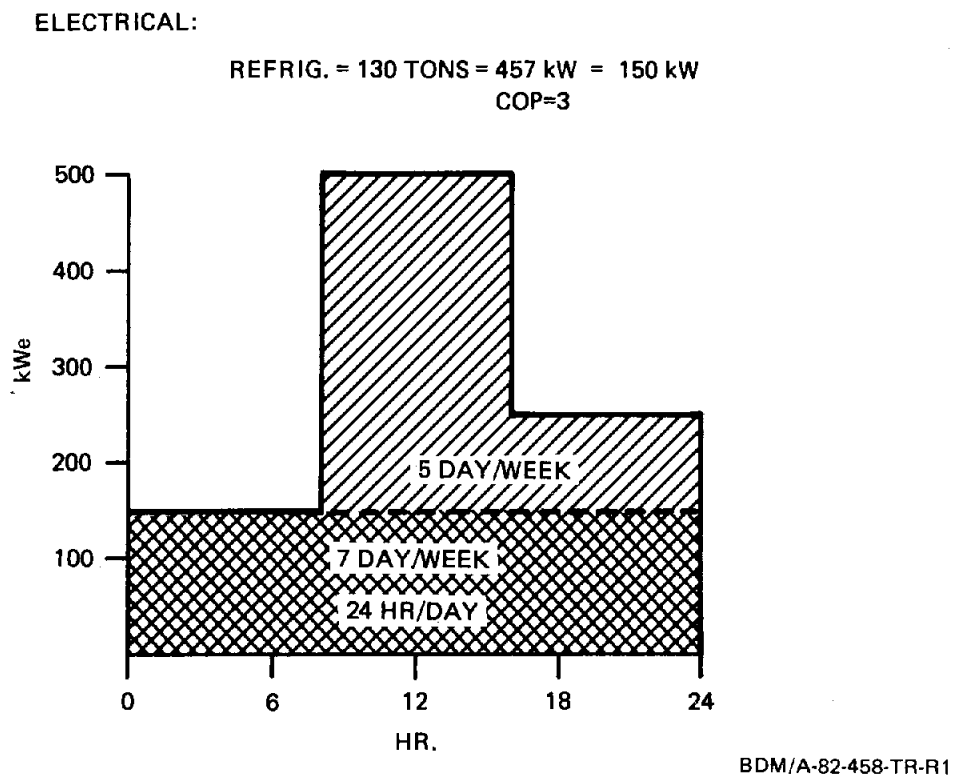

Figure III-17. Dixon, California Meat Packer Electrical Load Profile (Armour Meat Packing Co.)

system can provide hot water, thereby replacing the boiler with an auxiliary heater to ensure the required temperature of 60°C (140°F) is attained. It is also assumed that the clean-up water goes to waste and the return from the load is make-up at 18.3°C (65°F).

Man-made fiber finishing (2262) was ranked sixth. The process was considered within the broader heading of textiles in the Inter Technology report (ref. III-13), but has never been separately studied for solar energy application. Finishing is a series of processing steps which treat woven cloth (grey goods). The Drexel report listed 12 separate operations in its generic process diagram. Besides these general operations, specific processes such as rubber or plastic coating, impregnation with flame retardant compounds, and application of water repellant finishes may be part of a plant's processing train. Finishing operations are often combined with the initial weaving of the synthetic fiber cloth. Integrated plants have a higher boiler outlet temperature requirement, and much higher electrical requirements. These operations appear to be located nationwide if the manufacturers who produce specially coated fabrics have finishing operations. The American Textile Manufacturers Institute was contacted for information on finishing, and referred us to the current chairman of the Man-made Fiber Finishers Energy Council. The Council provided energy data on the plant in Thomaston, Georgia from which load profiles were developed. These load profiles (figures III-18 and III-19) are considered common for the industry.

The finishing of cloth at Thomaston Mills is a continuous process. The plant operates on three 8-hour shifts, five days a week with a single shift on Saturday. The load profiles show that the evening shifts are less energy intensive than the day shift. The plant turns out 91,000 - 113,400 kg (200,000 - 250,000 pounds) of fabric a day. The Thomaston Mills operation can use hot water in the 50-60°C range for desizing, scouring, mercerizing, washing, rinsing and dying. These processes account for 90 percent of the current steam demand. However, discussions with the plant manager indicate a reluctance to replace steam with hot water since the steam is currently cascaded through the process.

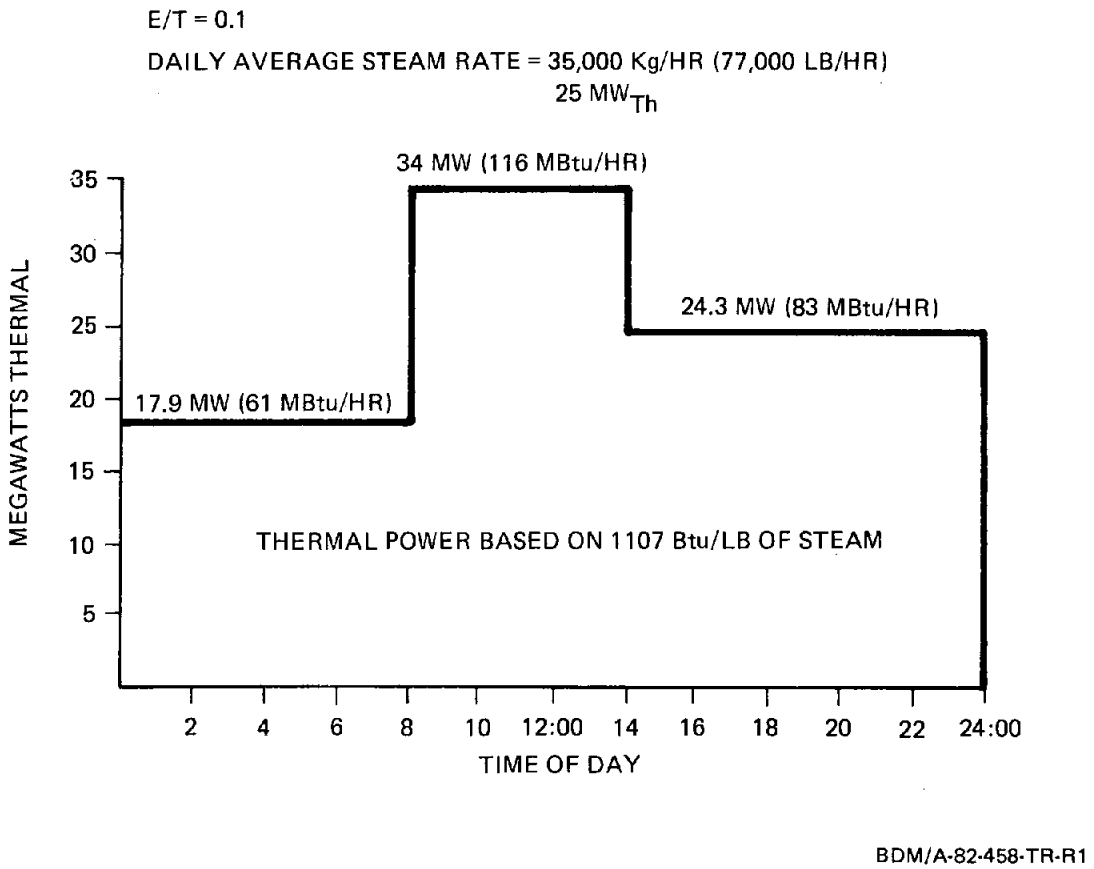

Figure III-18. Thomaston, Georgia Fiber Finishing Plant Thermal Load Profile (Thomaston Mills)

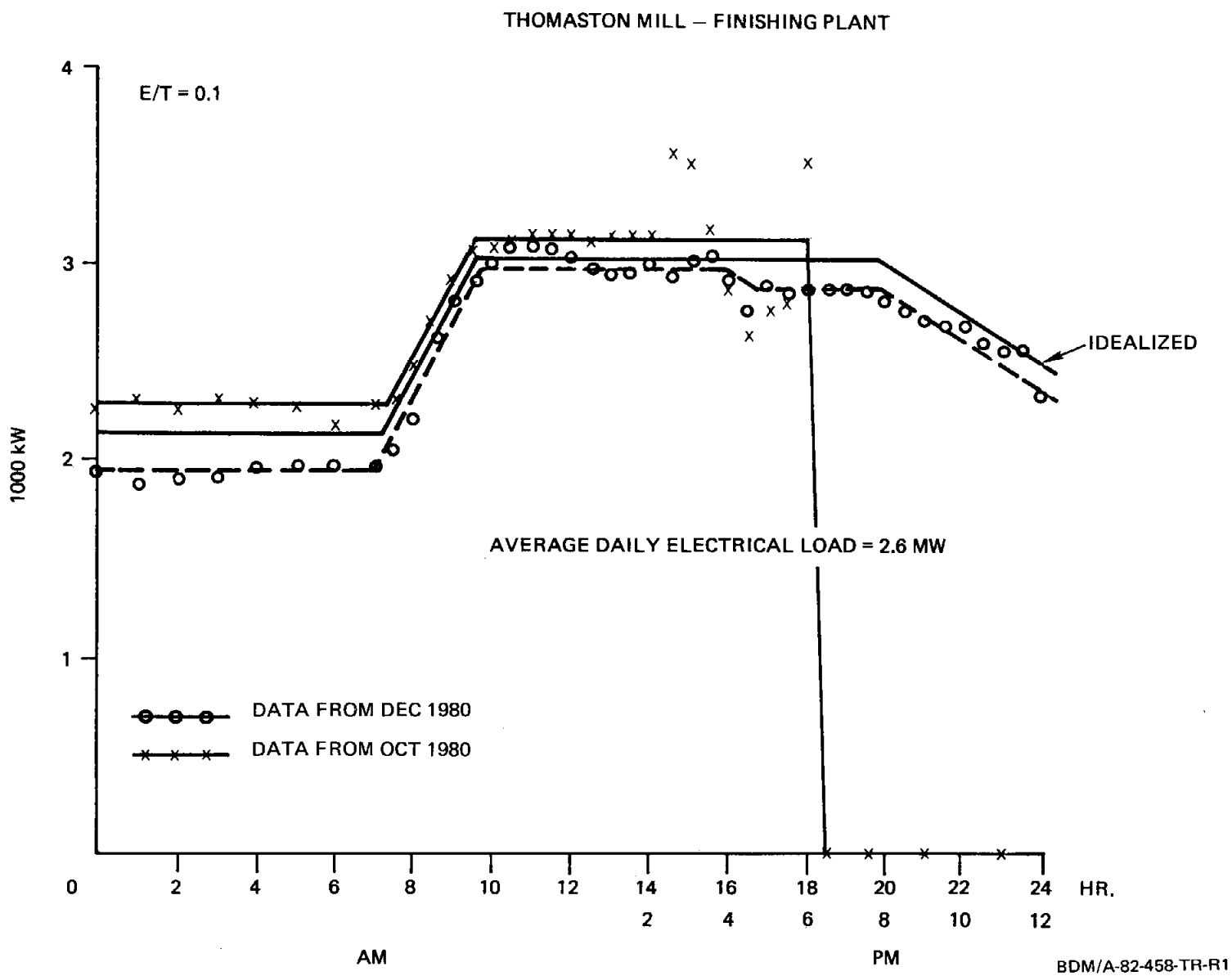

Figure III-19. Thomaston, Georgia Fiber Finishing Plant Electrical Load Profile

Thomaston Mills has 64000 m^2 (685,000 ft^2) of available roof space over its finishing plant. Large, long, one-story buildings are common to this industry which continuously moves wet fabric lengths from process to process.

Rayon production placed seventh in the combined rankings. This industry is located in the South Atlantic, where 10 plants owned by four companies are in operation. Ranking in other regions reflects the aggregation of energy data for all man-made and synthetic fibers. The industry is extremely competitive, not only between the rayon producers but also with other fibers which compete for the same markets. The demand for rayon has been rising for the last 5 years. The fiber is made from cotton linters and wood pulp, so its raw materials costs have not changed as rapidly as those of fibers made from petro-chemicals. Fiber production has not been included in solar application studies. Each of the four rayon manufacturers was contacted. None would supply energy load profiles, therefore this industry will not be considered further.

Fluid milk processing (2026) was not ranked as high as the other selected industrial processes. The Drexel report process diagram included the production of cottage cheese as well as the pasteurization of whole milk. Dairies are located in all regions. In 1977, over 1900 dairies were operating and processed 2.8×10^{11} kg ($61,900 \times 10^6$) pounds of milk. Plant size varies from farm operations (30 percent of all dairies), to plants employing more than 500 people. There are more than 400 plants in the median one-shift, 20-50 employee, range. Process temperatures are low, and there is a need for hot water clean-up. The production of related products designed to use excess milk (such as cottage cheese, buttermilk, and dried milk) requires higher temperatures. Some dairies store products which requires 24-hour refrigeration. Storage versus related product production may be an important trade-off in dairy capital expenditure. Per capita consumption of dairy products is falling but related product demand (yogurt) is rising slowly. Fluid milk processing has been considered in several solar industrial application studies (refs. III-2, 13, 18, 19). Electrical and thermal load

profiles were prepared for a dairy without refrigerated storage in El Paso, Texas (figures III-20 and III-21). The electrical refrigeration load is based on a COP of 3.

Raw milk is pasteurized, homogenized, and bottled at this plant (ref. III-18). Since there is no refrigerated storage, the electrical demand is primarily from pumping requirements and process cooling. Pasteurization systems are equipped with a flow diversion valve, which returns improperly heated milk to the raw milk side of the system in the event of malfunction. The pasteurization system operates between 72°C and 85°C. Holding time is matched to operating temperature, and ranges from 16 seconds at 72°C to negligible as the temperature rises. The hot pasteurized milk is cooled by the incoming raw product.

The El Paso plant operates on a single 8-hour shift, 5 days a week. Larger plants may operate on two shifts; typically, one from midnight to 10:00 a.m. when milk is pasteurized, and a second shift from noon to 8:00 p.m. for clean-up. The early morning milk processing schedule facilitates distribution to grocery stores on the same day. Milk is dated and must be sold promptly.

Concrete-block manufacturing was not part of the Drexel report. The process has been reviewed in a solar total energy study (ref. III-19), and there is an operating solar industrial process heat application (hot water) for concrete-block curing at York Building Products in Harrisburg, Pennsylvania. Steam curing is currently used by many producers; however, steam temperatures are not required. Temperatures between 55-90°C (130-190°F) are sufficient. Steam is used primarily to maintain adequate humidity, but aeration of pools of hot water will also provide the required humidity. Concrete blocks are produced in every region of the country to avoid transport problems. Operations are often divided into two shifts, with the blocks being formed during the day (electrical cycle) and cured overnight (thermal cycle). This schedule has been convenient but is not unchangeable if daytime operations are more energy efficient. Load profiles were prepared for a concrete block plant in Tucson, Arizona (figures III-22 and III-23). The electrical demand is

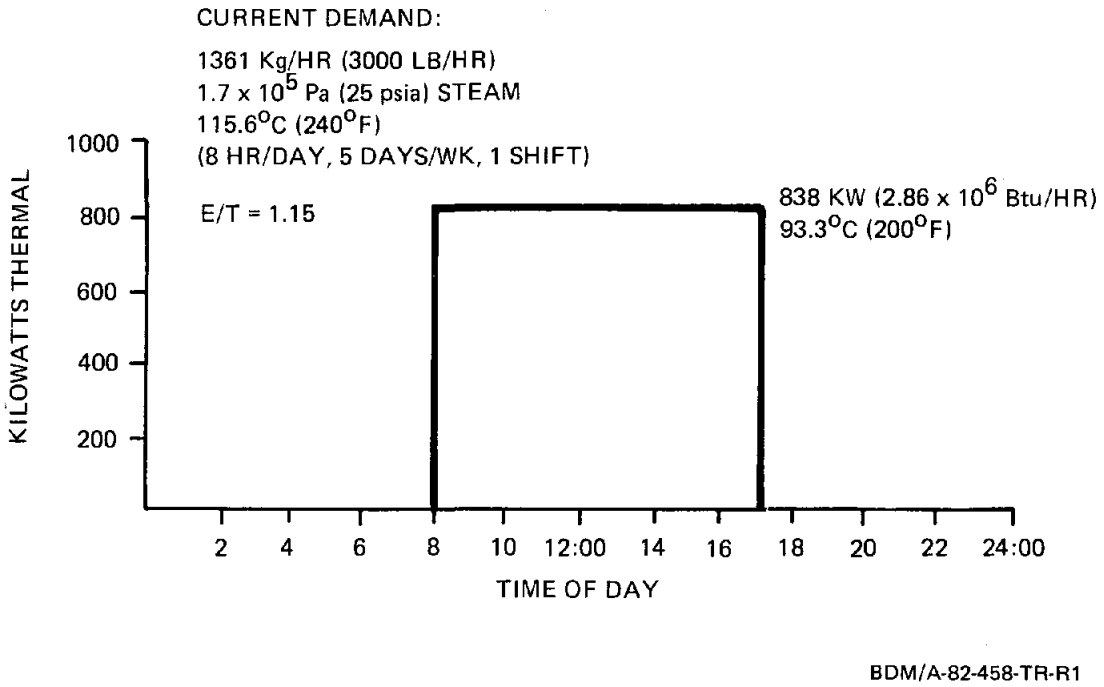

BDM/A-82-458-TR-R1

Figure III-20. El Paso, Texas Fluid Milk Plant Thermal Load Profile

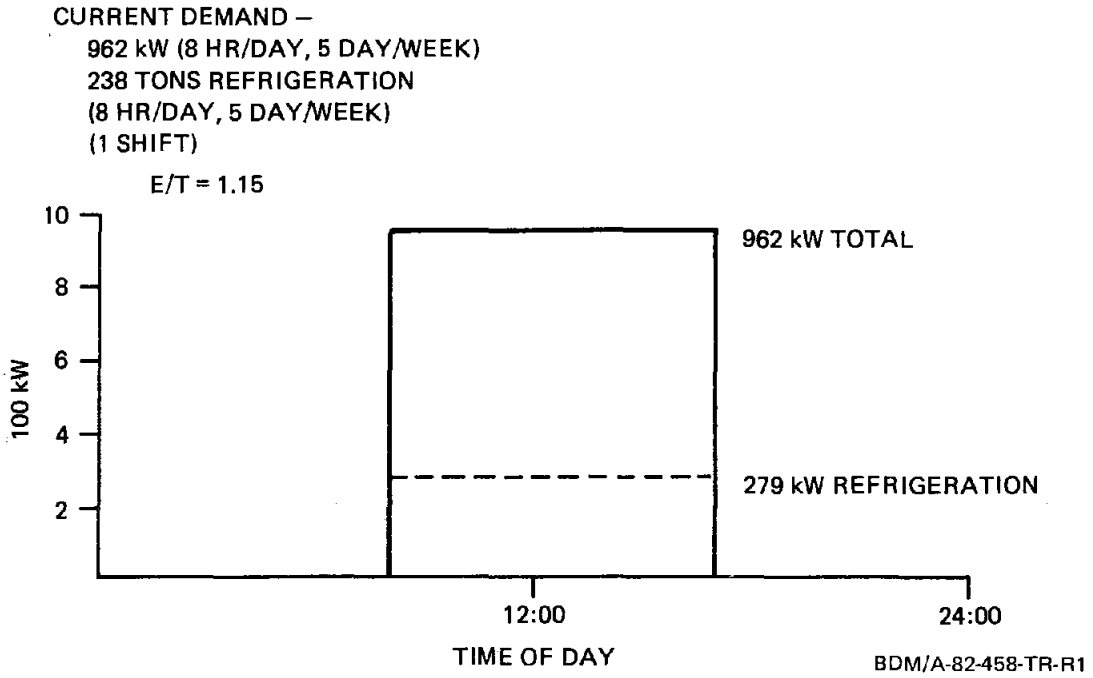

Figure III-21. El Paso, Texas Fluid Milk Plant Electrical Load Profile

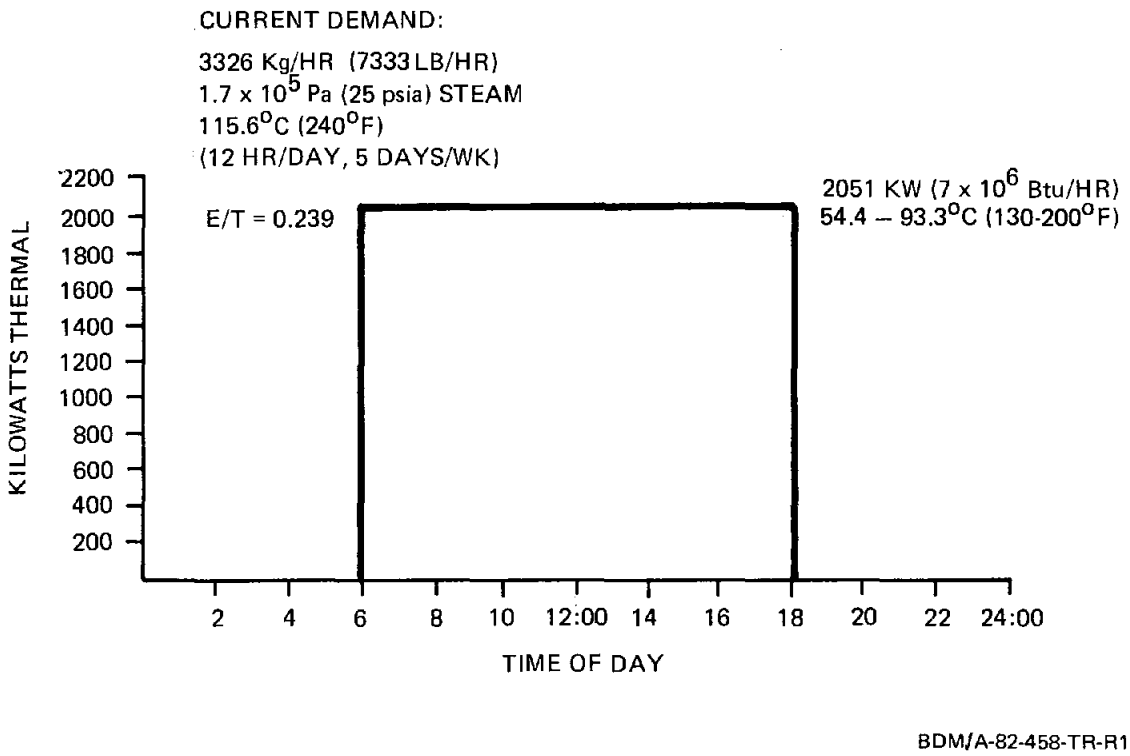

BDM/A-82-458-TR-R1

Figure III-22. Tucson, Arizona Concrete Block Plant Thermal Load Profile

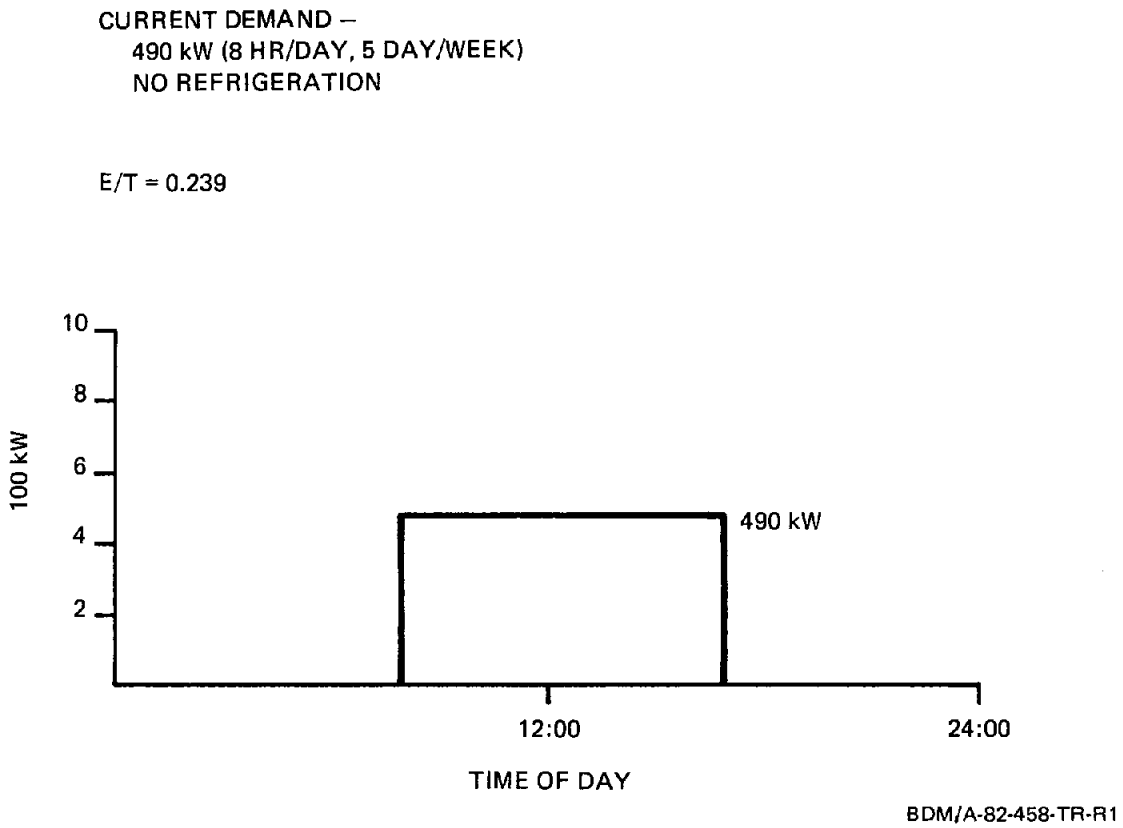

Figure III-23. Tucson, Arizona Concrete Block Plant Electrical Load Profile

for crushers and mixers. The experience at the York solar curing facility indicates that curing in the 43°-57°C solar range takes 24 hours, as opposed to 3 hours with steam curing, and 8-12 hours with an 82°C cure. There will probably be a site specific trade-off between the cost of storing blocks (while they cure) and the cost of steam. Based on information in reference III-19, we assumed a process temperature of 82.2°C (180°F) in an open loop with a make-up water return of 18.3°C (65°F).

The seventh industrial process chosen for further study was paper finishing (2621-1). This process was ranked tenth overall. It has not been considered in any solar application studies. There are 218 plants producing paper in the U.S. (1.5×10^{10} kg in 1977). Of these, approximately 121 are integrated plants not only finishing paper but making it, starting with cut logs. The Drexel study indicates that two of the eleven process steps require thermal energy in the 60-65°C range. An estimated E/T ratio would be .306. In attempting to develop load profiles for paper finishing the first step was to identify finishers. This was still being attempted when load profiles for the other five industries were completed. It was decided to concentrate our efforts on those industries.

In addition to the industrial processes chosen based on information from the Drexel report and the concrete block plant, it was felt that a laundromat would also be a reasonable application to consider due to its use of large amounts of hot water and electrical power. To obtain load profiles and typical use rates we contacted Ford Commercial Sales in Dallas, Texas. This company operates several solar laundromats in the Dallas area and was extremely helpful in providing us information from which load profiles were developed.

The typical temperature increase of the wash water is from 18.3°C (65°F) to 51.7°C (125°F) with an average of 28.4 m^3 (7500 gallons) per 14-hour day for a facility with 30 washers. A typical 30-washer facility uses either fifteen 30-pound dryers or thirty 15-pound dryers. The electrical load is due primarily to washer and dryer motors, lighting, and

air conditioning. Due to the low cost of natural gas compared to electricity, the great majority of dryers are gas dryers. Washer motors draw an average of 10 amps, and dryer motors an average of 15 amps at 120 VAC. Typical air conditioning loads are 15 tons (45 amp, three phase, 220 V unit).

Assuming gas dryers, and only the hot water thermal load, load profiles were developed and are shown in figure III-24. As indicated, the weekday and weekend thermal and electric loads are significantly different, with the weekday minimum load occurring during the best time of day for solar. These load profiles assume a 30-washer facility with fifteen 30-pound dryers. As indicated previously, these load profiles are "typical." The time of day useage may vary significantly for a particular laundromat location, such as a facility near a university or a facility near an apartment complex with young working couples.

D. SITE/APPLICATION PAIR ANALYSIS

A systems analysis was performed for the 11 site/application pairs identified in table III-18. This analysis was performed on an hour-by-hour basis for an entire year using SOLCEL II, which was modified to include the thermal system components shown in figure III-1. This initial analysis was performed to determine which site/application pair had the lowest LCCR (defined in equation III-1), and to determine the optimum array size. Given a load profile for a particular application, and SOLMET data for a specific site, the annual array output, life cycle costs, and the LCCR were calculated using the total array area as a parameter. Those site/application pairs with LCCR > 1 are not economically feasible. However, the calculated LCCR is highly dependent on the assumed process temperature, load profiles, and assumptions made concerning component costs, sell-back of electricity, and fuel costs.

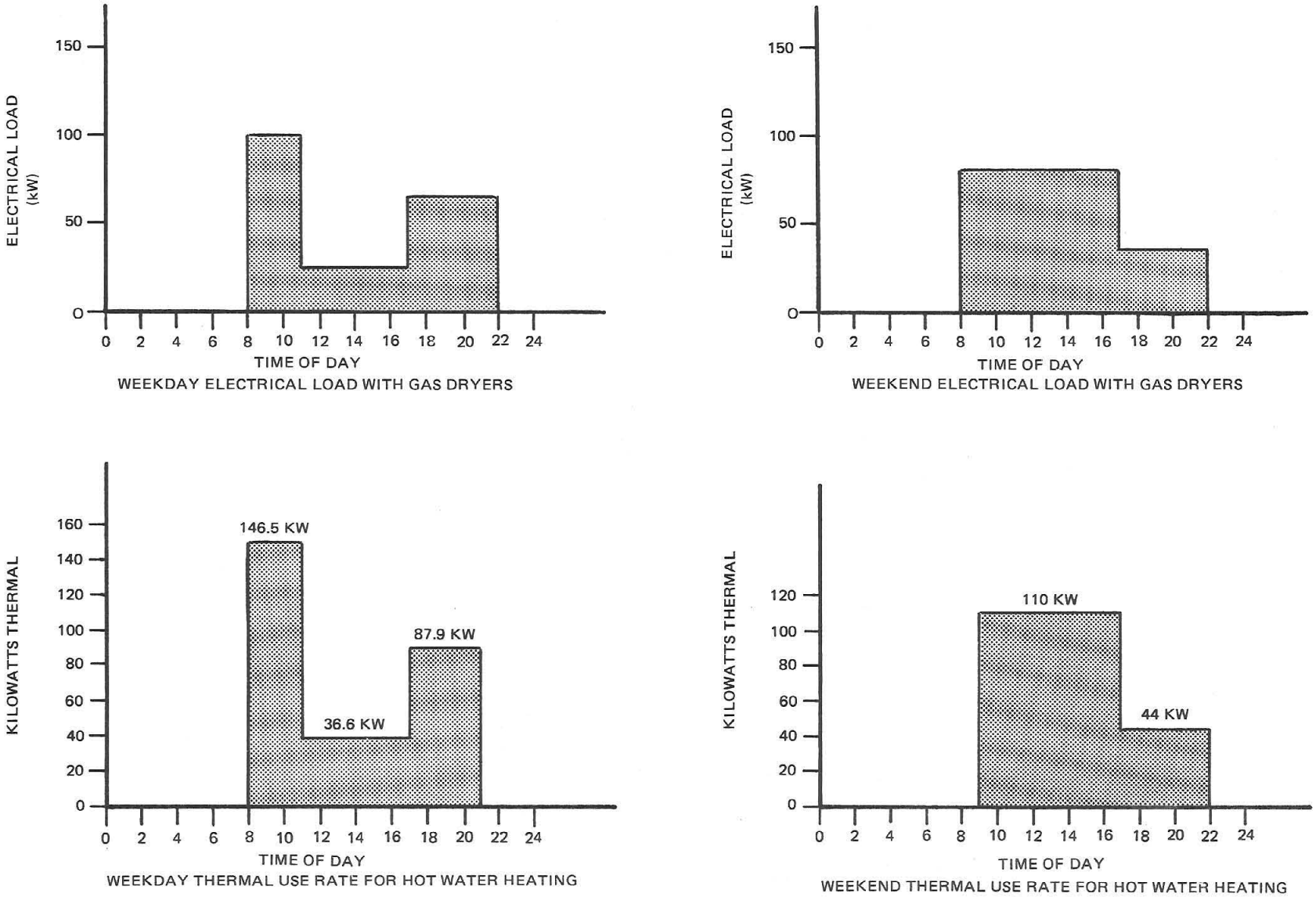

BDM/A-82-458-TR-R1

Figure III-24. Electrical and Thermal Load Profiles for a Typical Laundromat

TABLE III-18. SELECTED SITE/APPLICATION PAIRS

Site	Application	E/T*
Thomaston, GA	Man-Made Fiber Finishing	0.1
El Paso, TX	Fluid Milk Mfg.	1.15
Denver, CO	Bread Baking	0.46
Dixon, CA	Meat Packing	0.47
Tucson, AZ	Cement Block Mfg.	0.16
Fresno, CA	Hospital	0.61
Seattle, WA	Hospital	0.18
Albuquerque, NM	School	0.35
Boston, MA	School	0.28
Phoenix, AZ	Public Administration	0.72
Fresno, CA	Laundromat	0.71

$$*E/T = \frac{\text{Annual Electric Load}}{\text{Annual Thermal Load}}$$

1. Economic Parameters

In these analyses the array costs have been assumed to be $\$275/m^2$. Although this is a low figure, it is within the projected range of costs ($\$250-\$400/m^2$) for PV-T systems in the 1990 time frame for large production quantities. Initial analyses indicated that few of the selected applications would be economically feasible at the higher end of this price range. This is consistent with the findings by Rios, et. al. (ref. III-21) in which break-even costs were found to be between $\$300-\$400/m^2$ for a meat packing plant and a hospital. Although an array cost of $\$275/m^2$ may not be realistic in the near term, it allows the determination of those site/application pairs which are the most economically feasible, and allows a starting point for development of a detailed system design.

The $\$275/m^2$ cost figure is based on the assumptions that concentrator module costs will reach $1/Wp in the 1990's and field electrical efficiency will reach 15 percent. The concentrator module consists of PV cells and receiver structure, and the concentrating system (Fresnel lens and lens structure). This cost of $1/Wp for a concentrator module may not be too unreasonable, considering E-System's and Westinghouse's work with dendritic web cells, which are expected to cost about $\$0.05/cm^2$, and the work by E-Systems on a low-cost extrusion/embossing process for linear Fresnel lenses.

The derivation of the $\$275/m^2$ cost using the above stated assumptions uses an economic analysis performed by GE (ref. III-22) as a baseline. This analysis projects concentrating PV costs for 1980 vintage technology. Using the assumptions of $1/Wp and a 15 percent efficient field, the module cost would be

$$C_m = (\$/Wp)\eta I = (\$1/Wp)(1000\ W/m^2)(0.15) \qquad \text{(Eq. III-24)}$$

$$C_m = \$150/m^2$$

This may be compared to GE's predicted cost of $\$191.8/m^2$ for a concentrating LFF module.

GE predicts additional hardware costs to be $\$73/m^2$, installation costs to be $\$76/m^2$, and shipping costs at $\$16.70/m^2$. The additional hardware costs include such items as module support structure, tracking hardware, controls, and cooling hardware such as fittings and flex hoses. We have assumed shipping costs would remain fairly constant due to opposing effects of lighter loads (i.e., lighter structure) and higher fuel costs. The remaining costs (hardware and installation) should decrease with increased experience and production rates.

The effect of experience on production costs may be expressed as

$$C_T = C_o R^K \qquad \text{(Eq. III-25)}$$

where

$$K = \frac{\ln (C_T/C_o)}{\ln 2}$$

C_T = unit cost of array at time T
C_o = unit cost of array at time 0
R = experience factor
P_T = cumulative production at time T
P_o = cumulative production at time 0

An experience factor (R) of 0.95 is selected to apply to the hardware and installation costs. This factor represents a conservative estimate of the effects of large production volumes. For analogous manufacturing processes, experience factors of 0.8 have been observed for the production of electric power (30 years of data).

The expected installed cost of $\$275/m^2$ consists of the component costs defined in equation III-26.

Expected installed cost = module cost + shipping cost + hardware cost + installation cost (Eq. III-26)

Therefore, the expected hardware and installation costs must be reduced to $\$108.3/m^2$ from the GE projection of $\$149/m^2$.

Using GE's assumed production level of 10^5 m^2 in equation III-25, a cumulative production level of 7.5×10^6 m^2 must be achieved in order for the additional hardware cost and installation costs to be reduced to $\$108.3/m^2$, and the total array installed cost to be reduced to $\$275/m^2$.

Other assumptions which were made for the initial analysis of the 11 site/application pairs are:

Row Length		
	LPT	12 collectors/row
	LFF	12 arrays/row, four modules per array
Flow Rate		
	LPT	6.3×10^{-4} m^3/sec (10 gpm)
	LFF	3.15×10^{-4} m^3/sec (5 gpm)
Array Installed Cost		
	LPT	$\$275/m^2$
	LFF	$\$275/m^2$
No storage		
Heat Exchanger		
	Number of transfer units	2.5
	Heat Transfer Coefficient	4540 $W/m^2{}^oC$ (800 BTU/hr ft^2F)
	Cost	$\$344/m^2$ ($\$32/ft^2$)
Cooling Tower		Sized for the no load condition $\$1500+\$3.5 \times 10^5 G^*$
Inverter		Sized for the array output
	Cost	$700 + $180/kw
Sell-back ratio		0.75

*G = coolant flow rate in m^3/sec

Economic parameters for life cycle cost analysis are given in table III-19. An initial calculation was made using a 10 percent investment tax credit. The change from 10 percent to 25 percent tax credit made a significant change in the economic feasibility of several site/application pairs, as discussed in the next section. Conventional energy costs and energy escalation rates depend on the region of the country and are given in tables III-20 and III-21, respectively.

TABLE III-19. ECONOMIC PARAMETERS FOR PV-T LIFE CYCLE COST ANALYSIS

Discount Rate	20%	Price year	- 1982
Interest Rate	15%	System Life	- 20 yrs
General Inflation	9%	Loan period	- 10 yrs
Tax Rate	50%	Depreciation Life	- 7 yrs
Investment Tax Credit	25%	O&M Costs	- 1.5% of IC*/yr
Year of Operation	1986	Salvage Value	- 0
Depreciation	SOYD	Down Payment	- 20%

*IC = Initial Cost

TABLE III-20. CONVENTIONAL ENERGY COSTS, 1982 DOLLARS*

Site	DOE Region	Electricity $/Kwh	Natural Gas $/Kwh
		Industrial Sector	
Thomaston, GA	4	0.0365	0.0145
El Paso, TX	6	0.0389	0.0100
Denver, CO	8	0.0277	0.0103
Dixon, CA	9	0.0517	0.0142
Tuscon, AZ	9	0.0517	0.0142
Fresno, CA	9	0.0517	0.0142
		Commercial Sector	
Fresno, CA	9	0.0639	0.0183
Seattle, WA	10	0.0288	0.0183
Albuquerque, NM	8	0.0370	0.0149
Boston, MA	1	0.0820	0.0224
Phoenix, AZ	9	0.0639	0.0183

* January, 1980 Federal Register

A systems analysis for the industrial site/application pairs was performed using the LPT and the LFF collector systems. The LFF provided significantly better performance as indicated in chapter IV, and therefore, was more economical than the LPT in terms of the LCCR. Therefore, the commercial site/application pairs were analyzed using only the LFF collectors.

TABLE III-21. ENERGY COST ESCALATION RATES (23 YEAR AVERAGE OF JANUARY, 1980 FEDERAL REGISTER VALUES INCLUDING GENERAL INFLATION)

Site	DOE Region	Electricity	Natural Gas
	Industrial Sector		
Thomaston, GA	4	0.1019	0.1414
El Paso, TX	6	0.1057	0.1322
Denver, CO	8	0.0979	0.1255
Dixon, CA	9	0.0862	0.1281
Tuscon, AZ	9	0.0862	0.1281
Fresno, CA	9	0.0862	0.1281
	Commercial Sector		
Freson, CA	9	0.08545	0.0974
Seattle, WA	10	0.1010	0.1045
Albuquerque, NM	8	0.0938	0.1196
Boston, MA	1	0.08756	0.1044
Phoenix, AZ	9	0.08545	0.0974

2. Industrial Site/Application Pairs

The life-cycle cost ratio (LCCR) versus the collector area is shown for the LFF system in figure III-25 for five industrial site application pairs. These initial calculations assumed a 10-percent income tax credit and did not include the laundromat. Subsequent calculations used a more realistic income tax credit of 25 percent, which is currently available from the Federal Government. The results of these calculations are shown in figure III-26. Increasing the tax credit made a significant

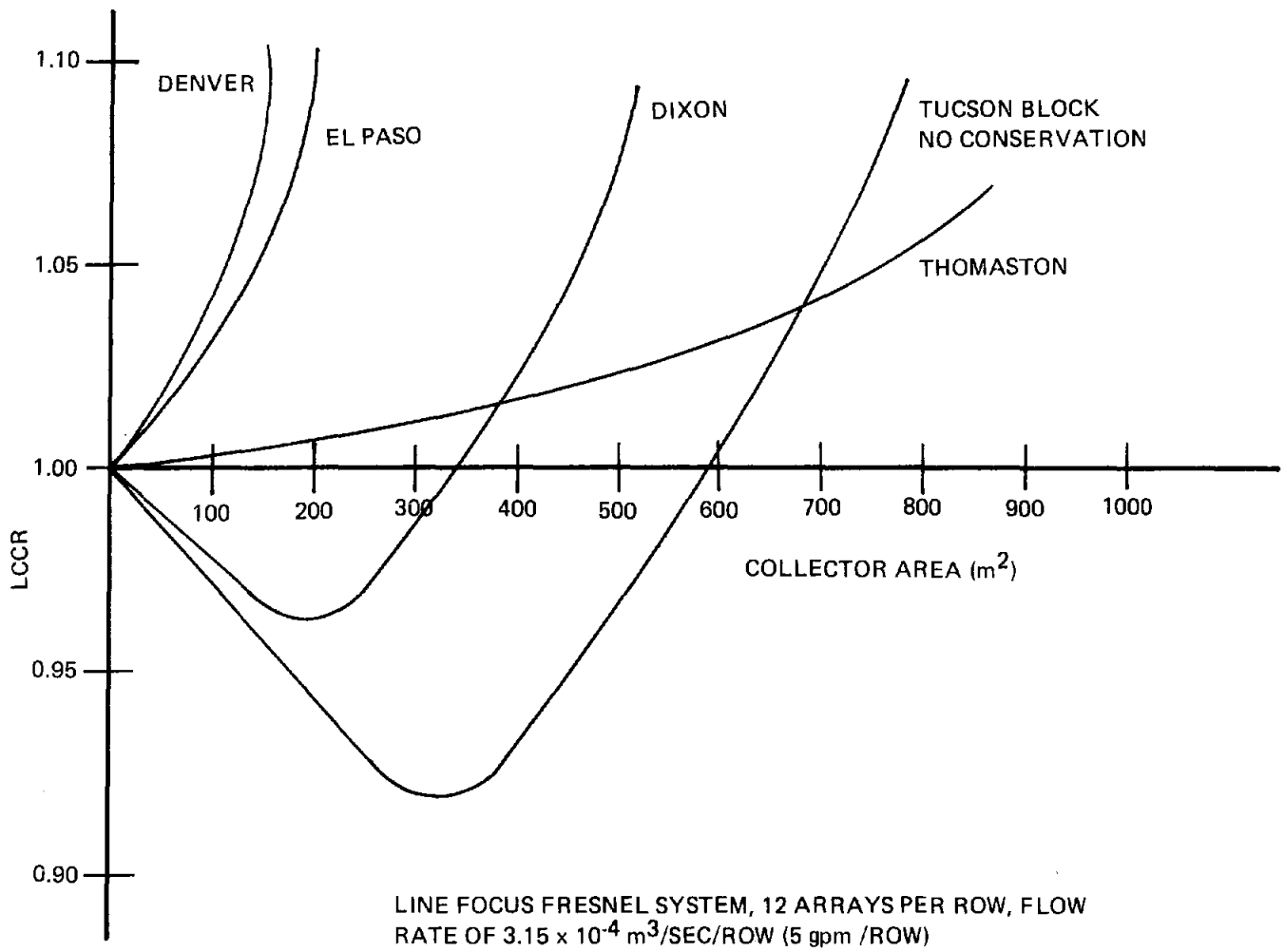

BDM/A-82-458-TR-R1

Figure III-25. Life Cycle Cost Ratio Versus Array Area for LFF Collectors and for the Industrial Sector -- Income Tax Credit is 10 Percent

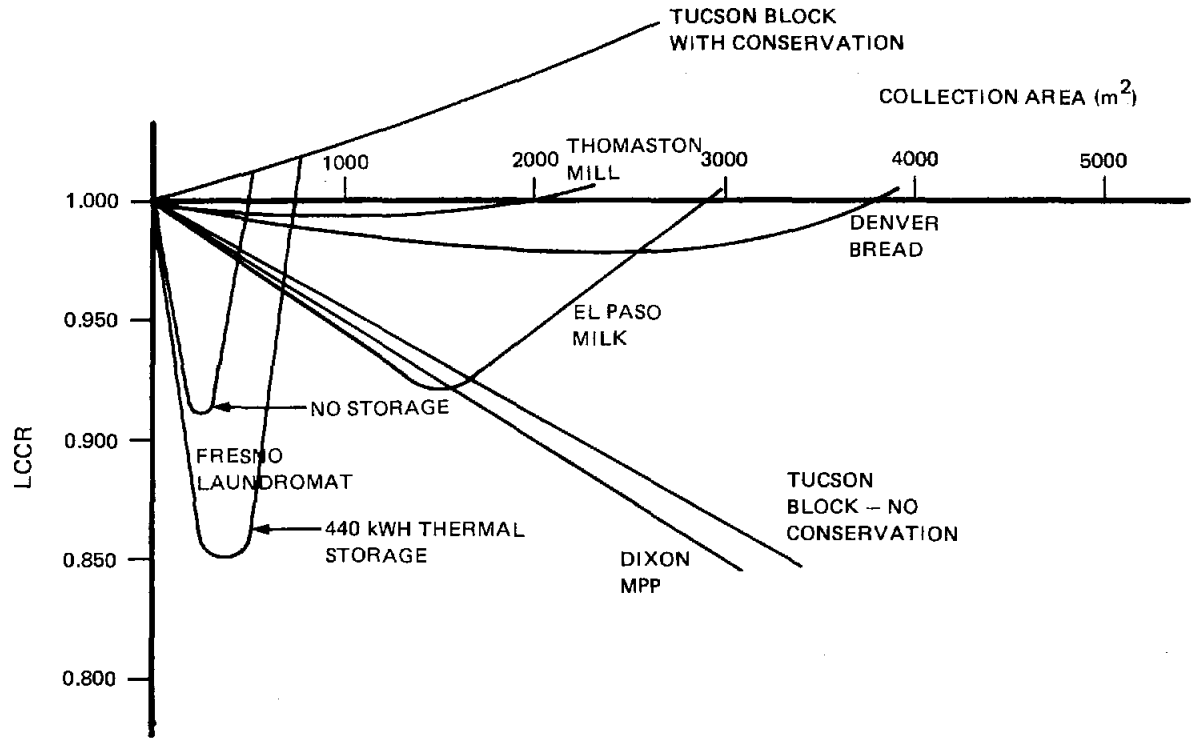

(a) LCCR VERSUS ARRAY AREA FOR THE INDUSTRIAL SECTOR, 12 ARRAYS PER ROW, FLOW RATE OF 3.15×10^{-4} m^3/SEC/ROW (5 gpm PER ROW)

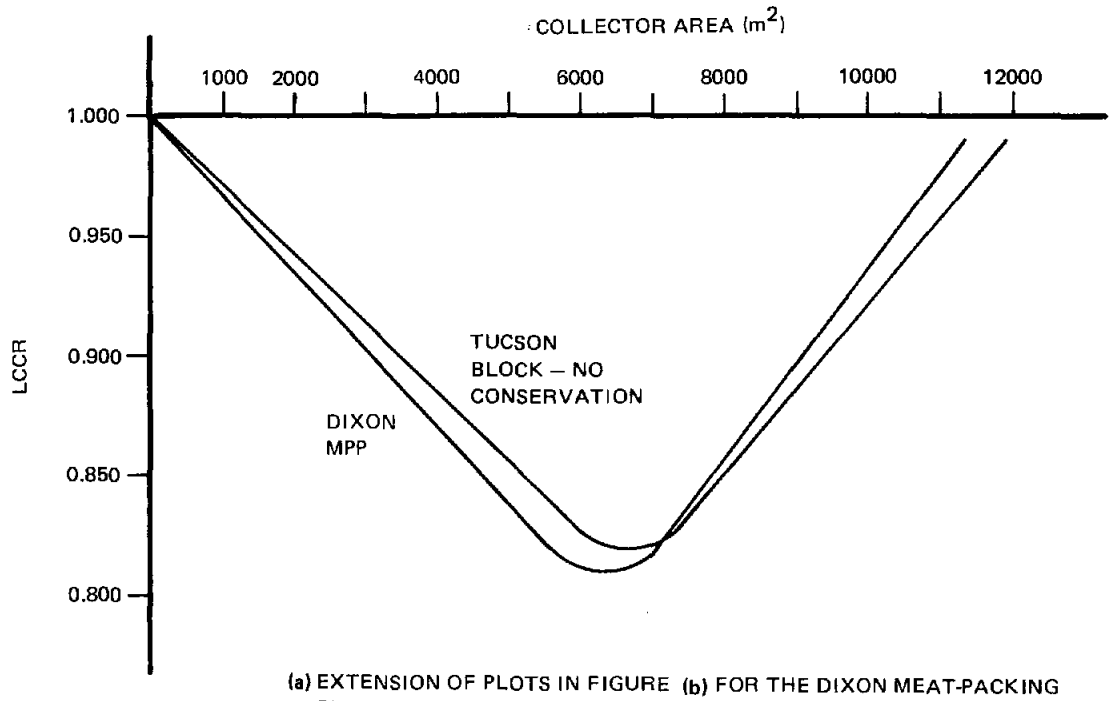

(a) EXTENSION OF PLOTS IN FIGURE (b) FOR THE DIXON MEAT-PACKING PLANT AND THE TUCSON CEMENT BLOCK PLANT

BDM/A-82-458-TR-R1

Figure III-26. Life Cycle Cost Ratio Versus Array Area of LFF Collectors for the Industrial Sector -- Income Tax Credit is 25 Percent

difference in three of the applications: the Denver bread bakery, the El Paso milk plant, and Thomaston mills. Increasing the tax credit caused these site/application pairs to become economically feasible. This change also significantly improved the LCCR for the Dixon meat-packing plant and the Tucson cement block plant.

In performing these calculations we assumed 12 LFF arrays per row with a flow rate of 3.15×10^{-4} m^3/sec (5 gpm). Preliminary calculations indicated that variations in the flow rate within this range have a minor effect on the LCCR. In all applications, the return temperature from the load was assumed to be 18.3°C (65°F) except for the fiber-finishing plant. This plant has a large steam load with a 50-percent condensate return at 82°C (180°F). Therefore, the return temperature from the load is about 51°C (125°F).

Based on this analysis, the selected applications in Denver and El Paso are not economically feasible for tax credits of 10 percent. This may be due to the low cost of electricity and natural gas in Colorado and Texas. Another factor affecting the El Paso application is that the facility for which a load profile was available has a very small thermal load compared to the typical loads specified in the Drexel report (where an E/T of 0.48 was identified). The Thomaston, Georgia plant is not economically feasible for 10-percent tax credits, and is barely feasible for 25-percent credits. This may be due to the very high thermal requirements for process steam and the high return temperature from the load. This indicates that a PV-T system may not be feasible for a preheat application since it would be more economical to use steam blowdown to heat makeup water or mix the condensate return directly with makeup water.

Subsequent to performing these calculations, plant managers were contacted at three meat-packing plants, two concrete block manufacturing plants, and a milk-processing plant. It was found that within the last few years significant energy conservation measures had been installed at the facilities contacted. The hot water used in the cement block curing process is recycled through a heat exchanger to preheat the

makeup water to about 65.6°C (150°F) to 71.1°C (160°F). A system analysis of this type of plant resulted in an LCCR greater than 1, indicating that PV-T would not be feasible for cement block plants using current heat recovery techniques.

Discussions with plant managers of meat-packing and milk-processing facilities indicate that various heat recovery techniques are in use. In one meat-packing facility, heat exchangers are used in drains to recover energy from hot clean-up water to preheat make-up water. In another facility, thermal energy is recovered from the refrigeration condenser to preheat make-up water. In a third meat-packing plant, the steam blowdown from the beef rendering plant was used to preheat make-up water to 48.9°C (120°F). Thus, the feasibility of PV-T systems in the meat-packing industry depends on the specific process and on energy conservation measures. The major requirement for a plant which processes beef is steam for the rendering operation. The steam is cascaded to preheat water used for clean-up. A plant which is too small for a rendering operation, such as the Dixon facility, uses steam primarily to produce hot water for clean-up. This type of meat-packing facility appears feasible for PV-T applications. At this time, it remains unclear whether the bakery or the milk plant would be feasible for a PV-T application once the current energy conservation techniques are considered.

At this stage of the survey and analysis of industrial site/application pairs, it appears that PV-T application is most feasible for a small meat-packing plant which does not require large amounts of steam in the process, and which has not installed any energy recovery equipment. A preliminary analysis indicates that thermal storage improves the economics of the system.

The primary conclusion of this study is that applications that can recover significant waste heat from the process water, or that require steam that can be cascaded to preheat process water, may not be feasible for PV-T application. Those applications which require hot water, and cannot recover significant amounts of waste heat to preheat the make-up water, appear to be viable candidates for PV-T systems.

3. Commercial Site/Application Pairs

A SOLCEL-II analysis was performed on the five selected commercial applications listed in section III.2.a., and with load profiles shown in figures III-4 through III-13. The results of this analysis are shown in figure III-27. These calculations were performed with a 25-percent tax credit. The two best applications are the Fresno, California hospital and the Albuquerque, New Mexico public school.

The Seattle, Washington hospital is not an economical application because of low insolation and low energy costs. The application to a school in Boston, Massachusetts is barely economical due to the low incidence of insolation at the site. The Phoenix, Arizona public administration building is not feasible for PV-T, apparently due to the low thermal energy requirement as indicated by the E/T ratio of 0.721. In this application much of the thermal energy produced by the array must be dissipated through the cooling tower.

As indicated in figures III-26 and III-27, the optimum collector field for a commercial application is much smaller than that for an industrial application due, of course, to the smaller, intermittent thermal loads versus the much larger and continuous loads of an industrial process. Somewhat larger arrays might be expected if thermal storage were included. Storage will be considered for the Fresno hospital and the Albuquerque school during the design phase of this project.

In making economic calculations for the industrial sector, we found that the line focus fresnel lens system was by far the most economical. Therefore, this system was used for the commercial sector calculations. Again, an installed cost of $\$275/m^2$ of array was assumed.

E. SIDE-BY-SIDE STUDY

In addition to the previously described calculations for a PV-T system, calculations were performed to determine the feasibility of supplying only the thermal load using a concentrating solar thermal

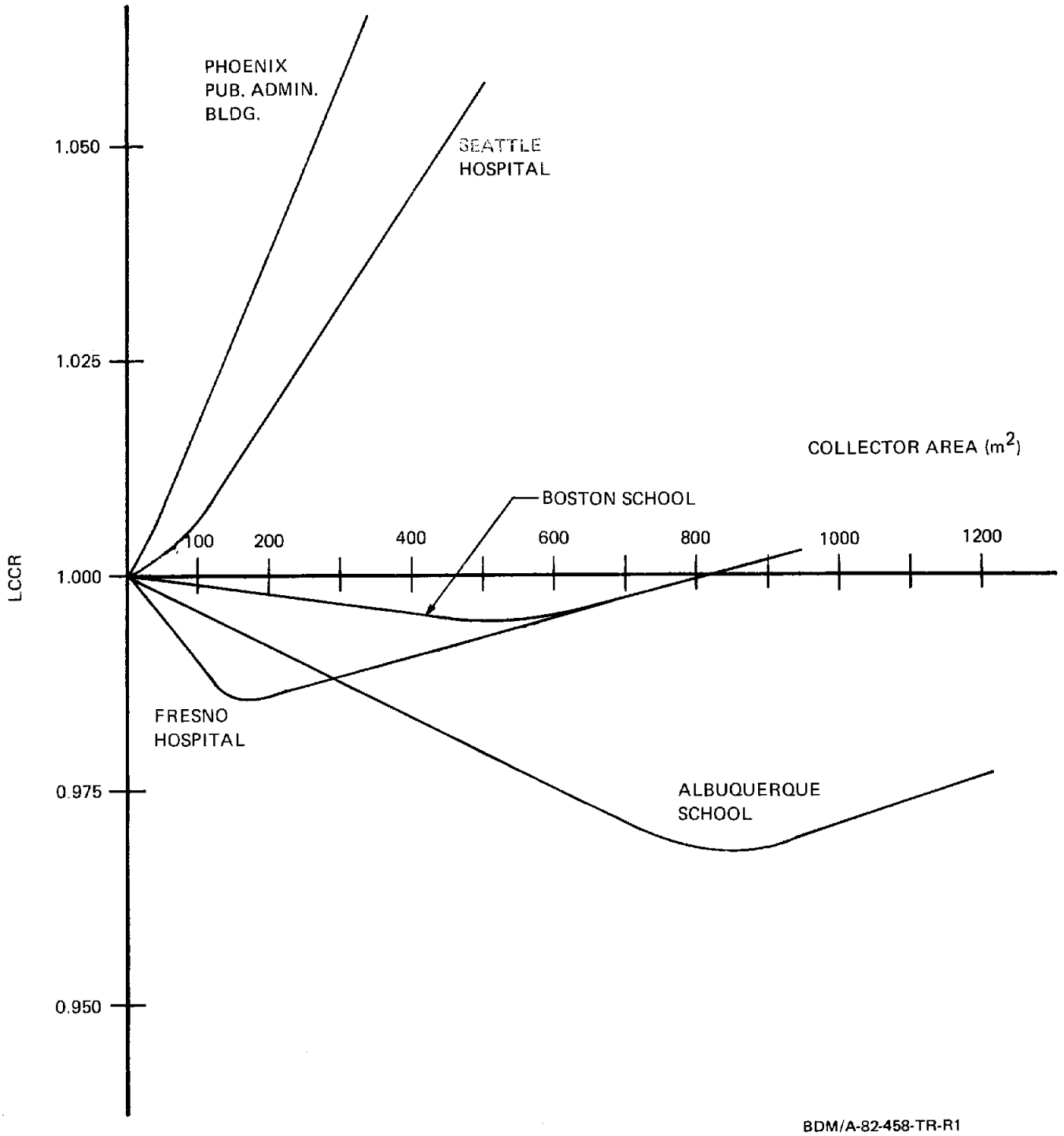

Figure III-27. Life Cycle Cost Ratio Versus Array Area for Commercial Applications Using LFF Collectors and a 25 Percent Tax Credit

system, or supplying only the electrical load using a passively cooled PV array. Before these calculations could be performed, collector array costs needed to be determined which are equivalent to the projected $\$275/m^2$ for the PV-T array. The development of these costs is discussed in the next section, and the results of the side-by-side analysis are provided in the following section.

1. Collector Array Costs

Collector array costs were determined for thermal-only and passively cooled PV-only LFF collectors, thermal-only LPT collectors, and flat plate PV collectors. GE's analysis (ref. III-22) was again used as a basis, and production volume costs were projected using equation III-25.

Using the previous assumptions of $1/Wp module cost and 15 percent field efficiency the LFF PV-only concentrator module again will cost $\$150/m^2$, the same as the PV-T concentrator module. For a production level of 7.5×10^6 m^2, the additional hardware and installation costs decrease to $\$88.6/m^2$, down from the GE projection of $\$121.9/m^2$ for a production level of 10^5 m^2. This is less than the PV-T cost since piping and plumbing fixtures are no longer required. With shipping costs of $\$16.7/m^2$, the PV-only LFF array installed cost comes to $\$255.3/m^2$.

Compared to the PV-T cost, the LFF thermal-only array cost decreases due to the elimination of PV cell costs and field wiring costs. The projected installed cost is $\$208.9/m^2$ with a cumulative production level of 7.5×10^6 m^2. The experience factor is applied to GE's projected cost for the LPT thermal-only system to give a cost of $\$196/m^2$.

In the GE analysis, the flat plate PV module cost was taken as $\$268/m^2$, or 1.4 times the cost of a LFF concentrating PV module. It was assumed that the same ratio would hold at higher production volumes and improved cell costs, so that a flat plate PV module cost in the 1990 time frame of $\$210/m^2$ was determined. Again, shipping costs were assumed not to vary, and installation costs decreased by the experience factor so that total installed costs for the flat plate PV array was $\$258/m^2$.

These costs are summarized in tables III-22 through III-24. Table III-22 shows the GE projected installation costs and table III-23 shows the GE projected hardware and fabrication costs, shipping costs, and total array installed costs. These costs are for 1980 technology and a production rate of 10^5 m^2/year. Table III-24 shows the predicted array costs assuming improved technology ($1/Wp and 15 percent efficiency) and a cumulative production level of 7.5×10^6 m^2.

2. Results of Side-By-Side Analysis

For the thermal-only system, we chose to use a linear parabolic trough in the analysis because its cost is lower than the LFF thermal-only collector. The T-800 LPT manufactured by Solar Kinetics, Inc. (SKI) of Dallas, Texas was chosen for simulation. This collector is 6.1 m (20 ft) long and 2.4 m (8 ft) wide with efficiency characteristics shown in figure III-28. Another reason for choosing this LPT is that its efficiency is equal to or greater than LFF thermal-only collectors (for example, see ref. III-24). The collector used for the PV-only analysis was the LFF passively cooled collector because of its low cost and high efficiency compared to the flat plate collector.

The results of the thermal only study are shown in figure III-29 for the industrial applications and figure III-30 for the commercial applications. Initial studies indicated that the north-south orientation of the LPT collector was optimum for all applications except the schools, which have a high winter load and a negligible summer load. All of these simulations were performed without thermal storage.

Comparing figure III-26 with figure III-29 shows that the fluid milk, laundromat, and cement block (without heat recovery or storage) applications have significantly lower LCRRs with a thermal-only system than with a PV-T system. However, the meat-packing plant exhibits a lower LCCR with the PV-T system.

Figures III-27 and III-30 indicate that only the Fresno hospital has a lower LCCR with a thermal-only system, as compared to a PV-T system. The Albuquerque school is also an economically feasible application for the thermal system. However, all other commercial applications are not economical.

TABLE III-22. GE INSTALLATION COSTS USING 1980 TECHNOLOGY AND A PRODUCTION RATE OF 10^5 m^2/YEAR (REF. III-22)

	LFF COLLECTOR			LPT	FLAT PLATE
	PV-T	T-ONLY	PV-ONLY	THERMAL	PV
Site Work					
Soil Sterilization	3.7	3.7	3.1	3.1	3.5
Ground Surfacing	11.6	11.6	11.6	9.9	10.8
Fencing	14.4	14.4	14.4	13.1	14.7
Foundation	29.7	29.7	29.7	30.6	--
Support/Tracking					
Install Steel	14.2	14.2	14.2	7.0	--
Wood Truss	--	--	--	--	19.1 (109.2)
Collector Installation	37.9	37.9	37.9	37.9	16.6
Electrical					
Array Wiring	17.3	--	17.3	--	6.9
Field Wiring	5.8	--	5.8	--	5.7
Control Wiring	1.6	1.6	1.6	5.8	--
Mechanical					
Array Piping	26	26	--	22.9	--
Field Piping	22.9	22.9	--	24.0	--
Subtotal (K$)	185.1	162.0	136.2	154.3	186.5
Burden (32%)	59.2	51.8	43.6	49.4	59.7
Aperture Area (400 KW)	3214	3214	3214	3680	4160
$/$m^2$	76	66.5	55.9	55.4	59.2

TABLE III-23. GE COST STUDIES USING 1980 TECHNOLOGY AND 10^5 m^2/YEAR PRODUCTION LEVELS (REF. III-22)

	LFF COLLECTOR			LPT	FLAT PLATE
	PV-T	T-ONLY	PV-ONLY	THERMAL	PV
Cell/Receiver				18.30*	268.80**
Solar Cells	75.70	--	75.70		
AL Receiver	32.70	32.70	32.70		
Assemblies	4.40	4.40	4.40		
Concentrator	79.00	79.00	79.00	107.40	
Module Support	27.70	27.70	27.70	--	
Tracking Hardware	33.10	33.10	33.10	55.60	
Controls	5.20	5.20	5.20	22.40	
Cooling	7.00	7.00	--	2.40	
Total Hardware and Fabrication Cost ($\$/m^2$)	264.8	189.1	257.8	206.1	268.80
FOB Selling Price	264.8	189.1	257.8	206.1	268.80
Shipping	16.7	16.7	16.7	6.0	4.8
Installation	76.0	66.5	55.9	55.4	59.2
Total Cost ($\$/m^2$)	357.5	272.3	330.4	267.5	332.8
Module Cost ($/Wp)	1.54		1.54		2.80

*Thermal receiver cost based on a study (ref. III-23) which indicated the receiver was 14.5 percent of the total collector cost.

**Flat plate PV module cost is 1.4 times the LFF concentrator module cost (cell/receiver and concentrator).

TABLE III-24. PROJECTED 1990 COSTS WITH NEW TECHNOLOGY AND 7.5×10^6 m^2 PRODUCTION LEVEL

	LFF COLLECTOR			LPT	FLAT PLATE
	PV-T	T-ONLY	PV-ONLY	THERMAL	PV
Cell/Receiver					
Solar Cells	59.25	--	59.25		
AL Receiver	25.50	25.50	25.50		
Assemblies	3.45	3.45	3.45		
Concentrator	61.80	61.80	61.80		
Total Module Cost ($/m^2)	150.00	90.75	150.00	91.30	210.00
Additional Hardware and Fabrication Cost	53.10	53.10	48.00	58.50	--
FOB Selling Price	203.00	143.85	198.00	149.70	210.00
Shipping Cost	16.70	16.70	16.70	6.00	4.80
Installation Cost	55.20	48.30	40.60	40.20	43.00
Total Installed Cost ($/m^2)	275.00	208.85	255.30	196.00	258.00
Module Cost ($/Wp)	1.00	--	1.00	--	1.75
Installed Cost ($/Wp)	1.83	--	1.70	--	2.15

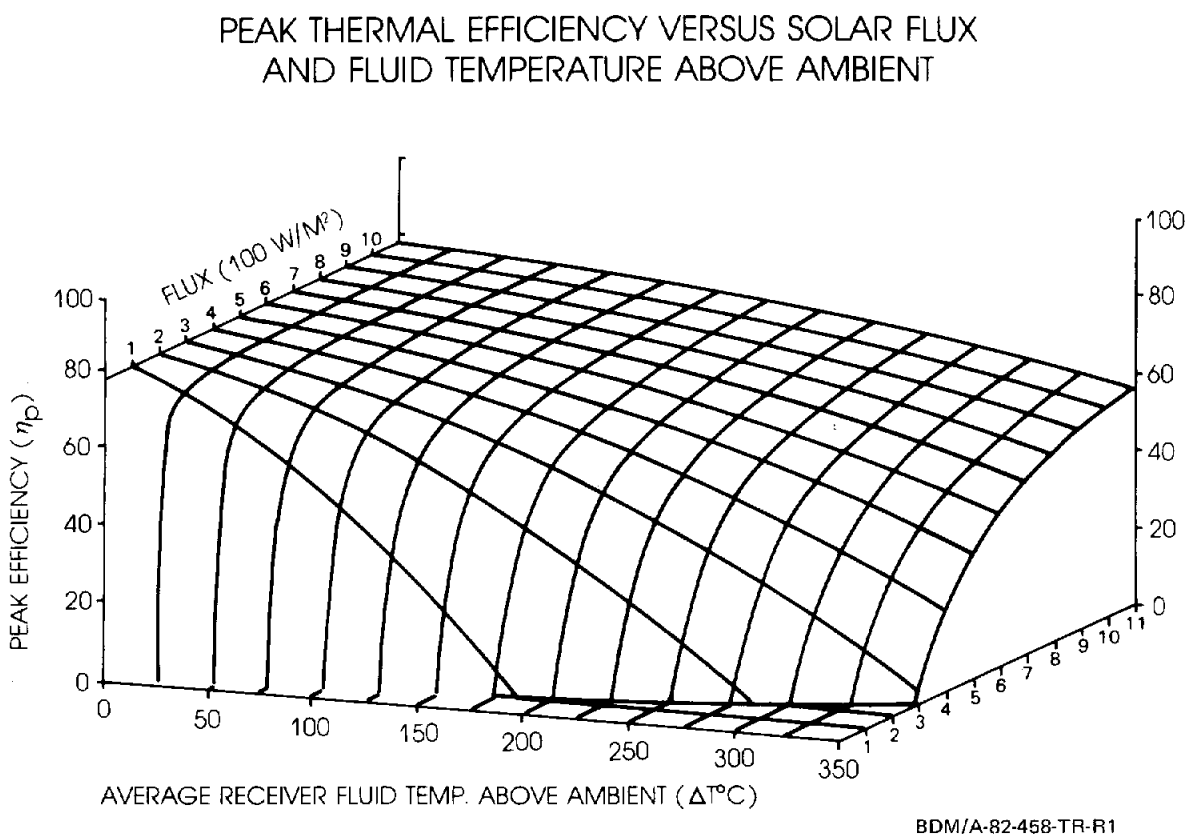

Figure III-28. Solar Collector Thermal Performance SKI T-800

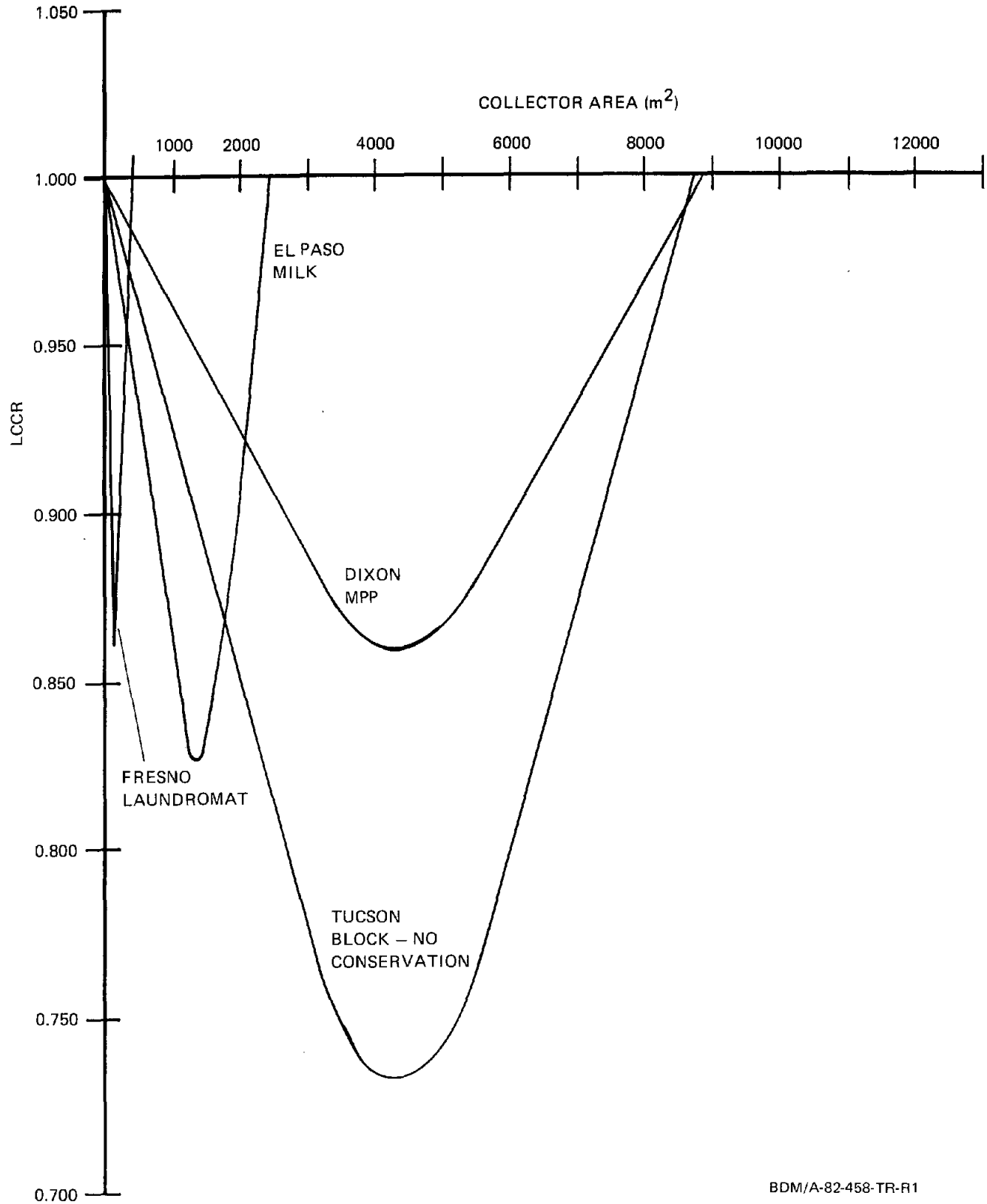

Figure III-29. Life Cycle Cost Ratio Versus Array Area for Concentrating Solar Thermal Collectors Only and Industrial Applications

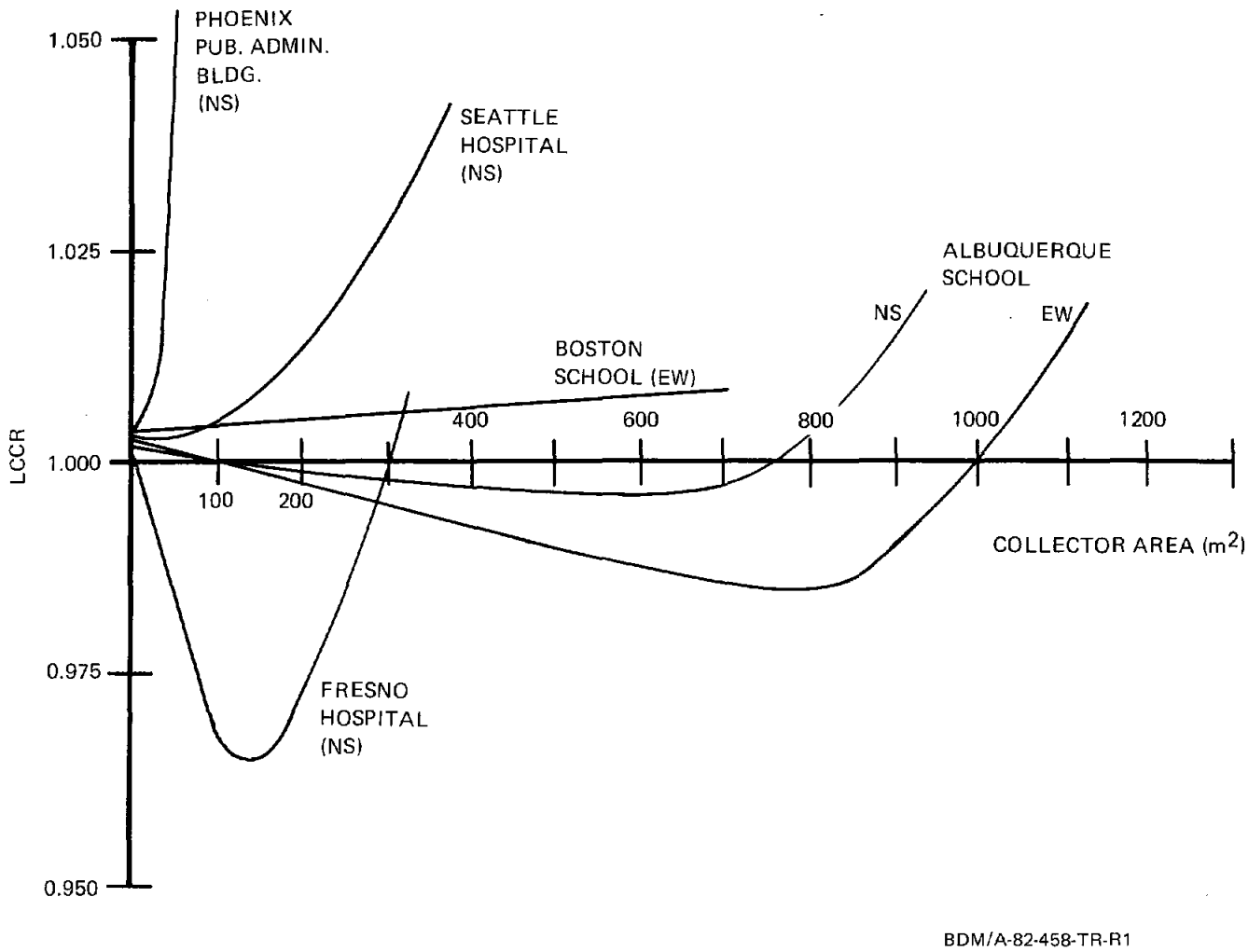

Figure III-30. Life Cycle Cost Ratio Versus Array Area for Concentrating Solar Thermal Collectors Only and Commercial Applications

The results of the PV-only calculations are shown in figure III-31 for the industrial applications and figure III-32 for the commercial applications. As seen in these figures, a PV-only system is not feasible for any of the proposed applications.

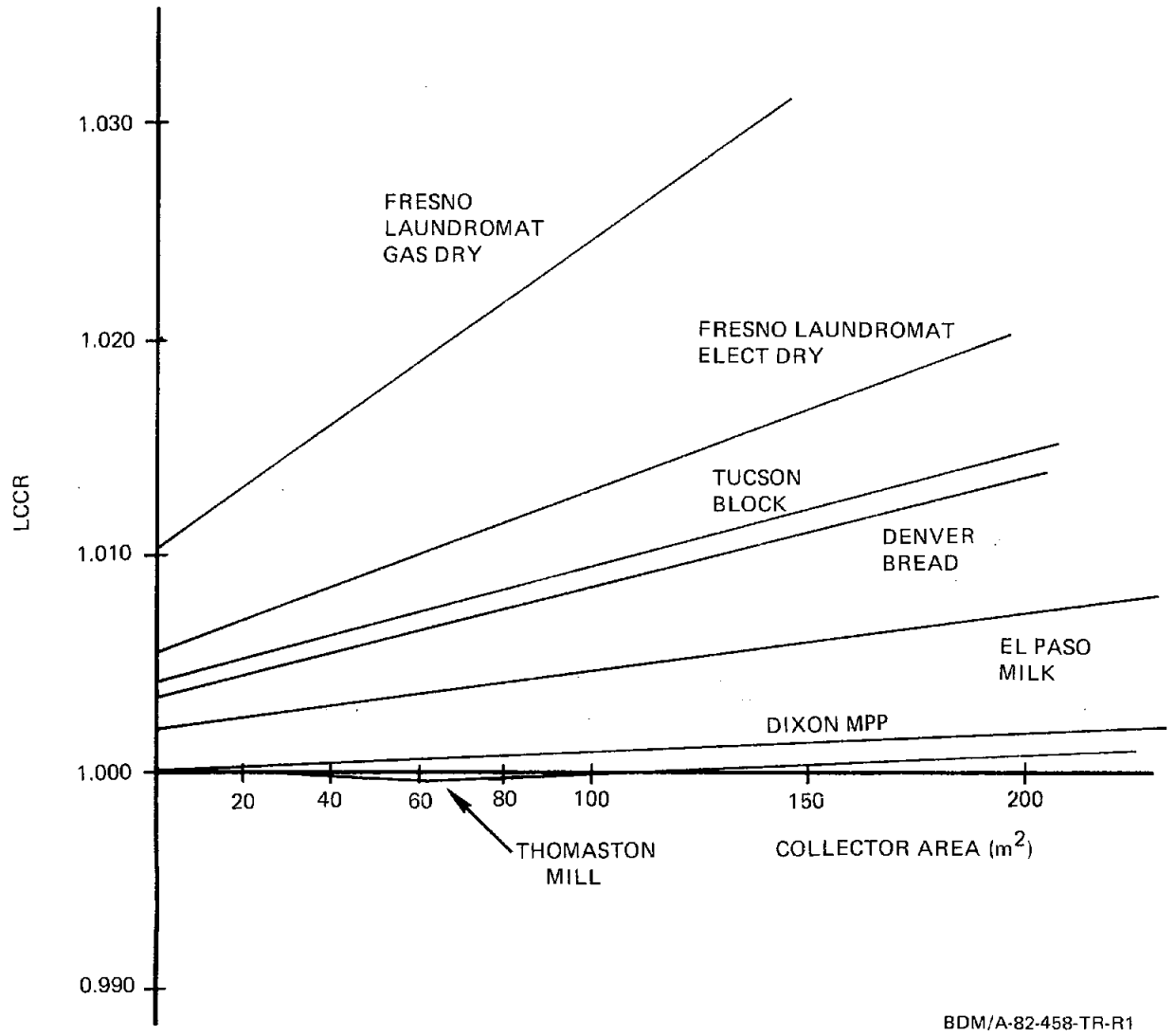

Figure III-31. Life Cycle Cost Ratio Versus Array Size for a LFF PV System Only and Industrial Applications

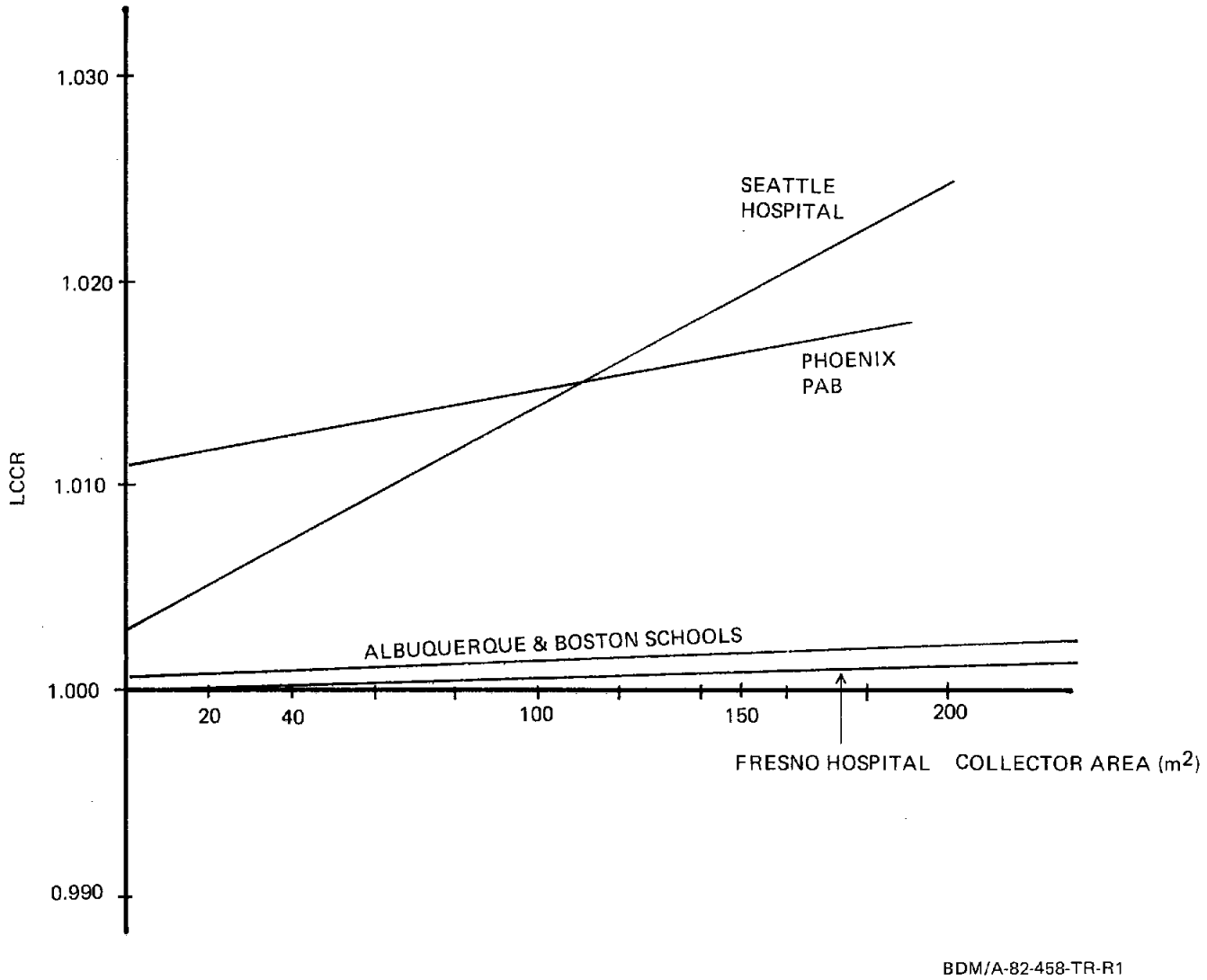

Figure III-32. Life Cycle Cost Ratio Versus Array Area for a LFF PV System Only and Commercial Applications

F. REFERENCES

III-1. C. D. Parker, et. al., A Study of Potential Photovoltaic/Thermal Applications in the Commercial Sector, Final Report, (Sandia National Laboratories, Albuquerque, New Mexico, July 1981), SAND 80-7175.

III-2. Bernard B. Hamel, et. al., 1980, Energy Analysis of 108 Industrial Processes, DOE Contract E(11-1) 2862, Drexel University.

III-3. A. M. Perino, A Methodology for Determining the Economic Feasibility of Residential or Commercial Solar Energy Systems, Sandia National Laboratories, Albuquerque, New Mexico, SAND 78-0931, January 1979.

III-4. H. A. Kaufman, Energy Consumption in Commercial Industries by Census Division - 1974, Jack Faucett Associates, Inc., Chevy Chase, Maryland, March 1977, TIC/NTIS #PB-268851.

III-5. U.S. Department of Energy, State Energy Fuel Prices by Major Economic Sector From 1960 Through 1973, DOE/EIA-0190, July 1979.

III-6. Federal Register, Volume 45, No. 16/Wednesday, January 23, 1980/Rules and Regulations.

III-7. The 1977 Ashrae Handbook of Fundamental, The American Society of Heating, Refrigerating, and Air-conditioning Engineers, Inc., New York, New York.

III-8. Uniform Building Code, Chapter 53, Energy Conservation, International Conference of Building Officials, Whittier, California, amended 1977.

III-9. E. Hirst, J. Carney, P. Knight, Energy Use at Institutional Buildings: Disaggregate Data and Data-Management Issues, Oak Ridge National Laboratories, Tennessee, ORNL/CON-73, DE81-024147, June 1982, p. 37.

III-10. Engineering Guide for System Design, Load Estimating and Duct and Piping Design, The Carrier Corporation, Catalog #592-018, 1969, p. 772.

III-11. Technical Support Document for Notice of Proposed Rulemaking on Energy Performance Standards for New Buildings, U.S. Department of Energy, DOE/CS-0113, November 1979.

III-12. D. S. Teji, "Technical Assistance Report, Human Resources Center #3," The Arizona Energy Conservation Office, Phoenix, 1981.

III-13. Inter Technology Corporation, 1977, Analysis of the Economic Potential of Solar Thermal Energy to Provide Industrial Process Heat, COO-2829-76/1 (ERDA Contract EY-76-C-02-2829.000).

III-14. U. S. Department of Commerce, 1980, 1977 Census of Manufacturers Bureau of Census.

III-15. U. S. Department of Commerce, 1981, Annual Survey of Manufacturers Fuels and Electric Energy Consumed, 1978.

III-16. W. O'Keefe, 1981, "Cement-Block Plants Cut Energy Waste Uniquely," Power, December 1981, p. 96.

III-17. Advanced Technology, Inc., 1981, Photovoltaic Off-Farm Agricultural Applications, Sandia National Laboratory Contract 62-6590.

III-18. D. W. Hooker, E. K. May, and R. E. West, 1980, Industrial Process Heat Case Studies, Solar Energy Research Institute, SERI/TR-733-323.

III-19. McDonnell Douglas Astronautics Company, 1977, Industrial Applications of Solar Total Energy, (DOE Contract EY-76-C-03-1132), SAN/1132-2/4.

III-20. McDonnell Douglas Astronautics Company, 1980, Solar Total Energy Modularity Study, (Sandia National Laboratory Contract 07-7164), SAND 80-7060.

III-21. M. Rios, Jr., et. al. "Cost Effectiveness of Concentrating Photovoltaic-Thermal (PVT) Systems Versus Side-by-Side Systems for Two Intermediate Applications," IEEE Photovoltaic Specialists Conference, 1981.

III-22. J. Chan, Manufacturing Cost Analysis of 1980 Vintage Photovoltaic Arrays, Sandia National Laboratories, Albuquerque, New Mexico, April 1982, SAND 81-7010.

III-23. The BDM Corporation, 1978, Conceptual Design and Analysis of a 100 MWe Distributed Line Focus Solar Central Power Plant, VOL. II, DOE Contract ET-78-C-03-2073, BDM/TAC-79-375-TR.

III-24. E-Systems, Inc., Technical Bulletin, Fresnel Lens Solar Energy Collector.

CHAPTER IV
CONCLUSIONS

A survey of the state-of-the-art actively-cooled concentrating photovoltaic systems has been performed, and an analysis of the performance of the three types of PV-T systems was carried out. These systems included the line focus Fresnel lens, linear parabolic trough, and point focus Fresnel lens collectors. Based on these studies the following conclusions may be made:

(1) The industry has matured in surfacing initial problems associated with PV-T systems through the DOE National Photovoltaic Program, and subsequently solving these problems. However, additional work is required to improve field efficiency and lower array costs. Research and development is continuing in these areas by cell and module manufacturers.

(2) The LFF collector exhibits the highest electrical and thermal efficiencies over a large range of insolation and ambient temperature. The thermal efficiency is nearly constant at about 50 percent regardless of weather conditions, whereas the thermal efficiency of LPT and PFF collectors decrease significantly with increasing values of the parameter $(T_F - T_A)/I_{DN}$.

(3) For a given electrical power output for an array, the LPT and LFF systems required the least land area, and the LFF system was the least expensive in terms of dollars per kilowatt produced by the array.

Systems analyses of selected commercial and industrial site/application pairs using LFF and LPT systems showed that LFF collectors are more cost effective in terms of lower life cycle cost ratios for all applications considered. These analyses also showed the obvious--sites with low insolation or low energy costs were not feasible.

A study of industrial and commercial applications indicated few economically feasible site/application pairs for a PV-T system. For the industrial sector this was primarily due to the inability of the PV-T

system to operate at sufficiently high temperatures to provide the required thermal energy. However, when an application is found which requires large amounts of low temperature water, a PV-T system becomes promising. For both commercial and industrial applications, if the thermal load is too low the analysis indicates a life cycle cost ratio (LCCR) greater than one, which means the system is not economical. This may be due to the following: (1) excessive use of the cooling tower, which must be used to cool the array in the absence of a thermal load, thereby decreasing the net electrical output of the array, and (2) the return on investment comes primarily from displacing thermal energy.

Applications with a large steam requirement, such as Thomaston Mills fiber finishing plant, were not economically feasible since a large amount of conventional backup fuel is required to supply the heat of vaporization to produce steam. When a significant portion of the thermal requirement can be supplied by conservation measures, the application is not feasible for PV-T. For example, the concrete block plant has a very low LCCR if it is assumed that there is no energy recovery from the hot water; however, if energy recovery is used so that the thermal load is reduced and the return temperature from the load is increased then the LCCR becomes greater than unity and the PV-T system is no longer economically feasible. The Phoenix public administration building has a low thermal load compared to its electrical load. Even though this application is in an excellent region for solar systems, the LCCR for the PV-T system was greater than one.

These examples begin to indicate that the economics of PV-T systems are driven by the thermal load requirements and the ability of the system to meet these requirements. This conclusion is further confirmed by the side-by-side study in which a passively cooled LFF PV-only system was simulated to provide only electrical power to the load, and an LPT thermal-only system was modeled to displace a portion of the thermal load.

The results of the side-by-side study indicate that PV-only systems are not economically feasible. That is, no application had an LCCR

less than one for the PV-only system. On the other hand, most applications had a LCCR less than one when the thermal-only system was used to displace the thermal load. In most cases the LCCR for the thermal-only system was less than the LCCR for the PV-T system, indicating that the additional cost of the PV portion of the system is not offset by the displaced electrical power. However, the meat-packing plant and the Albuquerque school had a smaller LCCR for the PV-T system than for the thermal-only system.

For these site/application pair and side-by-side studies, the following conclusions may be drawn:

(1) For most applications the cost of the PV portion of a PV-T system is not recovered through the displacement of an electrical load. Thus, a thermal-only system used to displace the thermal load would be a more economical alternative. However, each collector system and application must be carefully analyzed to determine the most cost effective alternative. For some applications the extra cost of the PV portion of the system can be recovered by displacing the electrical load.

(2) PV-T systems are not feasible for applications which have a small thermal load, a large steam requirement, or a high load return temperature.

DISTRIBUTION LIST:

Acurex Corporation (1)
Attn: George Sutton
Bob Spencer
Dariush Rafinejad
485 Clyde Avenue
Mountain View, CA 94042

Arco Solar, Inc. (1)
Attn: Ray Kosanke
Library
P. O. Box 4400
Woodland Hills, CA 91365

Arizona State University
Attn: Charles Backus
College of Engineering
Tempe, AZ 85281

Battelle
Attn: Don Carmichael
505 King Avenue
Columbus, OH 43201

The BDM Corporation (3)
Attn: Bill Schwinkendorf
1801 Randolph Road SE
Albuquerque, NM 87111

Black & Veatch
Attn: Sheldon L. Levy
P. O. Box 8405
Kansas City, MO 64114

U. S. Dept. of Energy
Div. of PV Energy Technologies
Attn: R. Annan
A. Krantz
M. Prince
L. Herwig
A. Scolaro
1000 Independence Ave. SW
Washington, DC 20585

EPRI (2)
Attn: Roger Taylor
Ed DeMeo
P. O. Box 10412
Palo Alto, CA 94303

ENTECH, Inc.
Attn: Mark O'Neill
A. J. McDanal
P. O. Box 612246
DFW Airport, TX 75261

Intersol Power Corporation
Attn: John Sanders
Sid Broadbent
11901 West Cedar
Lakewood, CO 80228

Jacobs Engineering
Attn: Bob Martin
251 South Lake Ave.
Pasadena, CA 91101

Jet Propulsion Lab (3)
Attn: K. Shimada
R. Ferber
Solar Data Center
MS 502/414
4800 Oak Grove Drive
Pasadena, CA 91109

Martin Marietta
Attn: R. Hein
P. O. Box 179
Denver, CO 80201

Oak Ridge National Lab
Attn: Steve Kaplan
P. O. Box X
Oak Ridge, TN 37830

SERI, Library (2)
1536 Cole Blvd., Bldg. #4
Golden, CO 80401

SOLAVOLT
Attn: Ray Kendall
P. O. Box 2934
Phoenix, AZ 85062

Southern Cal Edison
Attn: Spencer Carlisle
2244 Walnut Grove Ave.
Rosemead, CA 91770

Spectrolab
Attn: Steve Olah
12500 Gladstone Avenue
Sylmar, CA 91342

United Energy Technologies
Attn: John Mackay
420 Lincoln Center Dr.
Foster City, CA 94404

Varian & Associates (1)
Attn: N. Kaminar
611 Hansen Way K-219
Palo Alto, CA 94303

6223 G. Jones
6223 M. Thomas
6224 D. Arvizu (10)
3141 C. M. Ostrander (5)
3151 W. L. Garner (3)
3154-3 C. H. Dalin (25)
For DOE/TIC
(Unlimited Release)
8424 M. A. Pound